ABSTRACT

Title of Document:	EVALUATION OF SKEWED SIMPLE SPAN TRANSVERSELY POST-TENSIONED ADJACENT PRECAST CONCRETE SLAB BRIDGES
	Timothy Levi Briner, Master of Science in Civil Engineering, 2012
Directed By:	Professor Chung C. Fu, P.E. Department of Civil and Environmental Engineering

Adjacent precast, prestressed concrete multi-beam bridges have recently become more prevalent due to their rapid construction time and cost effectiveness. However, longitudinal cracking primarily caused by insufficient and/or inadequate transverse connection between the beams has been discovered in the concrete overlays of recently built skewed bridges. Maryland State Highway Administration requested a research project be conducted to determine the cause or causes of the reflective cracking and propose revisions to the current state code concerning the number, orientation, and location of the transverse post-tensioning. This thesis contains a description of the behavior of skewed bridges, a survey of other states' practices, a field test conducted on a local bridge that has exhibited longitudinal cracking, the finite element model analyses simulating the field test and their corresponding results, and a parametric study conducted to determine the best practices for transversely post-tensioning this type of bridge in Maryland.

EVALUATION OF SKEWED SIMPLE SPAN TRANSVERSELY POST-TENSIONED ADJACENT PRECAST CONCRETE SLAB BRIDGES

By

Timothy Levi Briner

Advisory Committee:
Professor Chung C. Fu, Chair
Professor Amde M. Amde
Professor Yunfeng Zhang

Dedication

I would like to dedicate this first to my Lord and Savior, Yeshua. Thank You for Your love and faithfulness and for giving me the ability and opportunity to study and work excellently and to live life to the full. Second, I would also like to dedicate this to my mother. Mom, thank you for always being there for me, encouraging me, and advising me through both the good and difficult times in my life. I love you.

Acknowledgements

Table of Contents

List of Tables

List of Figures

Chapter 1: Introduction

1.1 History and Background

Short span concrete bridges have been an integral part of the United States' infrastructure system for over a century. Yet according to the U.S. Federal Highway Administration's (FHWA) bridge inventory data from 2011, almost 24% of the nation's 605,086 bridges are classified as either structurally deficient or functionally obsolete (Federal Highway Administration, 2011). Furthermore, approximately a quarter of the nation's bridges are single-span concrete bridges (Menassa et al., 2007). Over the past 70 years, concrete slab and girder bridges constructed in the 1920s and 1930s have been a reliable component of the Maryland road system; but due to time and deterioration, many Maryland bridges of this type need to be repaired or replaced (Narer, 1997). Adjacent precast concrete multi-beam bridges have been commonly built as a low cost, rapid construction alternative, especially where a shallow superstructure is required (Russell, 2009). One relatively new building technique implements transverse post-tensioning to improve the performance of precast concrete slab or box girder bridges and was initially developed in Europe during the 1960s to do the following: (1) maximize the length of cantilever overhangs, (2) minimize the number of webs, (3) improve the connection between longitudinal girders, and (4) provide better and less congested reinforcement layout at piers (Ramirez and Smith, 2003). Transverse post-tensioning practice in combination with the use of diaphragms was adopted in the United States and has become more prevalent in recent years as states have developed building standards to incorporate

this bridge reinforcement technique (Saber and Alaywan, 2011, and Schaffer, 1967). The FHWA has also begun to encourage the use of adjacent, precast, pre-stressed concrete girder bridges in the building of small- and medium-span bridges due to several advantages, including (1) simple structure, (2) standardized production, (3) in-plant quality control increasing the girder durability, and (4) ease of construction (Fu et al., 2011).

A recurring problem in adjacent multi-beam bridges is longitudinal cracks forming along the joints between the adjacent beams, leading to reflective cracks in the concrete overlay (Russell, 2009). These cracks may be caused by stresses due to temperature gradients, the live load, or even the post-tensioning, and can lead to leakage of road chemicals which can corrode the steel reinforcement and ultimately result in full cracks through the joint and the loss of load transfer between beams (Russell, 2009). Longitudinal cracks have recently been found in these types of bridges in Maryland (as well as other states), leading the Maryland State Highway Association (MDSHA) to request the Bridge Engineering Software and Technology (BEST) Center at the University of Maryland, College Park, to conduct a study regarding the post-tensioning force for the transverse post-tensioning (without regard to the bridge skew and tendon layout) to revise the state's standards (Fu et al., 2011). Since that study, cracks have been found in additional skewed bridges of this type leading to this current study on the best practice for transversely post-tensioning a skewed bridge.

1.2 Description of Normal and Skewed Bridges

Non-skewed bridges, also known as straight, normal, or right bridges, are built with the longitudinal axis of the roadway normal to the abutment. Similar to the AASHTO LRFD Bridge Design Specifications (2012), the skew angle of a bridge is defined as the angle between the longitudinal axis of the bridge and the normal to the abutment, or equivalently as the angle between the abutment and the normal to the longitudinal axis of the bridge as shown in Figure 1-1. With such a definition, a non-skewed bridge has a skew angle of 0^0. Skewed bridges are often built due to geometric restrictions, such as obstacles, complex intersections, rough terrain, or space limitations (Huang et al., 2004, and Menassa et al., 2007).
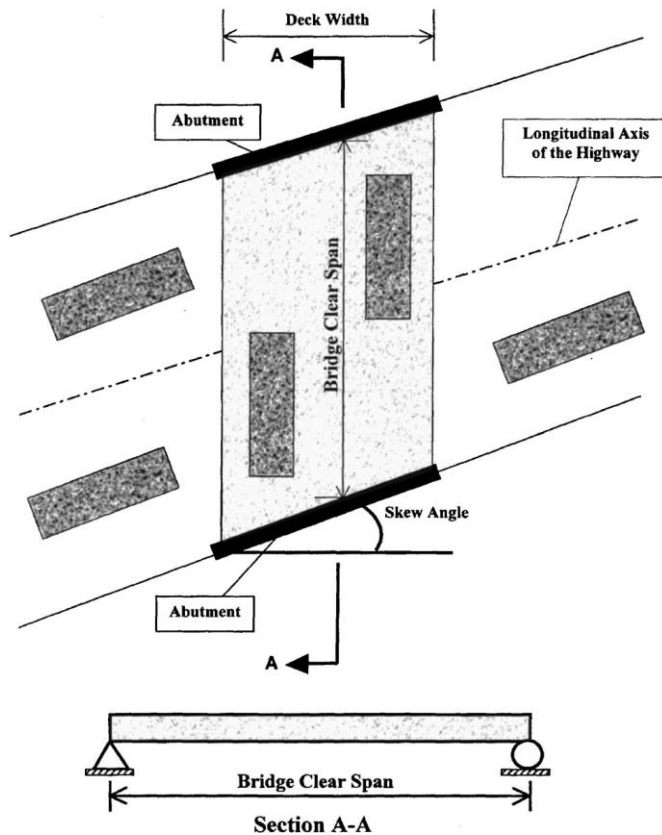
Figure 1-1: Description of a Skew Angle Using a Skewed Bridge over a Highway (Menassa et al., 2007).

1.3 General Building Practice

1.3.1 Summary of Building Practices

Adjacent precast concrete slab (or box beam) bridges are built using slabs or beams constructed in a factory and shipped out to the bridge site. The slabs or beams are then placed side by side across the abutments and tied together to form an integral structure. The space between the slabs or beams is filled with grout material to create a shear key and most times the slabs or beams are also transversely connected using post-tensioning (Fu et al., 2011). A wearing surface, generally cast-in-place concrete, is then placed over the slabs or beams. The superstructure of an adjacent precast multi-beam bridge can often be constructed within two weeks, which is significantly faster than most other alternatives (Narer, 1997). This also satisfied the Accelerated Bridge Construction (ABC) requirement recently promoted by the Federal Highway Administration (FHWA). State standards allow adjacent precast multi-beam bridges to span anywhere from 30 to 100 feet depending on the type of beams and transverse post-tensioning among other factors.

1.3.2 Precast Beams and Slabs

Precast box beams or voided slab sections are most commonly used for adjacent precast multi-beam bridges, though some states, including Maryland, use only solid slabs despite being less structurally efficient because they have proven to be more durable. In the past, salt chloride penetration has caused voided slab sections to deteriorate and undergo punching on the top portion of the slab thus proving a freezing as well as structural problem (Narer, 1997). In this study, only solid slab cases are studied.

1.3.3 Post-Tensioning

After the beams are placed, the transverse post-tensioning strands, tendons, or rods are inserted in the pre-drilled holes constructed in the solid slabs or in diaphragms constructed in the box beams or voided slabs. The transverse post-tensioning is provided using either steel strands or rods ranging from 0.5 to 1.375 inches in diameter. The ends of the transverse ties are clamped and tensioned to a specified force, the shear keys are filled in with grout, and the transverse ties are tensioned to the required force, ranging from 20 to 120 kips depending on the state, and bolted to the sides of the beams. The recesses where the transverse ties are bolted are then filled in with grout to create a smooth surface with the edge of the beam. On normal bridges, the transverse post-tensioning is placed parallel to the abutment, with the particular locations and number of transverse ties depending on the state standard. On skewed bridges, many states adopt the practice that transverse ties are placed parallel to the abutment up to 20° or 30° in skew, then, if beyond, placed normal to the girders and staggered, though each state has slightly different standards.

1.3.4 Shear Key Grouting

The shear key, either extending half-depth or full-depth of the beams depending on the state, is filled with non-shrink high-strength grout (usually a mixture of sand and mortar) which can be easily vibrated into the gap (Narer, 1997). This construction joint between the beams ties them together to help form an integral unit to distribute the stresses evenly and avoid any differential deflection between the beams (Badwan and Liang, 2007). These shear keys also allow for some fabrication and construction tolerance (Fu et al., 2011).

1.3.5 Cast-in-place Surface

The cast-in-place concrete overlay placed above the beams further helps the structure to perform monolithically as well as serving as a road surface and adding some protection to keep the beams and joints from deteriorating due to the salt chloride road treatments.

1.4 Slab Bridge Behavior

Either the American Association of State Highway and Transportation Officials (AASHTO) Standards Specifications for Highway Bridges or the AASHTO Load Resistance Factor Design (LRFD) Design Specifications are typically used to design highway bridges in the United States. Reinforced concrete slab bridges are generally designed as a series of beam strips due to AASHTO's simplified design procedure which uses a distribution width for highway loading to form a beam bending problem from a plate bending problem (Menassa et al., 2007). According to Article 4.6.2.2 of the AASHTO LRFD Bridge Design Specifications (2012), if the beams are sufficiently connected using some combination of shear keys, transverse post-tensioning, and structural overlay, then the structure will perform as a monolithic unit and may be designed as a whole-width structure. Articles 4.6.2.2.2b, 4.6.2.2.2d, 4.6.2.2.3a, and 4.6.2.2.3b from the AASHTO LRFD Bridge Design Specifications (2012) describe the calculations to find the distribution of live loads on a slab bridge for the moments in the interior beams, the moments in the exterior longitudinal beams, the shear in the interior beams, and the shear in the exterior beams, respectively (see Table 1-1).

Table 1-1: Distribution of Live Loads for a Superstructure Consisting of Concrete Beams Used in Multi-Beam Decks (AASHTO, 2012).

Load Description	Distribution Factors	Range of Applicability
Moments in Interior Beams	Regardless of Number of Loaded Lanes: $$S/D$$ Where: $$C = K*(W/L) \leq K$$ $$D = 11.5 - N_L + 1.4 * N_L * (1 - 0.2 * C)^2$$ When $C \leq 5$ $$D = 11.5 - N_L$$ When $C > 5$ $$K = \sqrt{\frac{(1 + \mu) * I}{J}}$$	Skew $\leq 45°$ $N_L \leq 6$
Moments in Exterior Longitudinal Beams	One Design Lane Loaded: $$g = e * g_{interior}$$ $$e = 1.125 + \frac{d_e}{30} \geq 1.0$$ Two or More Design Lanes Loaded: $$g = e * g_{interior}$$ $$e = 1.04 + \frac{d_e}{25} \geq 1.0$$	$d_e \leq 2.0$

Shear in Interior Beams	One Design Lane Loaded: $$\left(\frac{b}{130*L}\right)^{0.15} * \left(\frac{I}{J}\right)^{0.05}$$ Two or More Design Lanes Loaded: $$\left(\frac{b}{156}\right)^{0.4} * \left(\frac{b}{12.0*L}\right)^{0.1} * \left(\frac{I}{J}\right)^{0.05} * \left(\frac{b}{48}\right)$$ $$\frac{b}{48} \geq 1.0$$	$35 \leq b \leq 60$ $20 \leq L \leq 120$ $5 \leq N_b \leq 20$ $25{,}000 \leq J \leq 610{,}000$ $40{,}000 \leq I \leq 610{,}000$
Shear in Exterior Beams	One Design Lane Loaded: $$g = e * g_{interior}$$ $$e = 1.125 + \frac{d_e}{20} \geq 1.0$$ Two or More Design Lanes Loaded: $$g = e * g_{interior} * \left(\frac{48}{b}\right)$$ $$\frac{48}{b} \leq 1.0$$ $$e = 1 + \left(\frac{d_e + \frac{b}{12} - 2.0}{40}\right)^{0.5} \geq 1.0$$	$d_e \leq 2.0$ $35 \leq b \leq 60$

Where: S = spacing of beams or webs (feet)

D = width of distribution per lane (feet)

C = stiffness parameter

K = constant for different types of construction

W = edge-to-edge width of bridge (feet)

L = span of beam (feet)

N_L = number of design lanes as specified in Article 3.6.1.1.1

μ = Poisson's ratio

I = moment of inertia (in.[4])

J = St. Venant's torsional inertia (in.[4])

g = distribution factor

e = correction factor

d_e = horizontal distance from the centerline of the exterior web of exterior beam at deck level to the interior edge of curb or traffic barrier (feet)

b = width of beam (in.)

N_b = number of beams, stringers, or girders

1.5 Skewed Bridge Behavior

1.5.1 General Notes

It has been recommended to avoid building bridges with skew angles from as early as 1916 due to the many difficulties that arise when designing a skewed bridge, yet because of the increasingly complex site constraints, an increasing number of skewed bridges are being built (Coletti et al., 2011). In addition, it has been recognized that the skewness of a bridge does not depend solely upon its skew angle but that other factors affect the behavior of a skewed bridge. The Ontario Highway Bridge Design Code includes a measure of skewness made up of its skew angle, span length, bridge width, and girder spacing (Modjeski and Masters, Inc., 2002). In addition to the complex geometry and load distributions caused by the skew, the skew angle can affect the performance of the substructure in conjunction with the superstructure, causing a coupling of transverse and longitudinal modes due to wind and seismic loads (Precast/Prestressed Concrete Institute, 2003). Skew angles, in addition to the length to width ratio, also affect whether the bridge undergoes beam bending or plate action. As the skew increases or the length to width ratio of a bridge decreases, the bridge behaves more similarly to a plate than a beam.

1.5.2 Forces (Shear, Flexure, Moments, Thermal), Load Path, and Behavior

A complication that arises when designing a bridge with a skew angle is the introduction of alternate load paths and different distributions of loads (Coletti et al., 2011). Simply stated, depending on the transverse stiffness of the bridge, some of the load travels transversely to the obtuse corners of the skewed bridge abutments rather

than traveling along the longitudinal girders (see Figure 1-2) which reduces the longitudinal bending moments but increases the shear in the obtuse corners (Precast/Prestressed Concrete Institute, 2003).
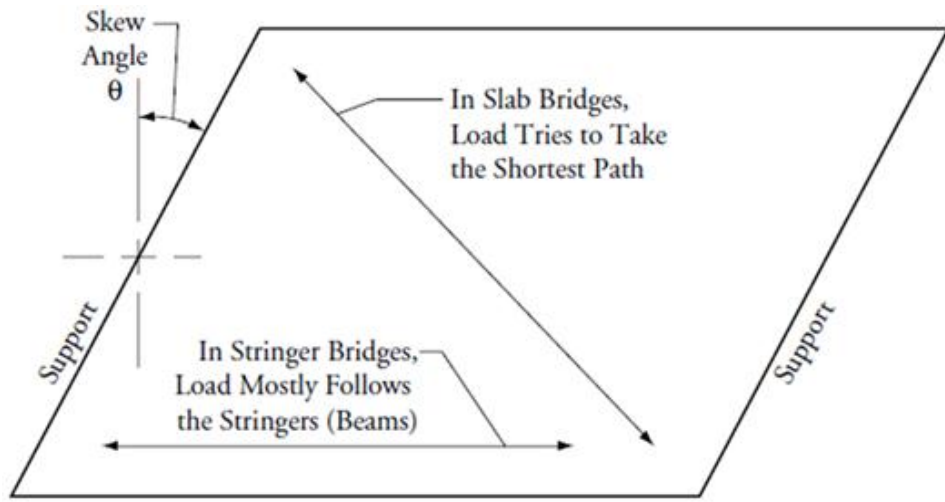
Figure 1-2: Load Path on a Skewed Bridge (Precast/Prestressed Concrete Institute, 2003).

This increase in the reactions at the obtuse corners of the bridge leads to a corresponding decrease in the reactions at the acute corners of the bridge which can sometimes cause uplift of the acute corners (Oregon Department of Transportation, 2004). This leads to an increase in the shear in the exterior beams near the obtuse corners and can produce transverse shear in the structure (Oregon Department of Transportation, 2004). In addition to increasing the shear on the exterior beams of a bridge, skew angles greater than 20° affect the bending moment applied to a bridge (Precast/Prestressed Concrete Institute, 2003). Menassa et al. (2007) showed that as the skew angle increases, the maximum longitudinal bending moment decreases but is offset by an increase in the maximum transverse moment. Corresponding with the decrease in the maximum longitudinal bending moment, the maximum live-load deflection also decreases.

Pertaining to these findings, the AASHTO LRFD Bridge Design Specifications (2012) reference corrections for longitudinal bending moments and support shear of the obtuse corner. Article 4.6.2.2.2e states that the bending moment in the longitudinal beams can be reduced based on the skew angle as long as the difference in skew angles of adjacent supports does not exceed 10^0 (see Table 1-2) (AASHTO, 2012). Article 4.6.2.2.3c conservatively applies a correction factor for the shear force at the obtuse corner to all of the beams but also states that that this correction is not necessarily conservative with respect to uplift at the acute corners and additional investigation should be done to determine the uplift on skewed structures (see Table 1-2) (AASHTO, 2012). See Figure 1-3 for how these equations behave with respect to the skew angle (using L = 40 ft., d = 20 in.).

Table 1-2: Corrections for Load Distribution Factors for Concrete Box Beams Used in Multi-Beam Bridges on Skewed Supports (AASHTO, 2012).

Load Distribution Factor Description	Correction Factor	Range of Applicability
Reduction for Moment in Longitudinal Beams	$1.05 - 0.25 * \tan\theta \le 1.0$	$0^0 \le \theta \le 60^0$ If $\theta > 60^0$ use $\theta = 60^0$
Correction for Support Shear of the Obtuse Corner	$1.0 + \dfrac{12.0 * L}{90 * d} * \sqrt{\tan\theta}$	$0^0 \le \theta \le 60^0$ $20 \le L \le 120$ $17 \le d \le 60$ $35 \le b \le 60$ $5 \le N_b \le 20$
Where: θ = skew angle (degrees) L = span of beam (feet) d = depth of beam or stringer (inch) b = width of beam (inch) N_b = number of beams, stringers, or girders		
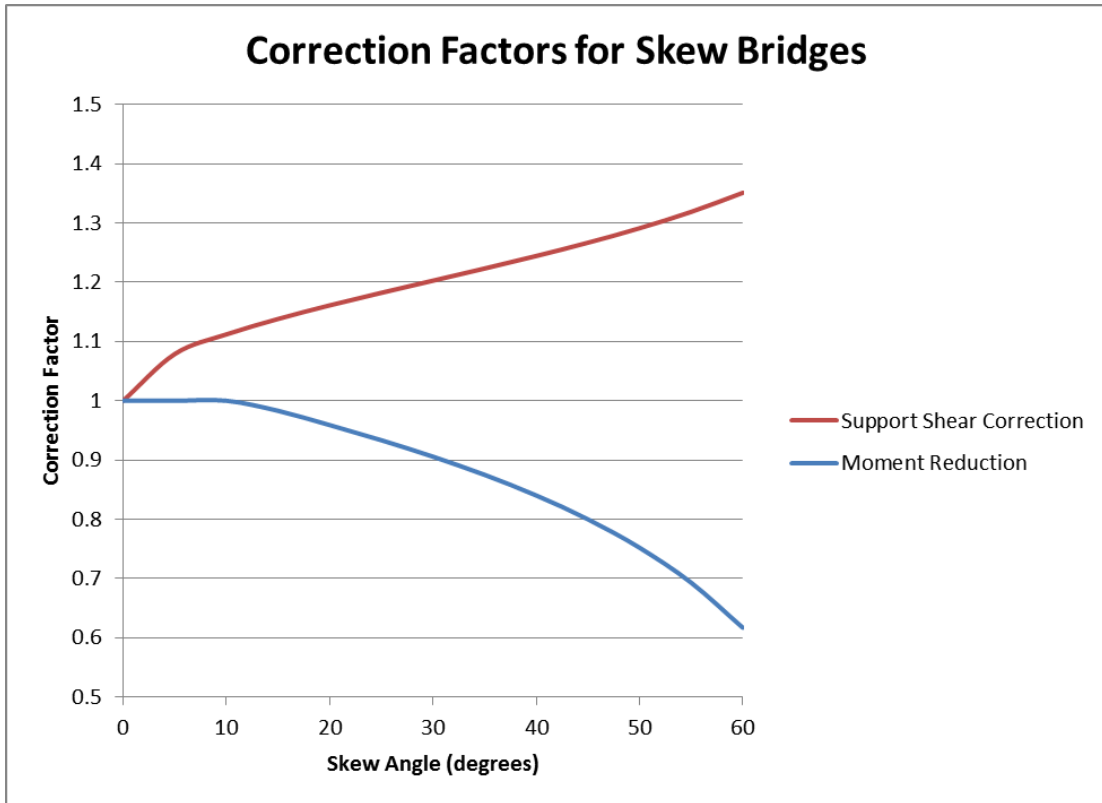
Figure 1-3: Corrections for Load Distribution Factors for Concrete Box Beams Used in Multi-Beam Bridges on Skewed Supports Based on L = 40 ft. and d = 20 in.

The torsional loads and deflections produced depend on the orientation of the diaphragms or transverse supports. For example, when the transverse supports are placed parallel to the skew, they connect longitudinally proportionate points along the beams which undergo consistent vertical deflections and thus can cause some lateral bending; while when the transverse supports are placed normal to the beams, they connect points on adjacent beams that are undergoing different vertical deflections and thus inducing some torsional loads in the beams (Coletti et al., 2011).

Thermal expansion effects should also be considered as the precast concrete slabs are often at least partially fixed to the abutments of the bridge. Because of their geometry, skewed bridges undergo differential thermal expansion unlike non-skewed

bridges. This causes the thermal movement of a skewed bridge to be asymmetrical, with the movement centered on a line between the acute corners of the skewed bridge as shown in Figure 1-4 (Coletti et al., 2011). Similar effects occur due to thermal contraction and shrinkage of the concrete (Precast/Prestressed Concrete Institute, 2003).
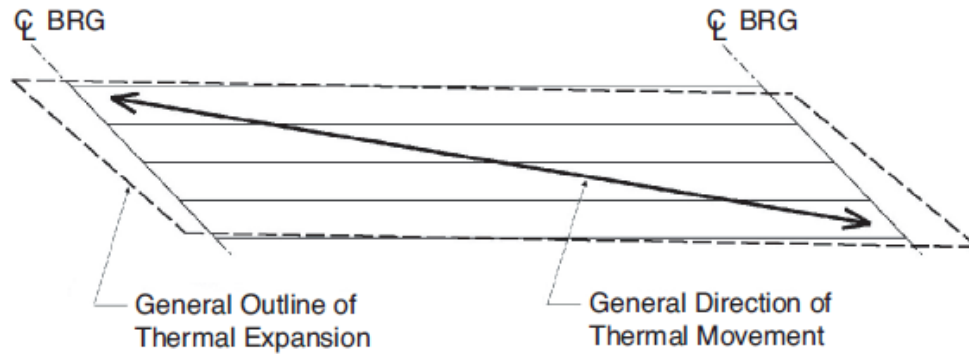
Figure 1-4: General Effect of Thermal Expansion on a Skewed Bridge (CL BRG = Centerline Bearing) (Coletti et al., 2011).

1.5.3 Methods to Avoid Skew Angles

Coletti et al. (2011) suggest multiple ways to eliminate or reduce skew in a proposed bridge design. These options include a change in roadway geometry, an increase in span length while moving the abutments to maintain horizontal clearance under the bridge, and the use of retaining walls to increase the possibility of using a normal abutment without concern of the abutment header slope encroaching on the horizontal clearance under the bridge. These alternatives should be evaluated with consideration to the cost of these changes versus the increasing cost and complexity of designing a skewed bridge. In addition, careful design of the post-tensioning near the skewed end can reduce the amount of load that the obtuse corner of a bridge

carries leading to an even distribution of the loads on the bearings (Oregon Department of Transportation, 2004).

1.6 Post-Tensioning Behavior

One important concept to consider concerning adjacent multi-beam bridges is shear friction. Discussed in section 11.6 of the American Concrete Institute (ACI) Building Code Requirements for Structural Concrete ACI 318-11 (2011), shear friction is to be applied where it is appropriate to consider shear transfer across a given plane, such as: an existing or potential crack, an interface between dissimilar materials, or an interface between two concretes cast at different times. Generally, steel reinforcement is placed across an area of anticipated cracking to increase the normal force to the crack. The reinforcement then acts as a clamp around the crack by creating friction to resist the shear (Badwan and Liang, 2007). The transverse post-tensioning placed on some precast multi-beam bridges, in combination with the shear keys, contributes to the shear friction produced between the adjacent precast beams and causes the beams to perform as a monolithic plate structure. This configuration, especially after a crack has occurred, helps ensure that stress is distributed among all of the adjacent beams and decreases the possibility of a single beam carrying the entire applied load.

Post-tensioning has previously been questioned as a useful tool for crack prevention due to the relatively low force some states use (about 30 kips) and the minimal amount of post-tensioning provided (2 or 3 strands). This small compression force (15 psi near the post-tensioning and 0 psi further from the post-tensioning) is not consistently applied to the shear keys and is miniscule compared to the

compressive force suggested to be provided at key points along the bridge, including the ends (Sharpe, 2007). Article 4.6.2.2 of the AASHTO LRFD specifications recommends a transverse post-tensioning stress of at least 0.25 ksi to sufficiently connect adjacent girders and suggests that post-tensioning is more effective than a structural overlay but does not give a depth over which the stress should be applied which may contribute to the variation in different states' practices (AASHTO, 2012, and Russell, 2011).

1.7 Crack Initiation and Occurrence

Cracks have often occurred in adjacent precast concrete multi-beam bridges, generally initiating due to high stresses near the supports instead of mid-span, possibly exasperated by trucks as they pass over the end of the bridge (Sharpe, 2007). Test results on a full-scale member of a multi-beam bridge system showed that cracks in the shear key developed due to thermal strains and propagated as the loads were applied (Badwan and Liang, 2007). This is further supported by observations of cracks on adjacent precast concrete multi-beam bridges occurring soon after construction was completed but before the bridges were opened for traffic. Early parametric finite element studies have also shown that secondary loads due to shrinkage of the shear key and overtopping slab or temperature changes are greater than the applied vehicular loads (Sharpe, 2007). These cracks generally have little effect on the load transfer between the beams if the transverse post-tensioning is intact but do cause problems due to leakage. It has been shown that composite deck slabs, full-depth shear keys, and transverse post-tensioning can reduce the stresses produced in the shear key with varying degrees of effectiveness (Sharpe, 2007, and

Russell, 2009). Full-depth shear keys can transfer transverse stresses more evenly between beams leading to less of a stress concentration at the bottom of the shear key than compared to partial-depth shear keys (Sharpe, 2007). Full-depth shear keys also been shown to reduce any hinge behavior that could occur with partial-depth shear keys, helping to transfer moments between beams (Sharpe, 2007). The Maryland state bridge design standards include the use of both composite deck slabs and transverse post-tensioning but do not include full-depth shear keys.

Chapter 2: Survey of State Practices for Transversely Post-Tensioned Bridges

2.1 Survey Methodology

A survey of state practices for constructing adjacent precast concrete multi-beam bridges was accomplished using each state's department of transportation website and the associated structures departments and bridge standards to compare with the bridge design standards used in Maryland (see Appendix A for source websites). The survey does not include the Maryland bridge design standards. Fewer than half of the states within the United States have adjacent precast concrete multi-beam bridge standards on their websites, and of those that do, not all have explicit standards for the following critical design elements: post-tensioning force, transverse tendon specifications, and skew particulars. Twenty states had some applicable specifications for adjacent precast concrete multi-beam bridges posted online, and seventeen states had some reference to skew limitations for this type of bridge. These are all current and relatively recent state standards with the oldest published in 2003 and the most recent in 2012.

2.2 Beam Types and Span Lengths

A few types of beams are used for adjacent precast concrete multi-beam bridges with different allowable span lengths. Box beams are the most commonly utilized beam type, but both voided and solid slabs are also used by different states for a variety of reasons. Maximum span lengths range from 50 feet to greater than

100 feet with spans between 20 feet and 80 feet being used most frequently (Russell, 2011).

2.3 Transverse Tendons

Because of the complexities of building transversely post-tensioned adjacent precast concrete multi-beam bridges, the post-tensioning specifications need to be fully detailed. The standards should include the following information about the transverse tendons: type, diameter, force, number, and location. Most, but not all, of the states surveyed included this information.

2.3.1 Type

There are basically only two types of post-tensioning tendons available to be used. States typically use unbonded strands which consist of six high tensile strength steel wires wrapped helically around a central wire or unbonded high strength steel threaded tie rods (bars) (Corven and Moreton, 2004). A few states use multi-strands, bonded strands, or bonded tie rods (Russell, 2011).

2.3.2 Diameter

The diameter of the transverse tendons generally ranges from 0.5 inches to 1.375 inches. States that use strands typically require a 0.6 inch diameter whereas tie rod requirements have wider range.

2.3.3 Force

States' standards include a large range of transverse post-tensioning force requirements. The majority of states use 30 kips, but the standards show a range from a minimum of 20 kips to a maximum of 120 kips.

2.3.4 Number and Location

As with the other transverse tendon specifications, the number and location of the tendons also varies from state to state. States require anywhere from one to ten transverse post-tensioning tendons with between two and four being most common. The tendons can be arranged in a variety of ways that include a regular discretization of the bridge span (i.e. locating tendons at the midspan, third points, quarter points, etc.) or specified distances (i.e. eleven feet apart). Figure 2-1 shows common ways to locate tendons depending on the number of tendons being used.
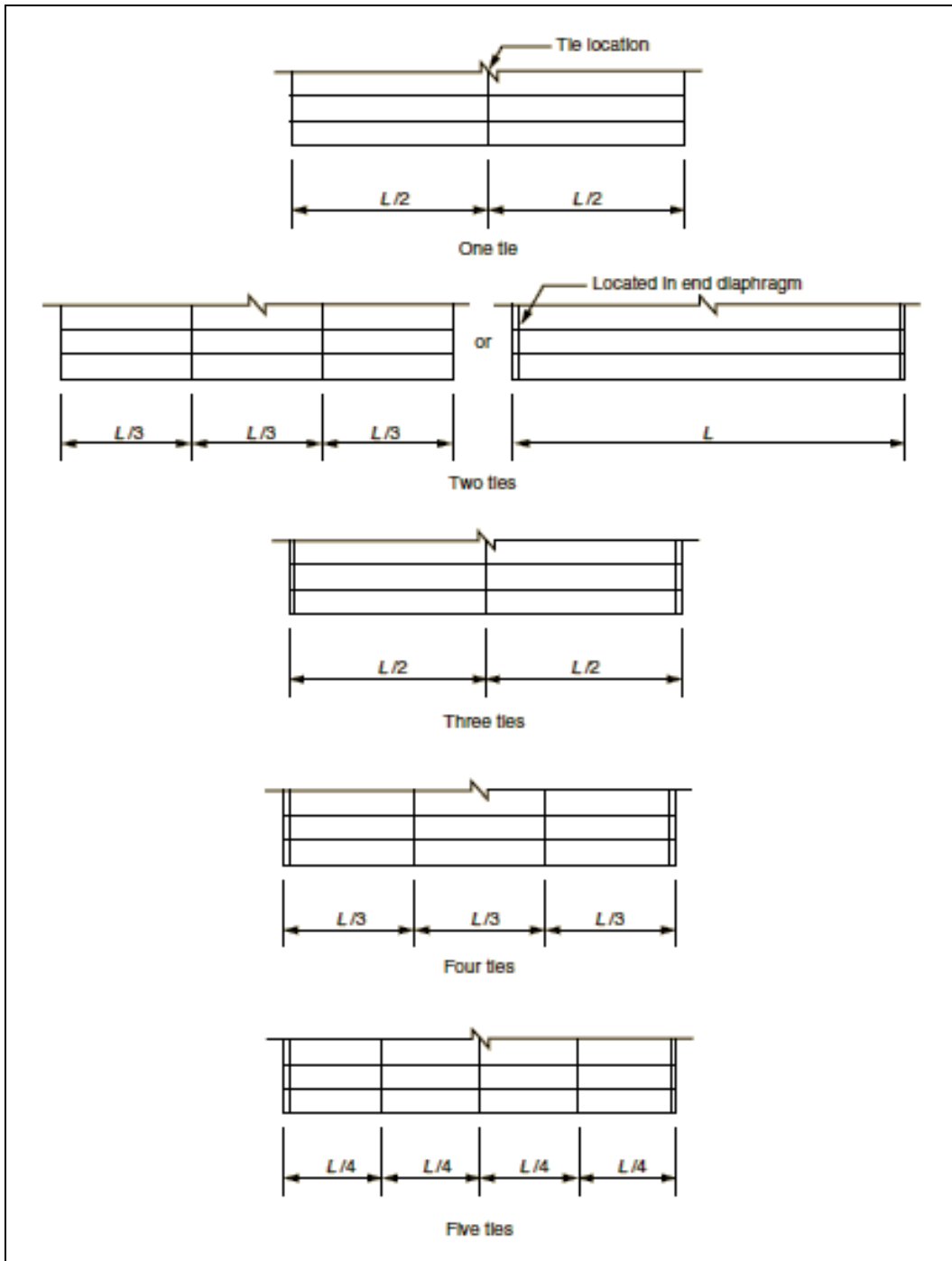
Figure 2-1: Common Transverse Post-Tensioning Tendon Locations Based on the Number of Ties (Russell, 2011). (Note: L = Length of Span)

2.4 Skew Specifications

In addition to specifying the requirements for the transverse post-tensioning, states standards should also include limitations for skewed bridges. The skew angle often determines both the transverse tendon orientation as well as whether the adjacent precast concrete multi-beam bridge is permitted to be constructed.

2.4.1 Tendon Orientation

The transverse tendons will transfer the applied loads to the connected concrete beams in different ways depending on their orientation. The tendons can either remain normal to the beams and staggered throughout the cross-section of a skewed bridge, or they can be placed parallel to the bridge's skew angle. A staggered orientation is often easier to install but it connects the beams at different relative distances along the beams. Though more difficult to install, tendons with a skewed orientation connect the beams at their same relative points thus making the bridge deformation behave more similarly to a normal bridge. Figure 2-2 shows the possible transverse tendon orientations and the corresponding possible diaphragm construction possibilities for box beams or voided slabs.
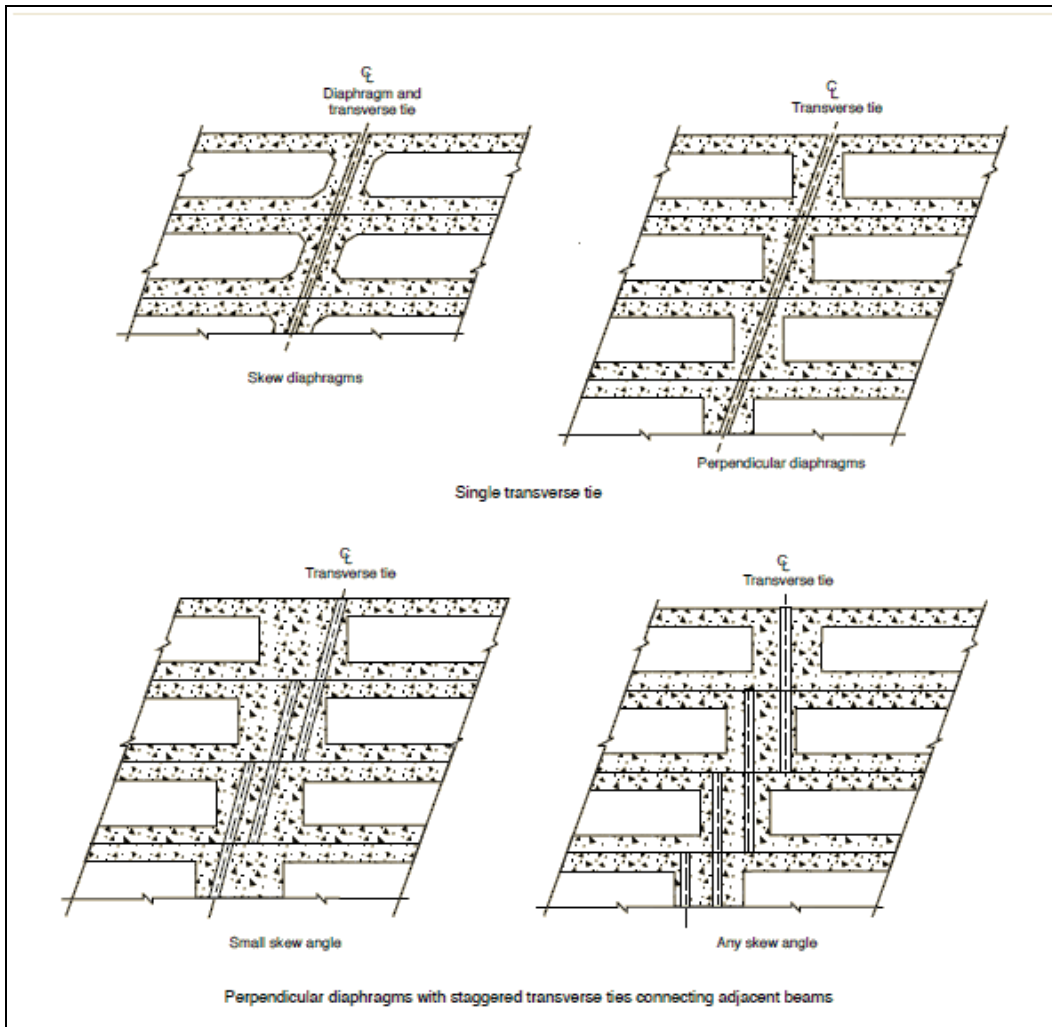
Figure 2-2: Transverse Tendon Orientation and Diaphragm Construction Possibilities (Russell, 2011).

2.4.2 Orientation Parameters

Both the skew angle and the span length affect the transverse tendon orientation practices as well as whether or not the bridge is permitted to be constructed. Most states recommend that the transverse tendons be built parallel to the skew when the skew angle is less than 20^0 or 30^0. Some states recommend placing the transverse tendons normal to the beams and staggered at skew angles greater than 20^0 or 30^0, while some restrict the maximum allowable skew angle to

30^0. Again, there is a wide variation in different states' practices as confirmed by a similar survey's findings shown in Figure 2-3. A summary of the skew specifications survey is shown in Table 2-1.
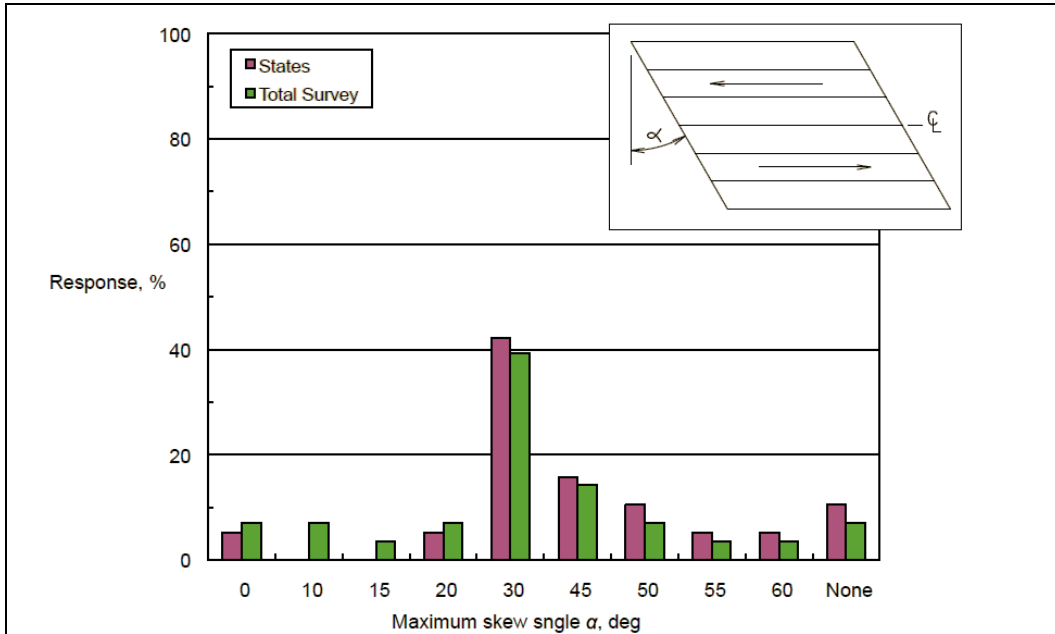
Figure 2-3: Alternate Survey Results for Maximum Skew Angle Specification (Russell, 2011).

Table 2-1: Summary of 17 States' Transverse Post-Tensioning Specifications for Skewed Adjacent Precast Prestressed Concrete Multi-Beam Bridges.

Skew	Placement of Transverse Ties	
	Parallel to Skew	Normal and Staggered
$\leq 20^0$	3	0
$\leq 30^0$	6	1
	Do Not Build	Normal and Staggered
$> 20^0$	0	3
$> 30^0$	8	3
$> 45^0$	2	0

2.5 Full Survey Results

The full survey results are shown in Tables 2-2 and 2-3.

Table 2-2: States' Transverse Post-Tensioning Specifications for Single Span Precast Prestressed Concrete Beam Bridges.

State	Beam Type (BB = Box Beam; SS = Solid Slab; VS = Voided Slab)	Span (ft)	Transverse Ties					Year
			Type	Diameter (in)	Force (kips)	Location	Number	
AZ	BB, VS	< 50	Tie rod	1.5	30	Midspan	1	2007
	BB, VS	50 - 75	Tie rod	1.5	30	Third Points	2	
	BB, VS	> 75	Tie rod	1.5	30	Quarter Points, Midspan	3	
CT	BI & BI Mod. BB, VS	≤ 50	Strand		30	Ends, Midspan	3	2003
	BI & BI Mod. BB, VS	> 50	Strand		30	Ends, Third Points	4	
	BII BB, VS	≤ 75	Strand		30	Ends, Third Points	4	
	BII BB, VS	> 75	Strand		30	Ends, Quarter Points	4	
	BIII BB, VS	≤ 75	Strand		30	Ends	2	
	BIII BB, VS	> 75	Strand		30	Ends, Quarter Points	4	
	BIV & BIV Mod. BB, VS	ALL	Strand		30	Ends, Quarter Points, Midspan	5	
DC	BB, VS		Strand or Tie rod	0.5 - 1.375				2009
IN	BB		Tie rod	1	20			2011
KY	BB	≤ 50	Tie rod	1	20	Midspan	1	2008
	BB	> 50	Tie rod	1	20	Third Points	2	
MA	BB	≤ 50	Strand	0.6	44	Ends, Midspan	3	2009
	BB	> 50	Strand	0.6	44	Ends, Quarter Points, Midspan	5	

State	Beam	Span	Type	Size	No.	Location	Count	Year
MI	BB	≤ 50			120	Ends, 2 at Center of Span (11 ft. apart)	4	2011
	BB	50 - 62			120	Ends, Quarter Points, Midspan	5	
	BB	62 - 100			120	Ends, Quarter Points, 2 at Center of Span (11 ft. apart)	6	
	BB	> 100			120	Ends, All Fifth Points	7	
NY	BB, SS, VS	≤ 50	3 Strands	0.5	28	Ends, Midspan	3	2011
	BB, SS, VS	> 50	3 Strands	0.5	28	Ends, Quarter Points, Midspan	5	
NC	BB, VS		Strand	0.6	44			2012
OH	BB	≤ 50	Tie rod	1		Midspan	1	2011
	BB	50 - 75	Tie rod	1		Third Points	2	
	BB	> 75	Tie rod	1		Quarter Points, Midspan	3	
PA	BB	≤ 45				Ends	2	2011
	BB	45 - 55				4 ft. from Ends	2	
	BB	55 - 77				16 ft. from Ends	2	
	BB	> 77				16 ft. from Ends, Midspan	3	
OR	BB, SS		Tie rod	7/8				2011
RI	VS	58	Strand	0.6	44	Ends, Midspan	3	2010
	BB	≤ 50	Strand	0.6	44	Ends, Midspan	3	
	BB	> 50	Strand	0.6	44	Ends, Quarter Points, Midspan	5	
	BB	≤ 50	Strand	0.6	44	Ends, Midspan (2 stacked for depth > 33 in.)	6	

State	Girder	Span	Method	Value	Num	Location	Count	Year
	BB	> 50	Strand	0.6	44	Ends, L/4 (2 stacked for depth > 33 in.)	10	
SC	VS		Strand or Tie rod	0.5	30			2007
	VS	30, 40, 50, 60	Tie rod	1.25		Third Points	2	2010
	VS	70	Tie rod	1.25		Quarter Points, Midspan	3	
TX	SS	40, 50	Strand	0.5				2012
	BB	max: 60-100	Strand	0.5				
VT	BB, VS	≤ 50	Strand	0.6	30			2011
	BB	50 - 90	Strand	0.6	30			2010
WA	BB, VS, SS		Strand	0.6		Ends, Midspan	3	2012
WV	BB	20 - 94	Strand	0.6	80			2004
WI	BB	≤ 24	Strand	0.6	86.7	Ends, Quarter Points, Midspan	5	2012
	BB, VS	24 - 92	Strand	0.6	86.7	Ends, Quarter Points, Midspan	5	
WY		≤ 40	Strand	0.6				2008
		40 - 80	Strand	0.6		Midspan	1	
		> 80	Strand	0.6		Third Points	2	

Table 2-3: States' Transverse Post-Tensioning Specifications for Skewed Precast Prestressed Concrete Beam Bridges Based on Skew Angle.

State	Skew	Placement of transverse reinforcement
AZ	$\leq 20^0$	Parallel to abutments and piers
	$> 20^0$	Normal to girders and staggered
CT	$\leq 30^0$	Parallel to abutments and piers
	$> 30^0$	Normal to girders and staggered
DC	$\leq 30^0$	Parallel to abutments at ends, normal to girders at midspan
	$> 30^0$	Do not build
IN	$\leq 25^0$	Parallel to abutments and piers
	$> 25^0$	Normal to girders and staggered
KY	$\leq 10^0$	Parallel to abutments and piers
	$> 10^0$	Normal to girders and staggered
NY	$\leq 50^0$	Parallel to abutments and piers
	$> 50^0$	Do not build
OH	$\leq 4^0$	Parallel to abutment (4 ft. wide beams)
	$\leq 5^0$	Parallel to abutment (3 ft. wide beams)
	4^0 - 30^0	Normal to girders and staggered (4 ft. wide beams)
	5^0 - 30^0	Normal to girders and staggered (3 ft. wide beams)
	$> 30^0$	Do not build
PA	$> 20^0$	Do not build if span > 131ft
	$> 30^0$	Do not build if span > 88ft
	$> 45^0$	Do not build
OR	$> 30^0$	Do not build if precast box
	$> 45^0$	Do not build if precast slab
RI	$> 30^0$	Do not build unless authorized by engineer
SC	$\leq 30^0$	Consider as straight bridge
TX	$> 30^0$	Do not build
VT	$> 30^0$	Fill the clipped void with foam filler prior to the overlay placement or using the overlay concrete to fill the void
	$> 45^0$	Do not build
WA	$\leq 30^0$	Parallel to abutments and piers
	$> 45^0$	Do not build
WV	$\leq 25^0$	Parallel to abutments and piers
	$> 25^0$	Normal to girders and staggered
WI	$\leq 30^0$	Parallel to abutments and piers
	$> 30^0$	Not recommended, Normal to girders and staggered if built
WY	$\leq 20^0$	Parallel to abutments and piers
	$> 20^0$	Normal to girders and staggered

Chapter 3: Field Testing Methodology and Results

3.1 Test Bridge Description

3.1.1 Summary of Test Bridge

The Maryland State Highway Administration (MDSHA) requested that the BEST Center at the University of Maryland, College Park, test one of five recently constructed transversely post-tensioned adjacent concrete slab bridges that were found to have cracks on their top surfaces to determine the cause or causes of the cracks and propose revisions and/or additions to the Maryland Bridge Standards. The test bridge selected is Structure No. 10381XO, a transversely post-tensioned prestressed concrete slab panel bridge built in 2007 and located in Knoxville, Maryland, on MD Route 180 crossing over a tributary of the Potomac River. It is a two-lane simply-supported single span bridge with a 22'-3.125" span and a 31.4° skew angle. The superstructure consists of eight adjacent 4'-0" wide x 1'-3" high x 23'-4.125" long prestressed concrete beams and a typical 5" minimum thick composite concrete deck. A 2'-0" wide x 3'-11" high concrete barrier parapet is located on each exterior slab along the entire length of the bridge.

3.1.2 Bridge Specifications

The eight concrete slabs were precast and prestressed to have a minimum 28-day strength of f'_c = 7,000 psi and a minimum compressive strength at the transfer of prestress of f'_{ci} = 5,800 psi. The pretensioning steel strands were Grade 270 0.5" diameter 7-wire bright low relaxation strands pretensioned to 31,000 lbs. All of the

reinforcing steel used was Grade 60. Each end of the slabs is supported by two 1"

thick elastomeric bearing pads with a design load of 36 kips.

The slabs were transversely post-tensioned using four 1" diameter tie rods

tensioned to 80 kips. The tie rods were staggered and placed normal to the beams in

2.5" diameter holes precast in the slabs. Two tie rods were placed at approximately

the third-points of the bridge 7' apart, each integrating five beams (one integrating

beams one through five; the other integrating beams four through eight). Two more

tie rods were placed 7' from the third-point tie rods towards the acute corners of the

bridge, each integrating three beams (one integrating beams one through three; the

other integrating beams six through eight). See Figure 3-1 for a schematic of the

post-tensioning placement.
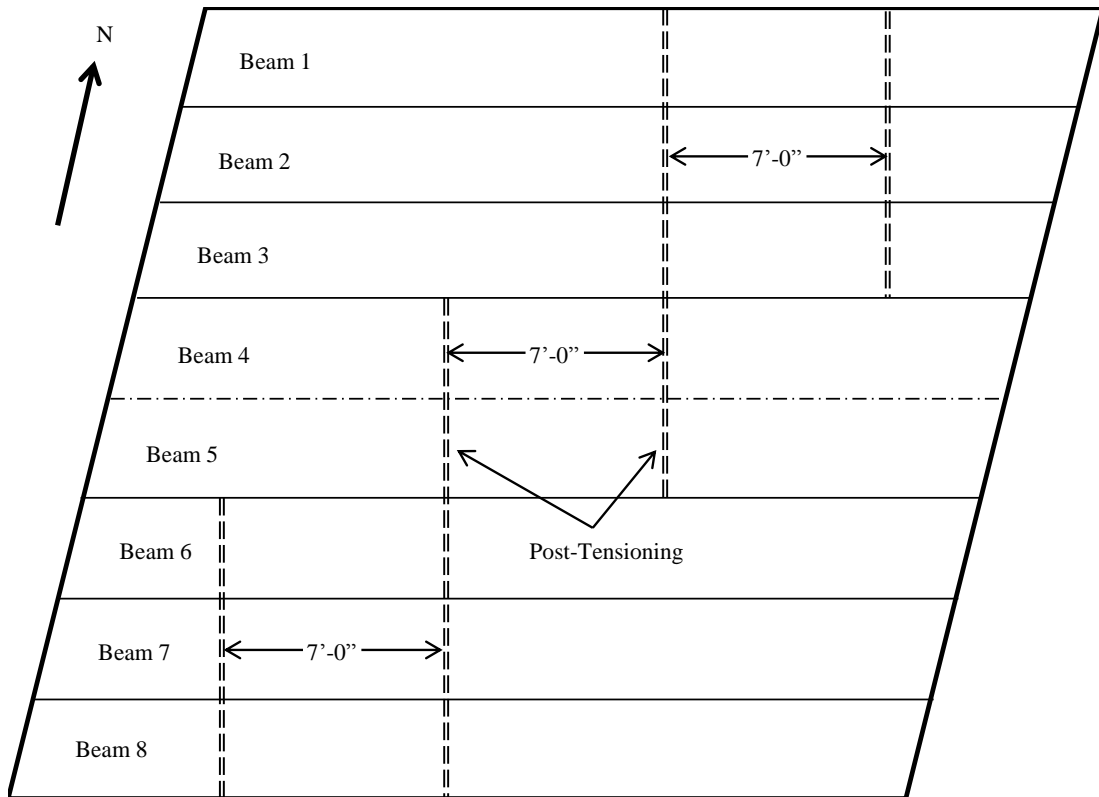
Figure 3-1: Locations of the Post-Tensioning Tie-Rods on the Knoxville Bridge.

The tie-rod bolt recesses were then grouted using nonshrink grout while the post-tensioning remained unbonded to the surrounding slabs. The slabs were then connected longitudinally with partial-depth (7.25" deep) shear keys using nonshrink grout.

3.1.3 Reasons for Construction and Testing

The old bridge at this location was an 18'-0" single-span concrete girder bridge that had been built in 1910. The bridge was replaced due to age and traffic conditions at the site. The available options were limited due to the private properties restricting the available area on all sides as well as the shape and depth of the Potomac tributary. To minimize traffic disruption and because of the limitations of the bridge site, a transversely post-tensioned adjacent concrete slab bridge with a skew angle of 31.4^0 was decided upon. Within three or four years of being built, longitudinal cracking was found on the top surface of the concrete overlay of the new bridge initiating MDSHA's request that testing be done to determine the cause or causes of the cracking.

3.1.4 Bridge Photos and Plans

The longitudinal cracking on the top surface of the Knoxville bridge can be seen circled in yellow in Figures 3-2 to 3-5. A clear pattern emerges when viewing the cracks – the cracks initiate perpendicular to the abutment, travel a couple of feet, then reorient to travel parallel to the bridge beams and seem to follow the shear keys between the slabs. Figures 3-6 and 3-7 show that no leakage was occurring on the underside of the bridge, indicating that the longitudinal reflective cracks on the top surface were probably not yet full depth and not affecting the steel reinforcement and

post-tensioning in the bridge. All of the relevant sheets from the Knoxville bridge plans pertaining to the major structural elements of the bridge superstructure are included in Appendix B.

Figure 3-2: Longitudinal Crack on the Top Surface of the Knoxville Bridge.

Figure 3-3: Longitudinal Crack on the Top Surface of the Knoxville Bridge.

Figure 3-4: Longitudinal Cracks on the Top Surface of the Knoxville Bridge.
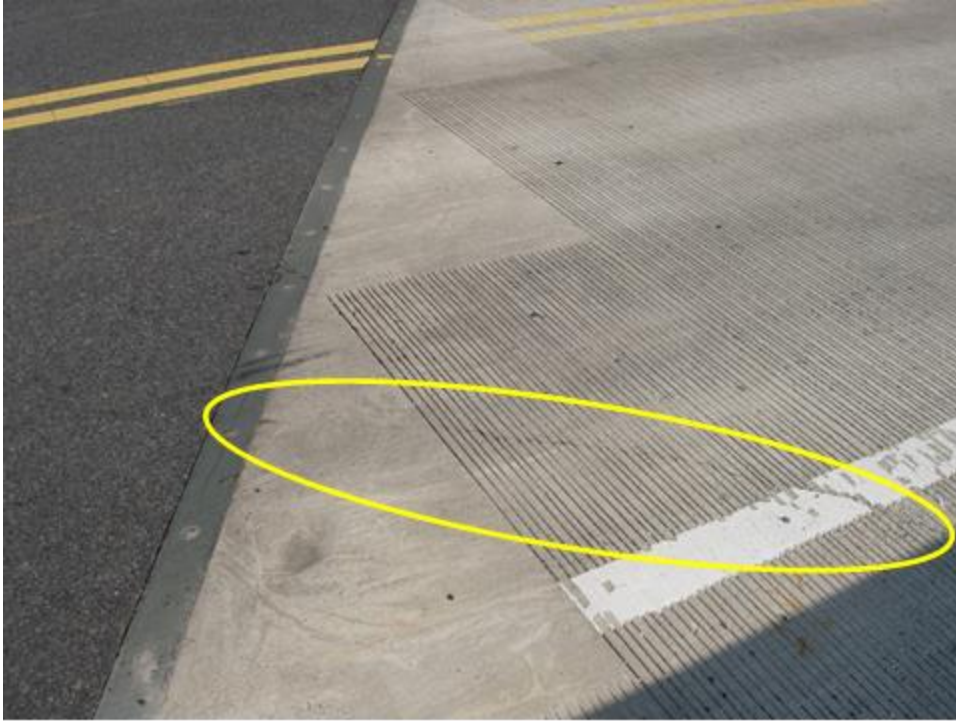
Figure 3-5: Longitudinal Crack on the Top Surface of the Knoxville Bridge.

Figure 3-6: View of the Bottom Surface and the East Abutment of the Knoxville Bridge.

Figure 3-7: View of the Bottom Surface and West Abutment of the Knoxville Bridge.

3.2 Instrumentation Plan

3.2.1 Summary of Instrumentation Plan

An instrumentation and testing plan was formulated to observe the short-term live load strains on the bottom and top surfaces of the bridge due to a testing vehicle driving over. Eight Bridge Diagnostic Inc. (BDI) strain transducers (strain gauges/sensors) were chosen to acquire the live load strains. The sensors were placed at approximately the same locations on the top and bottom surfaces of the bridge with the same orientations so as to determine the strains where the cracks were occurring. A Campbell Scientific data acquisition instrument in coordination with a software program run on a laptop computer was used to obtain the strain data from the sensors.

3.2.2 Strain Gauge Locations

The strain gauge locations were selected based on three important criteria: first, the necessary locations to characterize the bridge behavior; second, the locations of the longitudinal cracks in the bridge; and third, the ease of accessing similar points on the underside of the bridge. The cracks on the top surface of the bridge that corresponded in location with accessible area on the underside of the bridge were chosen for the sensor locations. One BDI sensor was placed on the top surface of the bridge parallel to the abutment across a crack near where the abutment supported the beams (#1644) with a corresponding sensor on the bottom surface of the beams (#3213). Two more BDI sensor were placed on the top surface of the bridge, one normal to the beams across another longitudinal crack (#1643) and one close by but parallel to the beams (#1641), with two more sensors placed approximately in the corresponding positions on the underside of the bridge (#3214 and #3215, respectively). The last two BDI sensors were placed on the underside of the bridge, one normal and across beams 6 and 7 and the other parallel to the beams on beam 3. A gauge location schematic and photos of the strain gauges on the bridge are shown in Figures 3-8 to 3-10.
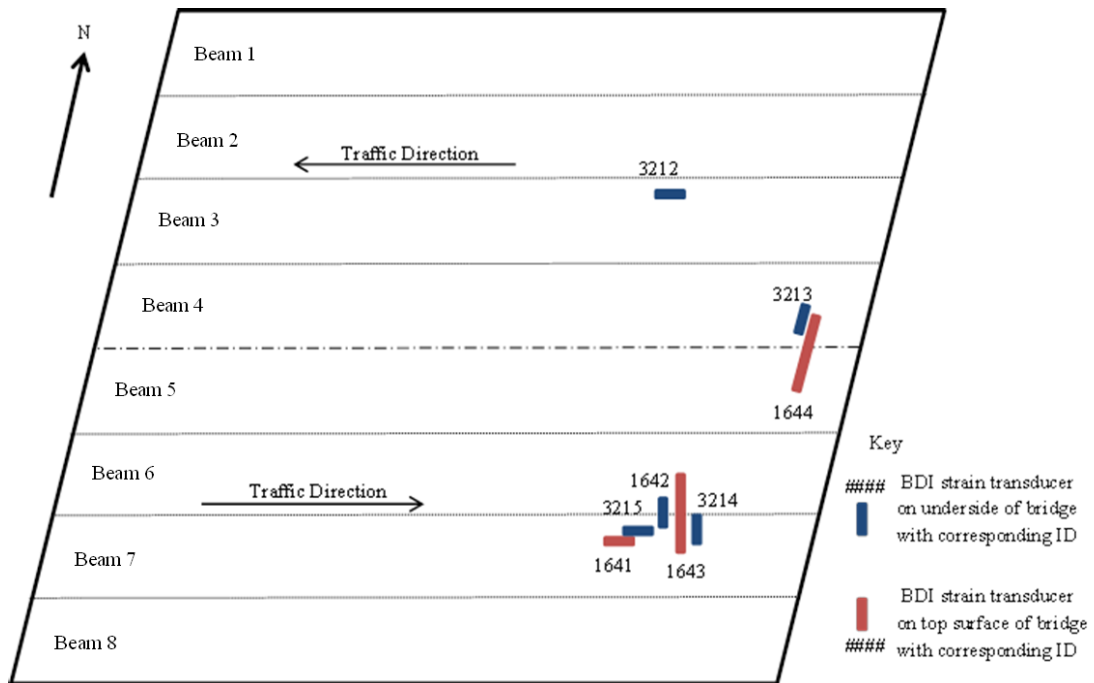
Figure 3-8: Strain Gauge Locations on the Knoxville Bridge.

Figure 3-9: Location of BDI Sensors on the Bottom Surface of the Knoxville Bridge.
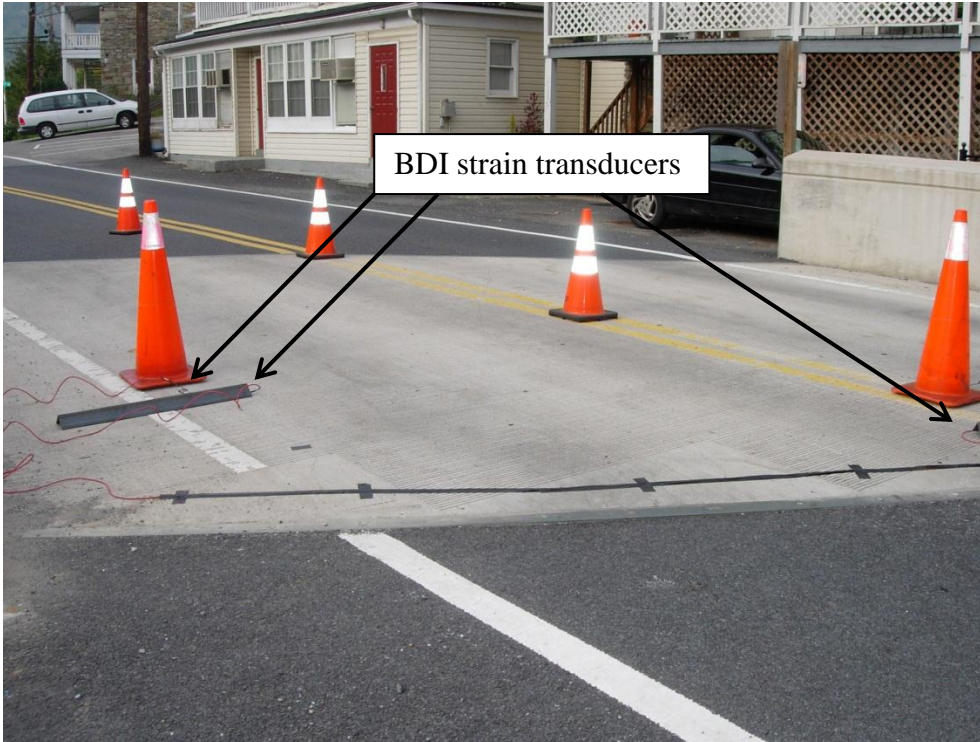
Figure 3-10: Location of BDI Sensors on the Top Surface of the Knoxville Bridge.

3.2.3 Instrumentation Setup

The instrumentation setup for the live load test consisted of multiple components. Eight prefabricated BDI sensors were connected to the Campbell Scientific CR5000 data logger. The CR5000 was powered by a small generator and connected to a laptop computer which was running the PC9000 software. The connections from the sensors to the data logger were correctly made on the same day as the field test and checked using a multi-meter and preliminary test runs. The data was recorded to the CR5000 and transferred using the PC9000 to the computer. A schematic of the data acquisition network and a photo of it during operation are shown in Figures 3-11 and 3-12; further descriptions of each component of the system are provided in the following section.

Testing Truck   Sensors   Generator

Bridge

CR5000   User

                                              Laptop
                                              Computer
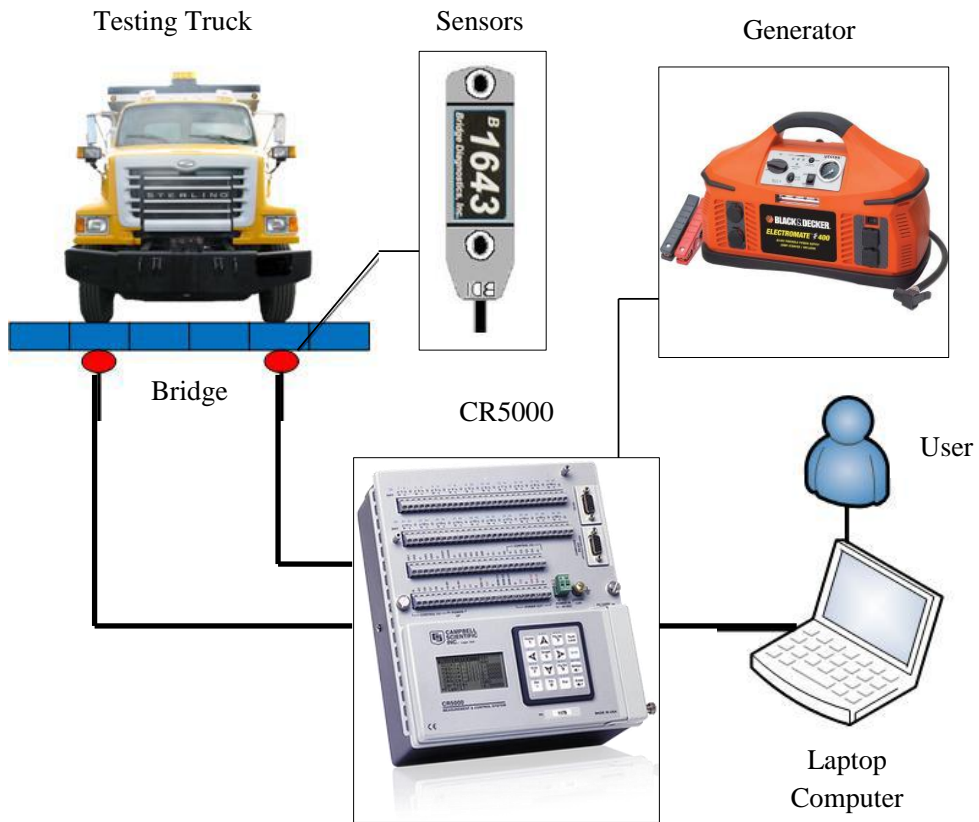
Figure 3-11: Data Acquisition Network (Jeong, 2009).

Figure 3-12: Data Acquisition System Monitoring the Strain Gauges During the Live Load Test.

3.3 Data Acquisition Network

3.3.1 Strain Gauge Description, Resistance, Strain, and Installation

Simple strain gauges operate on a relatively basic principle, that the resistance of a foil strain gauge is directly proportional its deformation (the amount of strain it is undergoing). When a load is applied to a structure, the attached strain gauges undergo a length deformation which changes the electrical resistance of the strain gauge. This resistance can then be directly correlated with the amount of deformation the gauge is undergoing, which (using the strain gauge's length) can be used to calculate the amount of strain in the gauge and therefore the amount of strain on the structure at the point where the gauge is located. A circuit arrangement known as the Wheatstone bridge is used to detect these small changes in resistance. This data – the changes in resistance, the corresponding deformation calculation, and the strain calculation – is recorded and can be used for further analysis or corrections. For a visual representation of the operation of a strain gauge and the Wheatstone bridge circuit, see Figures 3-13 and 3-14.
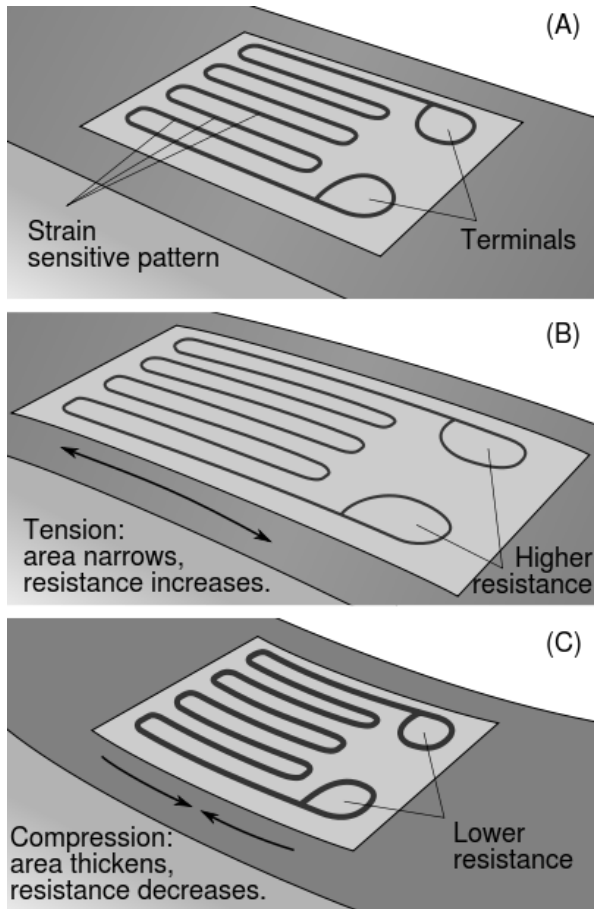
Figure 3-13: Strain Gauge Operation Concept ("Strain Gauge").
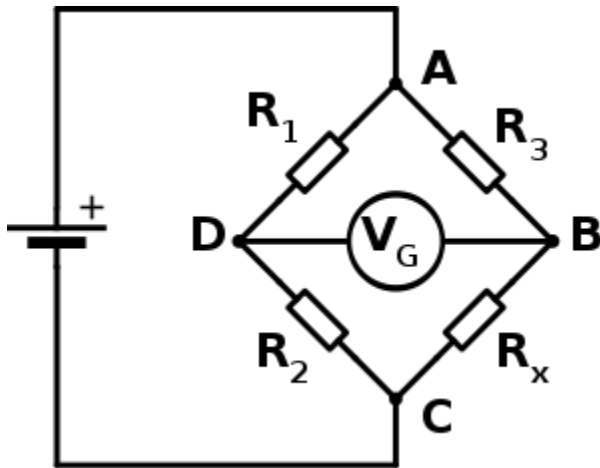
Figure 3-14: Wheatstone Bridge Circuit Used to Measure an Unknown Electrical Resistance ("Wheatstone Bridge").

In this case, it was most important to accurately measure the concrete strain on the bridge deck, so BDI strain transducers were chosen over other common strain gauges (such as Vishay strain gauges) because of their durability, ease of installation and use, and reusability. BDI strain transducers are highly accurate, prefabricated, pre-wired, rugged, weather-resistant, water-proof, reusable strain gauges made using a full Wheatstone bridge circuit with four active 350Ω foil gauge resistors and compatible with most data acquisition instruments. They are often used to measure strain in civil structures because they have a quick installation time (less than five minutes in some circumstances) and can be attached to a wide range of materials, including steel, polymers, timber, and concrete, using a variety of attachment methods, including mounting tabs and adhesives, weldable tabs, C-clamps, masonry or wood screws, and concrete anchors. The strain transducers have an effective gage length of three inches but aluminum extensions can be attached to increase their effective gage length in three inch increments all the way to two feet to average strain over greater distances. They have a strain range of ± 2000 $\mu\varepsilon$ with a sensitivity of 500 $\mu\varepsilon$/mV/V and an accuracy of less than $\pm 1\%$ (Bridge Diagnostics, Inc.). See Figures 3-15 to 3-17 for the BDI strain transducer dimensions and photos of the strain gauges installed on the bridge.
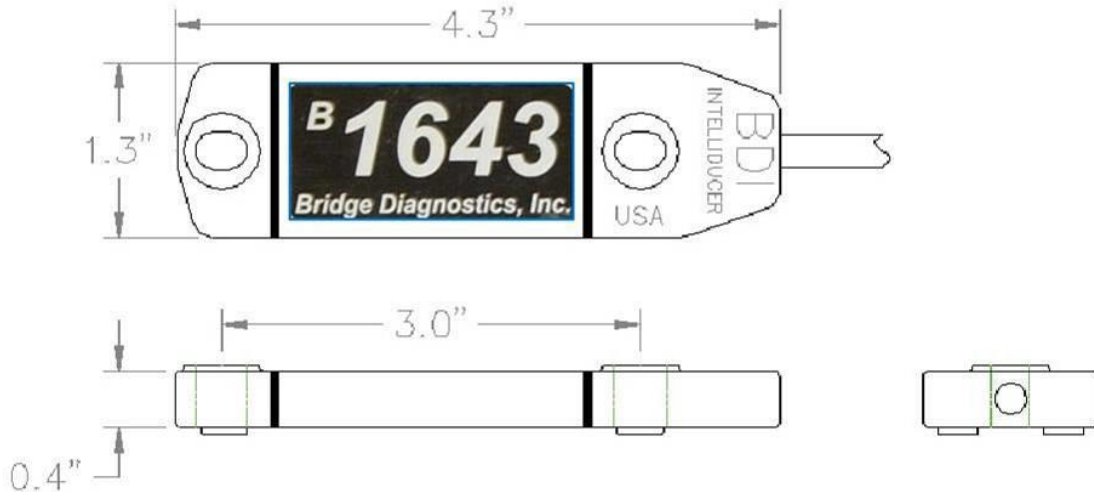
Figure 3-15: Bridge Diagnostics, Inc. (BDI) Strain Transducer Dimensions (Jeong, 2009).
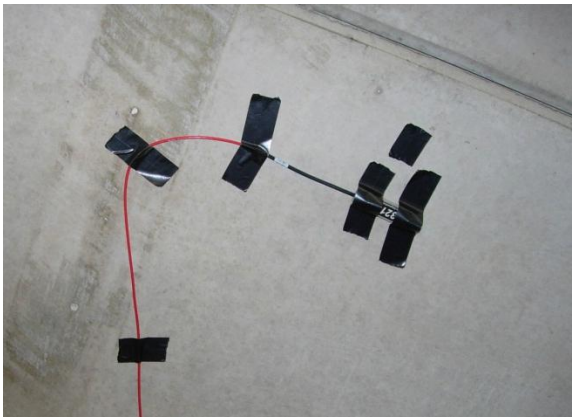
Figure 3-16: A BDI Strain Transducer Installed on the Bottom Surface of the Knoxville Bridge.
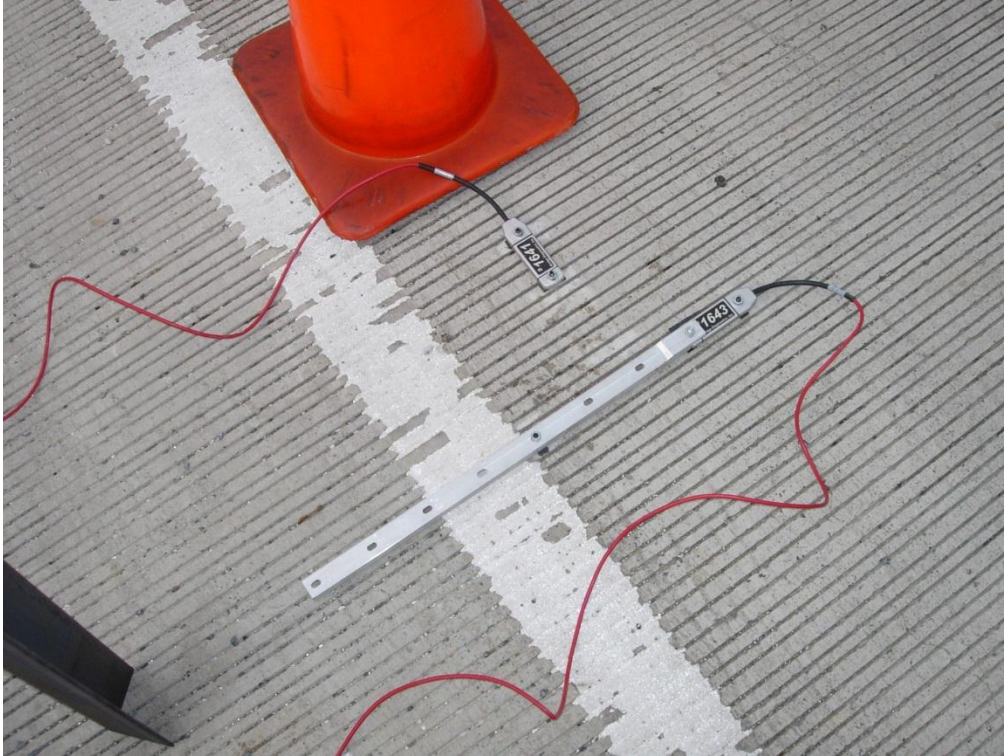
Figure 3-17: Two BDI Strain Transducers Installed on the Top Surface of the Bridge (BDI #1643 with an Extension Bar, BDI #1641 without an Extension Bar).

3.3.2 Campbell Scientific CR5000 Data Logger

For the live load field testing, the Campbell Scientific CR5000 Measurement and Control System was used to record the data obtained from the BDI strain transducers. The CR5000 is a rugged, high performance data acquisition system that can be used as an excitation source for sensors as well as recording data at a maximum rate of 5000 Hz (5000 measurements per second). It has twenty differential individually configured inputs that can be used for a wide variety of different sensor types, including strain gauges. See Figure 3-18 for a photo of the CR5000.

Figure 3-18: Campbell Scientific CR5000 Data Logger.

3.3.3 Dell Laptop with PC9000 Software

A computer is used to download the required operating code to the CR5000 using the PC9000 software for a Windows operating system. The software provides the user with various functionalities including, but not limited to, writing and compiling the required programming code, downloading it to the CR5000, confirming the CR5000's status, monitoring real-time data and the response of the attached sensors, graphing, and retrieving the data stored on the CR5000. The PC9000 software provides most of the communication functions between a computer and the CR5000.

3.4 Field Testing Procedure

3.4.1 Installation and Setup

The eight BDI sensors were installed on the testing bridge by the research team from the University of Maryland over the course of two days (October 10-11, 2011). The sensor locations were decided upon, marked, and the sensors located on the underside of the bridge installed on the first day. The sensors located on the top surface of the bridge were installed and the bridge testing was accomplished on the second day. The sensors were mounted on the bridge, connected to the data logger, and tested to confirm the proper connections. MDSHA provided the live load testing vehicle and maintenance of traffic during the testing.

3.4.2 Test Vehicle

The pre-weighted test vehicle was a two-axle dump truck provided by MDSHA and weighing 26,420 pounds. It weighed 5,200 pounds in each front wheel and 8,010 pounds in each rear tandem. The driver was instructed to drive across the bridge a total of eight times (four times in each direction) at varying speeds to obtain live-load strain data for the bridge. See Figures 3-19 and 3-20 for photos of the test vehicle.

Figure 3-19: Test Vehicle Provided by MDSHA Traveling Westbound across Knoxville Bridge.

Figure 3-20: Test Vehicle Provided by MDSHA Traveling Westbound across Knoxville Bridge.

3.4.3 Live Load Test

The test vehicle performed a total of eight runs across the test bridge for the live load test. The odd numbered runs (1, 3, 5, and 7) were made with the test vehicle driving east-bound across the bridge (i.e. on beams 5, 6, and 7). The even numbered runs (2, 4, 6, and 8) were made with the test vehicle driving west-bound across the bridge (i.e. on beams 2, 3, and 4). Runs 1, 2, 7, and 8 were made with the test vehicle driving at "crawling speed" (approximately 1 mph). Runs 3 and 4 were made with the test vehicle traveling at approximately 5 mph, and runs 5 and 6 were made with the test vehicle traveling at approximately 20 mph. Runs 3 through 6 were made to confirm that strain data obtained was consistent for a low range of varying speeds. The CR5000 collected the strain data at a rate of 2 Hz (2 per second).

The PC9000 program was used to retrieve the raw data from the CR5000. That data included both the resistance values of the BDI strain transducers as well as the calculation using a gage factor for each sensor to determine the strain. The strain data obtained was then plotted on graphs for a simple comparison and confirmation that the strain data was consistent and reliable among the multiple runs. Portions of the data for specific sensors were taken, further analyzed, and plotted using corrections for initial values and sensor drift. Most of the data included two peaks, corresponding to when the test truck's front axle and rear axle crossed near the location of each respective BDI sensor. Temperature effects were disregarded due to the short duration of each test run made by the testing truck (less than 30 seconds each time). The final results of the data are described in the following section.

3.5 Field Testing Results

3.5.1 Maximum Strain

Some of the maximum strain data acquired from the field test of the Knoxville bridge are listed in Table 3-1 along with the corresponding run number that the data was obtained from. A maximum strain for each sensor and for each direction of the test truck's runs is listed. The positive strain values indicate tensile strain; the negative strain values indicate compressive strain. The large strain values recorded by BDI sensor #1642 resulted from this sensor being placed transversely across two beams on the bottom surface of the bridge thus being affected by both the strain in each beam as well as any possible differential displacement of the beams. Though not all of the BDI sensors recorded significant strains because of their locations, the maximums are listed here for comparative purposes.

Table 3-1: Some Maximum Strain Data Results Obtained from the Field Test.

BDI Identification Number	microstrain	Run Number
1641	-0.5	8
	-5.85	1
1642	67.84	1
	-12.73	2
1643	1.01	2
	-5.25	1
1644	0.72	7
	-1.46	2
3212	3.14	2
	-0.37	1
3213	1.47	2
	-1.35	1
3214	-0.15	2
	-1.03	1
3215	4.06	1
	0.76	2

3.5.2 Strain Curves

The strain data was also plotted to view significant similarities or differences. The strain data from BDI sensors #1641 and #3215 located parallel to the beams on the top and bottom of beam 7, respectively, is shown in Figure 3-21. As can be seen, the data from the two respective runs in the same direction show both similar shapes and similar magnitudes with opposite signs (positive vs. negative) corresponding to the tension and compression that the bottom and top of the bridge, respectively, was experiencing during the live-load testing as expected.
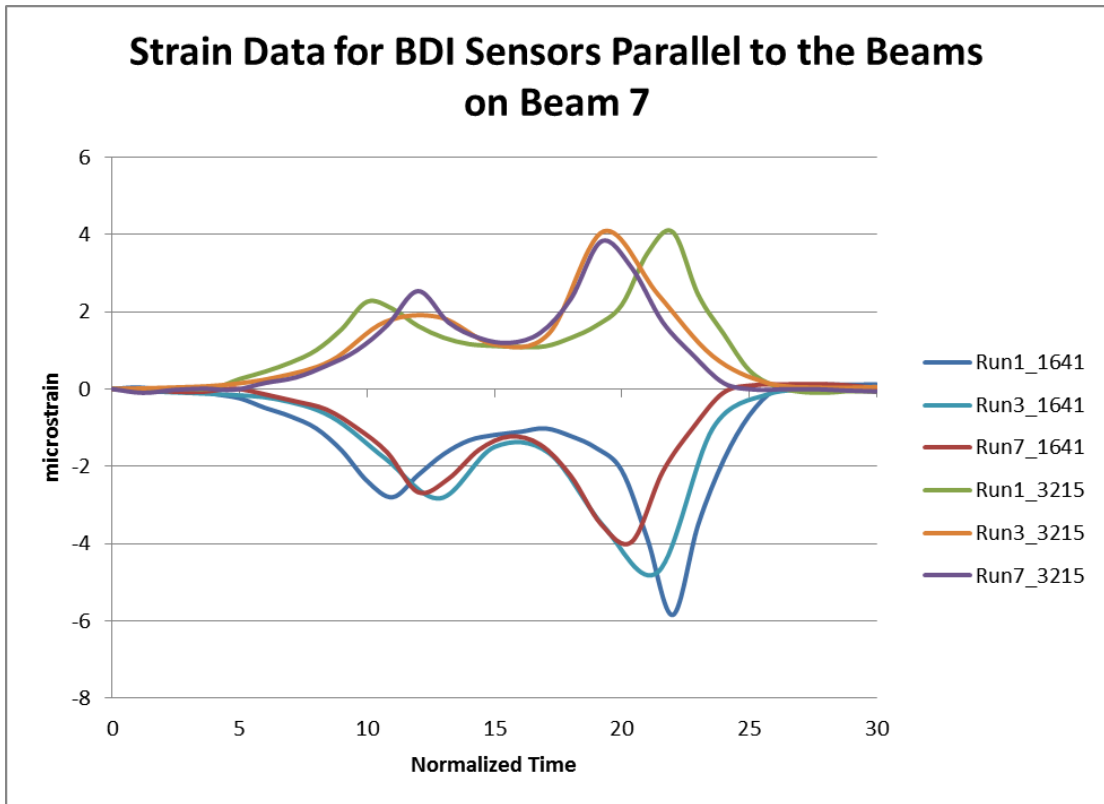
Figure 3-21: Strain Data for BDI Sensors #1641 and #3215 from Runs 1, 3, and 7.

The strain data from BDI sensors #1643 and #3214 located perpendicular to the beams on the top and bottom of beam 7, respectively, for the eastbound runs is

49

shown in Figure 3-22. As can be seen, the data from the runs in the same direction show similar shapes with all of the magnitudes in the same direction as expected. However, there are some discrepancies in the magnitude of some of the records, notably by the same sensor (BDI #1643). This may be explained by its location on the top surface of the bridge across a crack and very close to where the test truck made its run. It is important to note the absence of a return to the initial strain value in the data from both runs and the lack of some data from run 7 (removed because of an obvious error, possibly caused by the truck coming in contact with a portion of the sensors protective cover). Taking these into consideration, the data is not nearly as conflicting as it may first seem and seems in more agreement with the data from run 3.
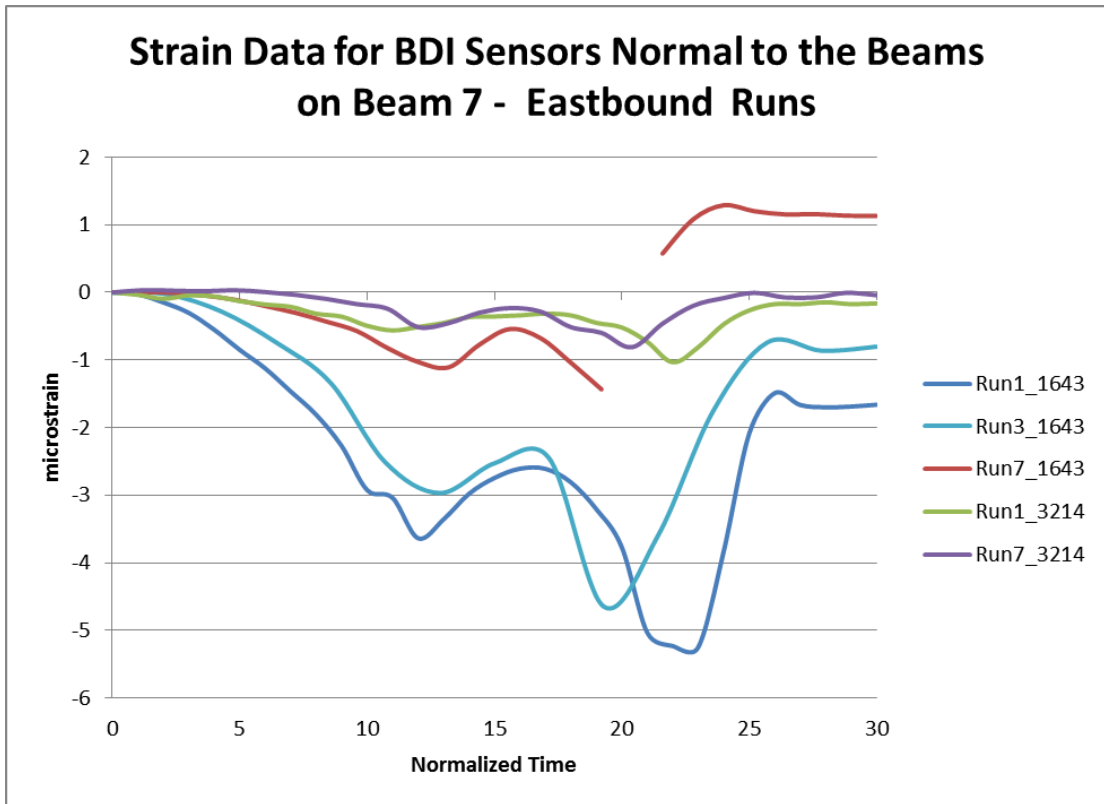
Figure 3-22: Strain Data for BDI Sensors #1643 and #3214 from Runs 1, 3, and 7.

The strain data from BDI sensors #1643 and #3214 located perpendicular to the beams on the top and bottom of beam 7, respectively, for the westbound runs is shown in Figure 3-23. As can be seen, the data from the runs in the same direction show similar shapes for each corresponding sensor. However, again, there are some discrepancies in the magnitude of some of the records by the same sensor (BDI #1643). This may again be explained by its location on the top surface of the bridge across a crack. It is important to note that while strain gauge on the top surface of the bridge (BDI #1643) recorded compression in the transverse direction when the test truck made the eastbound runs, it recorded tension in the transverse direction when the test truck made the westbound runs, possibly contributing to the cracking of the concrete overlay.
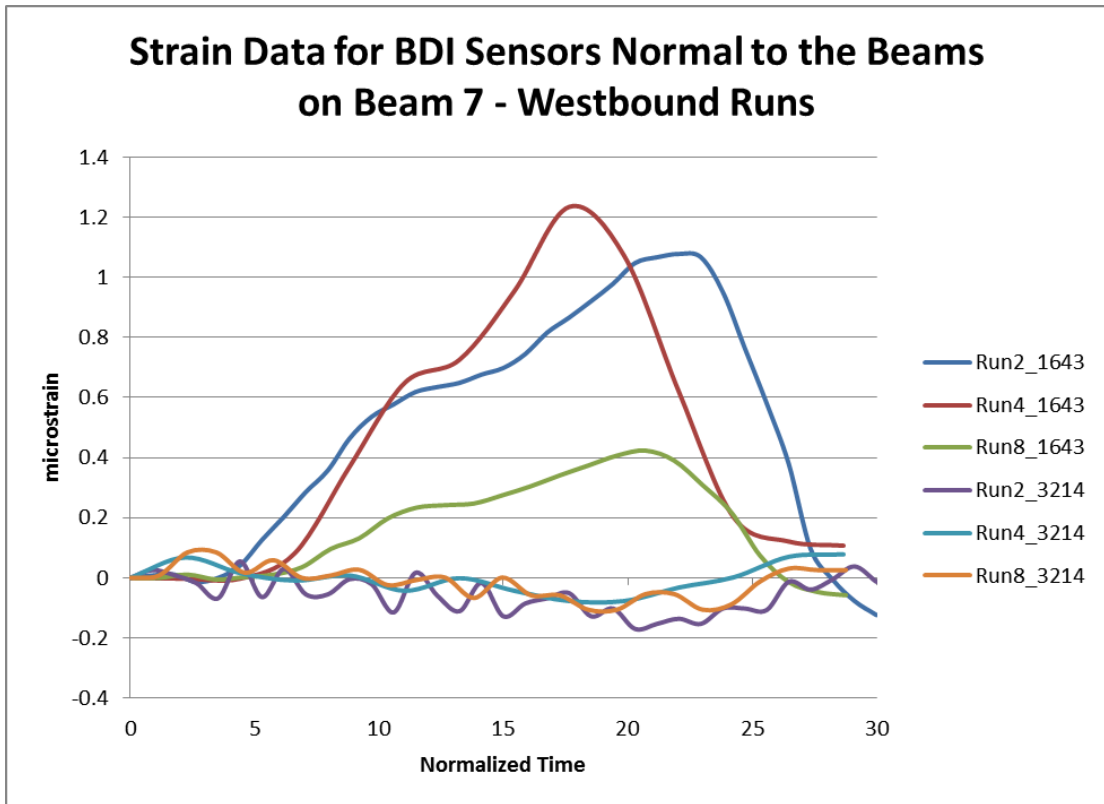
Figure 3-23: Strain Data for BDI Sensors #1643 and #3214 from Runs 2, 4, and 8.

The strain data from BDI sensors #1644 and #3213 located parallel to the abutment on the top and bottom of beam 4, respectively, is shown in Figure 3-24. As can be seen, the data from the two respective runs in the same direction show similar shapes and similar magnitudes in the same direction as expected.
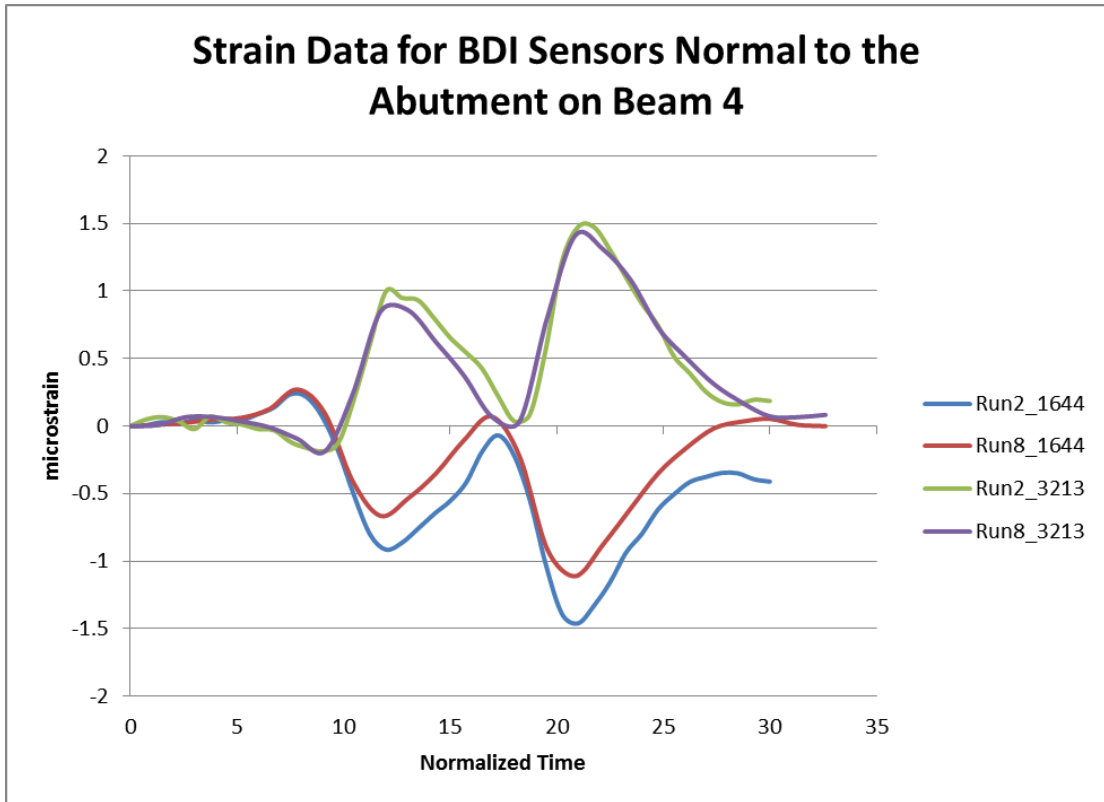
Figure 3-24: Strain Data for BDI Sensors #1644 and #3213 from Runs 2 and 8.

Chapter 4: Finite Element Model Analyses and Results of Knoxville Bridge

4.1 Summary of the Finite Element Model and Results for the Knoxville Bridge

A finite element model (FEM) of the Knoxville bridge was created and refined using the field test results to analyze possible causes of the longitudinal cracking found in the deck of the bridge (see Figure 4-1). Though other analysis methods have been used, such as grillage analysis or analytical methods, finite element analysis has proven to be both robust and accurate for refined analyses. Finite element analysis enables detailed forces and stress and strain distributions to be found in complicated structures while still allowing flexibility in analyzing specific material characteristics (Jeong, 2009). The strain data from the finite element model was compared to the strain data from the field test, following which the model was refined until close enough results were found. ANSYS version 10.0 was used to create this model. The model details are described in the following section.
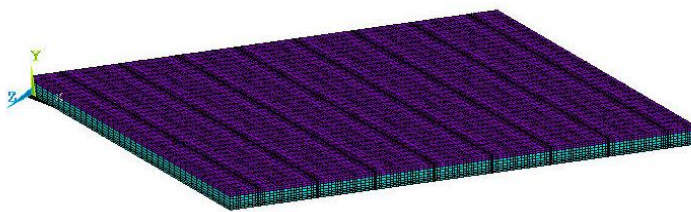
Figure 4-1: Finite Element Model of the Knoxville, MD, Bridge.

4.2 Finite Element Model Description

4.2.1 Sections and Elements

Four main sections were created to compose the finite element model of the bridge: the precast prestressed concrete slabs, the prestressing strands, the transverse

53

post-tensioning, and the concrete overlay (see Figures 4-2 to 4-5). One further simplification was the exclusion of a modeled shear key, due to the complexities of constructing and its minimal contribution. The concrete in the precast beams and the concrete overlay were modeled using solid brick elements (Solid 45), and the pretensioning strands in the precast beams and the post-tensioning tie rods were modeled using link elements (Link 8). Both the solid brick and the link elements have three degrees of freedom (translation) at each node. There were 46,080 solid brick elements and 3,520 link elements for a total of 49,600 elements.
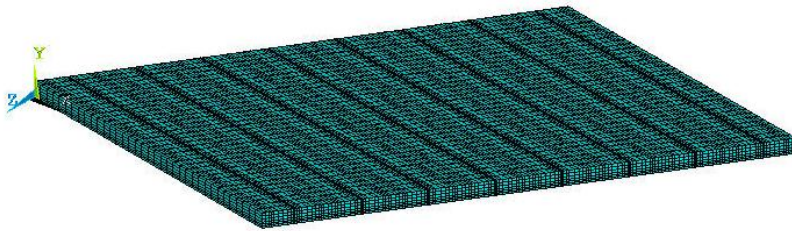
Figure 4-2: Finite Element Model Concrete Slabs/Beams.
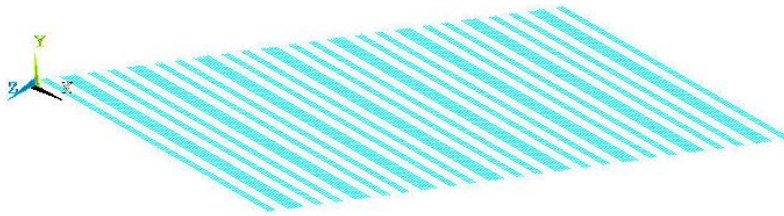
Figure 4-3: Finite Element Model Prestressing Strands.
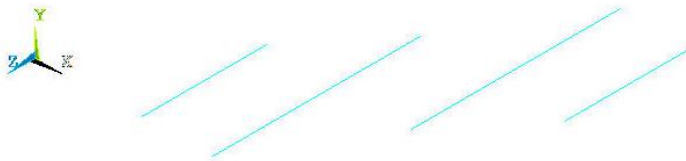
Figure 4-4: Finite Element Model Post-Tensioning Rods.
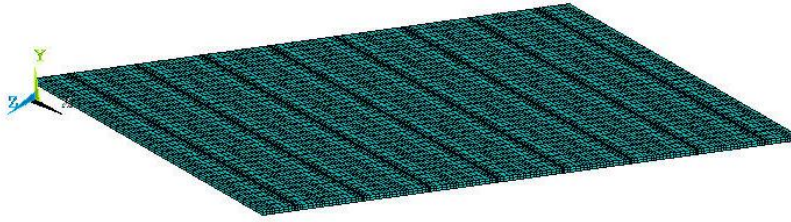
Figure 4-5: Finite Element Model Concrete Deck.

4.2.2 Material Properties and Tensioning Forces

The material properties for the model were obtained from the construction plans and are listed in Table 4-1. The isotropic reinforcing steel in the concrete overlay was not considered due to its negligible effect on the stiffness of the structure. The modulus of elasticity (i.e. stiffness) of the cast-in-place concrete for the concrete overlay and the precast concrete for the concrete beam were adjusted to refine the model. The prestressing and post-tensioning forces prescribed by the bridge plans were applied to the respective steel modeled elements.

Table 4-1: Material Properties of Finite Element Model of the Knoxville Bridge.

Material	Section	Properties
Concrete	Precast Beam	f'_c = 7000 psi E = 5224136 psi
Cast-in-Place Concrete	Concrete Overlay	f'_c = 4000 psi E = 3604997 psi
Prestressing Steel	Precast Beam	E = 28592160 psi A = 0.19625 in.^{2} P = 31,000 lbs
Post-Tensioning Steel	Post-Tensioning Tie Rod	E = 30043540 psi A = 0.7854 in.^{2} P = 80,000 lbs

4.2.3 Geometry

Two methods of modeling can be used in ANSYS: solid modeling and direct generation. Solid modeling consists of establishing the boundaries of the model and

setting some element specifications then allowing ANSYS to generate all of the nodes and elements. Direct generation allows the user to have more control over the process by having the user define the geometry, numbering, size, and connectivity of all the elements (Jeong, 2009). This model was created using direct generation with the command prompt window instead of the Graphical User Interface (GUI).

4.2.4 Loading and Boundary Conditions

The loads and boundary conditions applied to the model were made as similar as possible to the field test. The test truck load was applied as four groups of point loads corresponding to the wheel loads and defined as 5200 pounds for the front wheel loads and 8010 pounds for the rear wheels loads. A time-history analysis was used comparing the finite element model with the field test results under the modeled load (truck) traveling in a path that corresponded with runs 1, 3, 5, and 7 in the field (i.e. Eastbound across the bridge on beams 6 and 7). The model bridge was defined as simply-supported even though this bridge was partially fixed to the abutments which may have some impact on the results (Menassa et al., 2007).

4.2.5 Iterations for Strain Data Comparisons

The strain data from the model was taken at approximately the same locations as where the BDI strain transducers were placed during the field test then compared with the field test strain data results. The field test results were used to further refine the model to create as accurate a representation of the bridge as possible. As a guide, when the shape of the model strain data did not correspond with the shape obtained from the field test, the boundary conditions or structural geometry of the finite element model were refined; when the shapes of the model and field test results were

similar but the magnitudes were different, some of the members' stiffness (i.e. material properties) were refined (Jeong, 2009).

4.3 Finite Element Model Strain Comparison with Field Test Results

4.3.1 Finite Element Model and Field Test Results Comparison Introduction

The final model strain results are compared with the field test results in the following sections. It is important to note that due to the simplifications that were made in creating the finite element model in addition to the presence of cracks on the Knoxville bridge (which were not modeled) and the non-linear strain response with load positioning, a perfectly accurate model may be hard to obtain (Jeong, 2009).

The model was specifically refined based on BDI strain transducers #3215 and #1641 because of the consistent, significant results from the field test. As the finite element model iteration results grew closer to the field test results, further comparisons were made with the data from the other strain transducers. After a model was created that correlated well with the main BDI strain gauges that were considered, the rest of the strain data was compared with the strain data obtained from similar locations on the finite element model. Also note that the positive strain values indicate tensile strain while the negative strain values indicate compressive strain.

4.3.2 BDI Strain Gauge Sensors Placed Parallel to the Precast Concrete Slabs

The finite element model results correspond very closely to the field test results based on the data from the strain gauges placed parallel and on both the top and bottom surfaces of the precast concrete slabs. As expected, the model results for the strain gauges placed parallel to the slabs and on the bottom and top surfaces of beam 7 (BDI #3215 and #1641, respectively) are very similar to the field test data

(see Figures 4-6 and 4-7). The data show logical strain directions (tensile on the bottom surface of the beam and compressive on the top surface) and similar trends and maximum values of strain, with the bottom surface undergoing approximately 4 microstrain longitudinally in tension and the top surface undergoing approximately 6 microstrain longitudinally in compression. The model results for the sensor placed parallel to the slabs on the bottom surface of beam 3 do not seem to correspond as well with the field test results because of the minimal amount of strain that beam 3 undergoes due to the loading on the opposite side of the bridge, but the model result does show a similar trend and only differs by a little more than 0.3 microstrain (see Figure 4-8). When the corresponding point on the opposite side of the bridge was examined in the model and compared with the data obtained from runs 2 and 8 (when the testing truck was traveling westbound on beams 2 and 3, directly over the strain gauge), both the trends and the maximum peaks (3 microstrain longitudinally in tension) match well, confirming that the finite element model is a reasonably accurate model for the Knoxville bridge (see Figure 4-9).
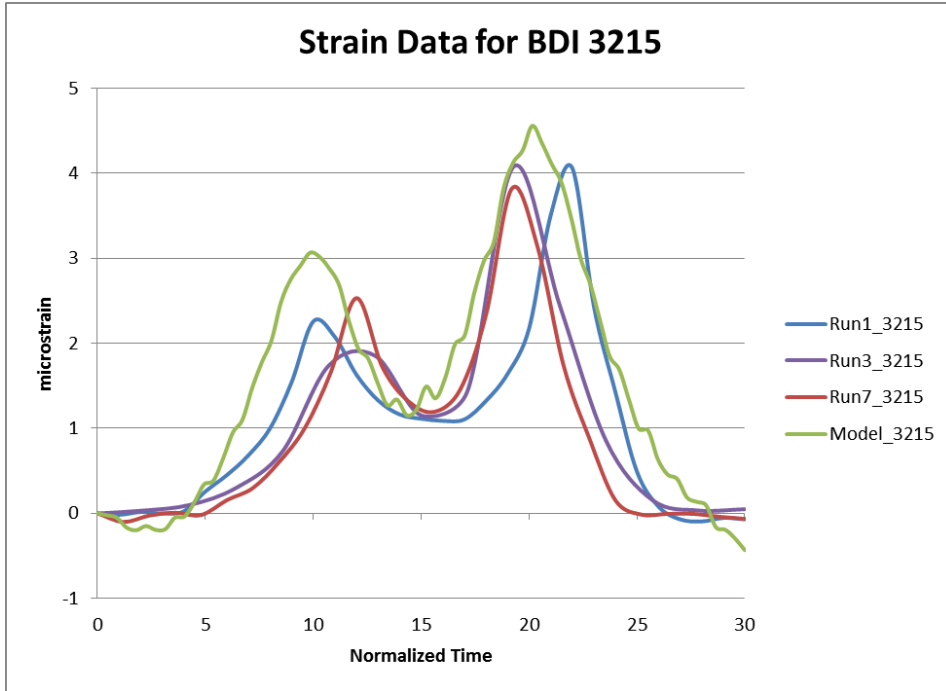
Figure 4-6: BDI Strain Transducer #3215 - Placed Parallel to the Slabs on the Bottom Surface of Beam 7.
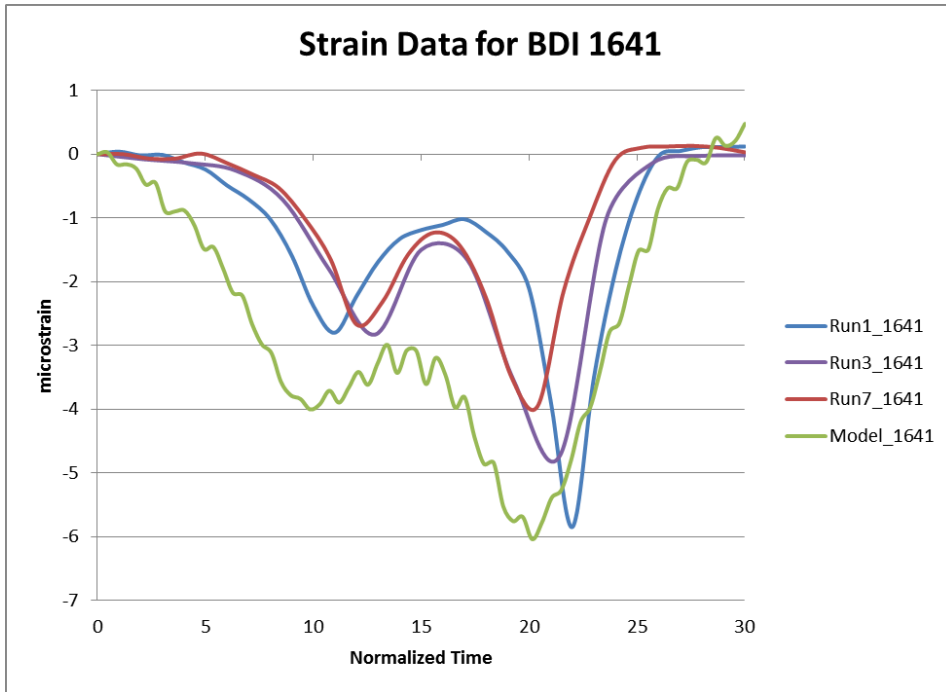
Figure 4-7: BDI Strain Transducer #1641 - Placed Parallel to the Slabs on the Top Surface of Beam 7.
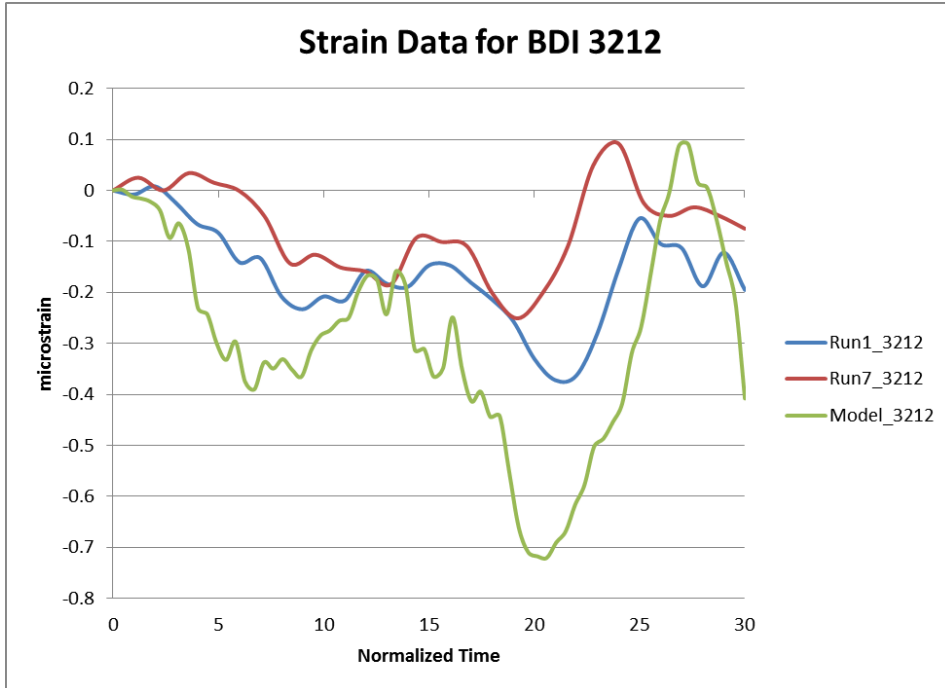
Figure 4-8: BDI Strain Transducer #3212 - Placed Parallel to the Slabs on the Bottom Surface of Beam 3.
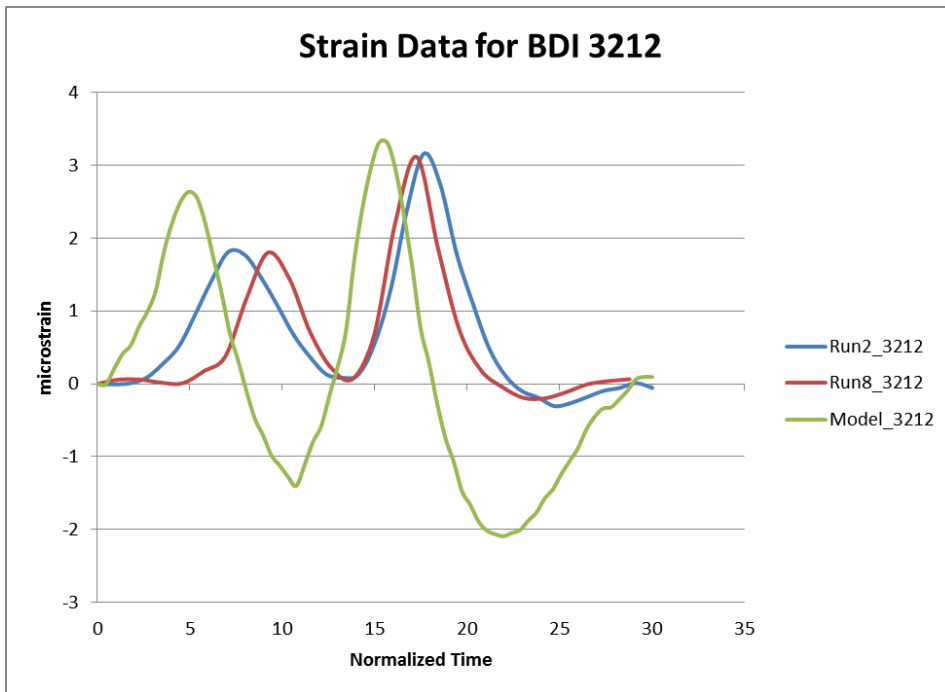
Figure 4-9: Field Test Data Based on BDI Strain Transducer #3212 - Placed Parallel to the Slabs on the Bottom Surface of Beam 3 Near the East Side of the Bridge; Model Data Based on an Equivalent Position on Beam 6 Near the West Side of the Bridge.

60

4.3.3 BDI Strain Gauge Sensors Placed Normal to the Precast Concrete Slabs

For further comparison and confirmation, the field test strain data obtained from the strain transducers placed normal to the precast concrete slabs was compared with the finite element model results. The model results for the strain gauge placed on the bottom surface of beam 2 (BDI #3214) matched well with the field test data, with both a similar trend and peak, with a maximum value of about 1 microstrain transversely in compression (see Figure 4-10). The model results for BDI #1643 which was placed on beams 6 and 7 across a crack that was present between the slabs did not correspond well with the field test results (see Figure 4-11). This may be because the strain gauge in the field was calculating strain across the two beams whereas only one node in the finite element model (i.e. only a point on beam 7) could be analyzed to determine the strain it was undergoing. An additional contribution may be that the finite element model did directly consider cracking or the consequences of it because of insufficient data about the cracks in the test bridge.
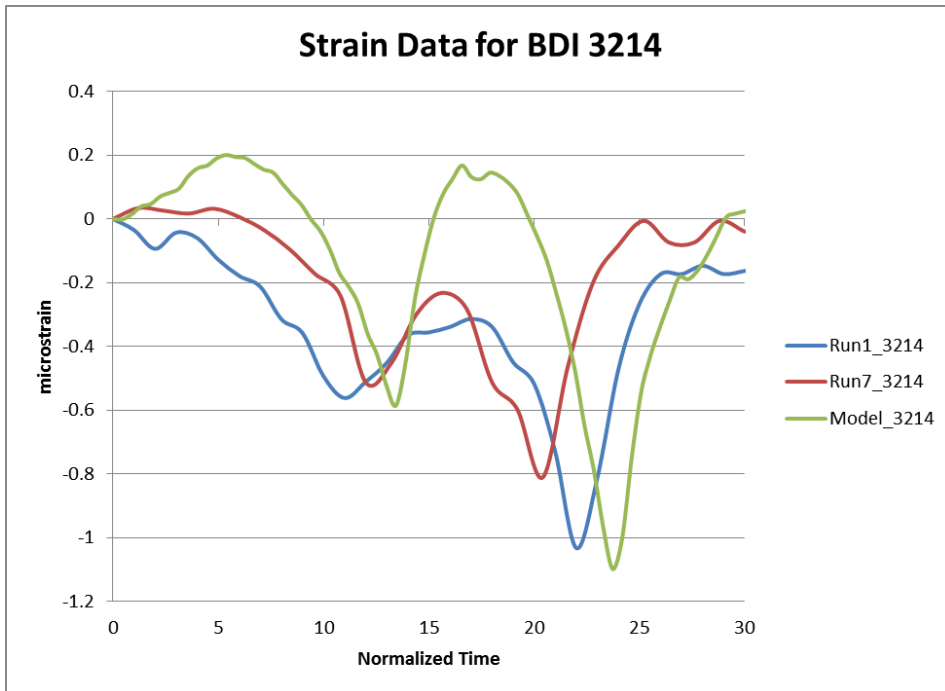
Figure 4-10: BDI Strain Transducer #3214 - Placed Normal to the Slabs on the Bottom Surface of Beam 2.
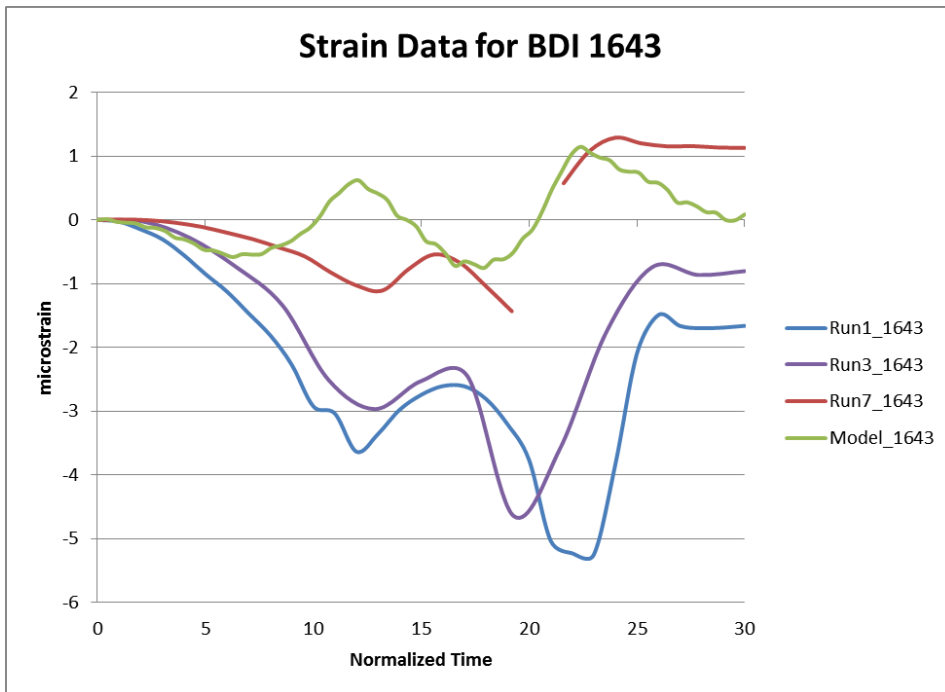
**Figure 4-11: BDI Strain Transducer #1643 - Placed Normal to the Slabs on the Top Surface across a Crack between Beams 6 and 7; Model Data Based on an Approximately Equivalent Position on Beam 7.**

4.3.4 BDI Strain Gauge Sensors Placed Normal to the Abutment

For further comparison, the model results were also compared to the strain data obtained by the strain gauges placed normal to the abutment (BDI #3213 and #1644). This comparison was made more difficult because of the orientation of the strain gauges in the field in combination with the ability to only examine the longitudinal and transverse strains at specific points in the finite element model. The longitudinal and transverse strains from the model were mathematically combined to form an approximate composite strain that could be compared to the field test results. The individual strains as well as the composite strain are shown in the following figures. The model results for the sensor located on the bottom surface of beam 4 for the eastbound loading case compared considerably well with the field test results, with a similar peak of 1.4 microstrain in compression (see Figure 4-12). There seems to be a major discrepancy when the corresponding point on the opposite side of the bridge was examined in the model and compared with the data obtained from runs 2 and 8 (when the testing truck was traveling westbound on beams 2 and 3). For the calculated composite strain data, the trends and magnitudes are almost exactly the same but the sign is opposite (i.e while the field test data indicates there was tensile strain, the model undergoes compressive strain) (see Figure 4-13). In contrast to this, the transverse strain from the model shows the closest results to the field test data. When the model results for the sensor placed on the top surface are compared with the field test results, further discrepancies are seen. For both the eastbound and westbound cases, the calculated composite strain data trends are similar but the magnitudes are significantly different (see Figures 4-14 and 4-15). However, for the

eastbound case, the longitudinal strain from the model shows similarities to the field test data; and for the westbound case, the transverse strain from the model shows similarities to the field test data. These discrepancies may be in part due to the orientation difficulties. For the strain gauge on the top surface, the differences may be compounded because that sensor was placed across a crack between beams 4 and 5, whereas the strain data from the model could only be calculated from one point on beam 5. Significantly, the transverse stress results from the model generally were closest to the field test results and thus were primarily used in the finite element model stress analyses for both this bridge and the parametric study.
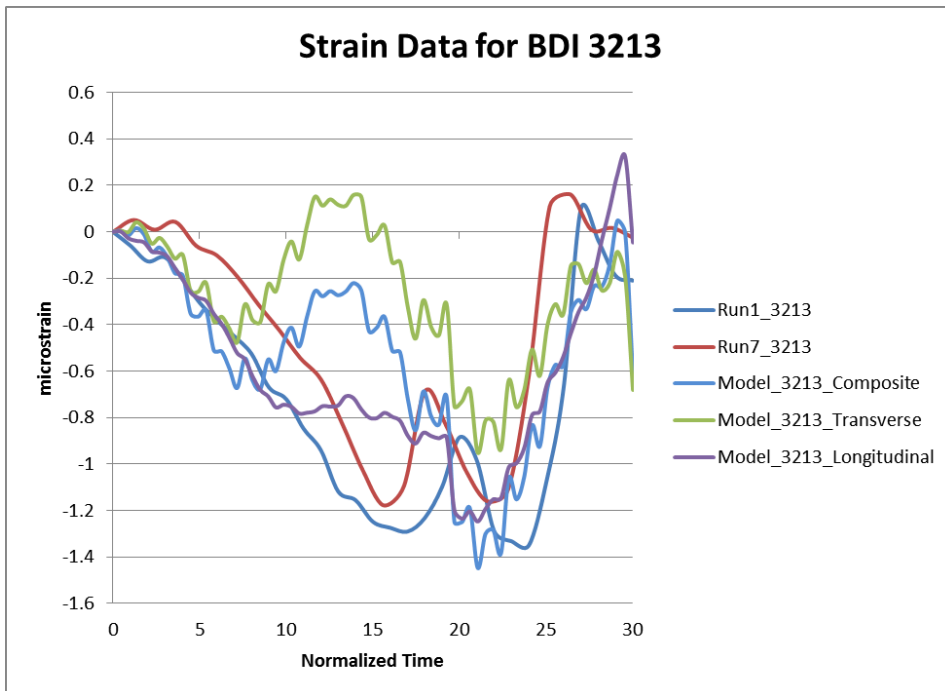
Figure 4-12: BDI Strain Transducer #3213 - Placed Normal to the Abutment on the Bottom Surface of Beam 4.

64
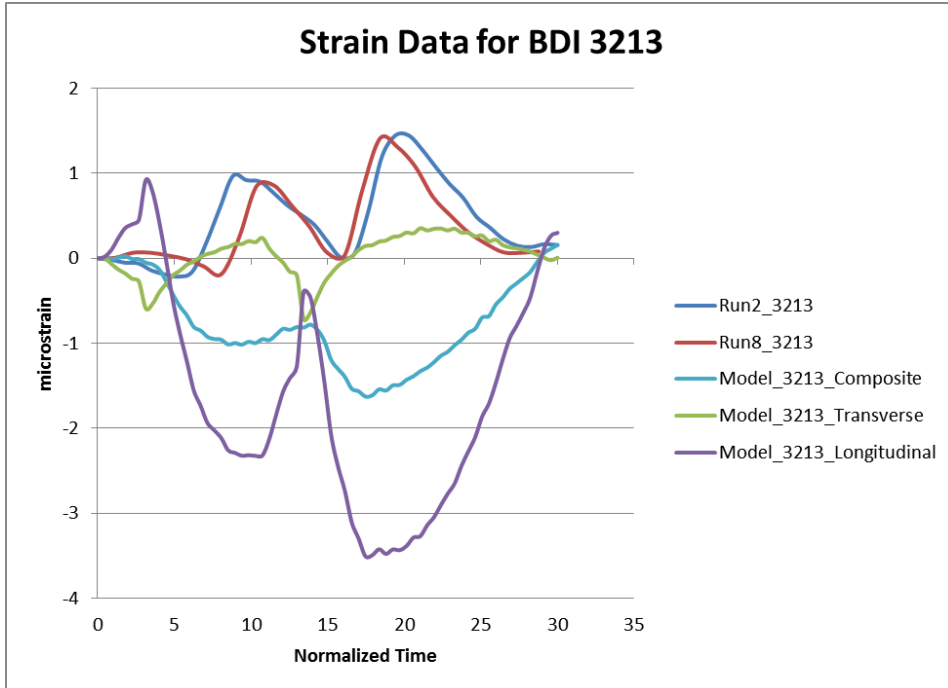
Figure 4-13: Field Test Data Based on BDI Strain Transducer 3213 - Placed Normal to the Abutment on the Bottom Surface of Beam 4 Near the East Side of the Bridge; Model Data Based on an Equivalent Position on Beam 5 Near the West Side of the Bridge.
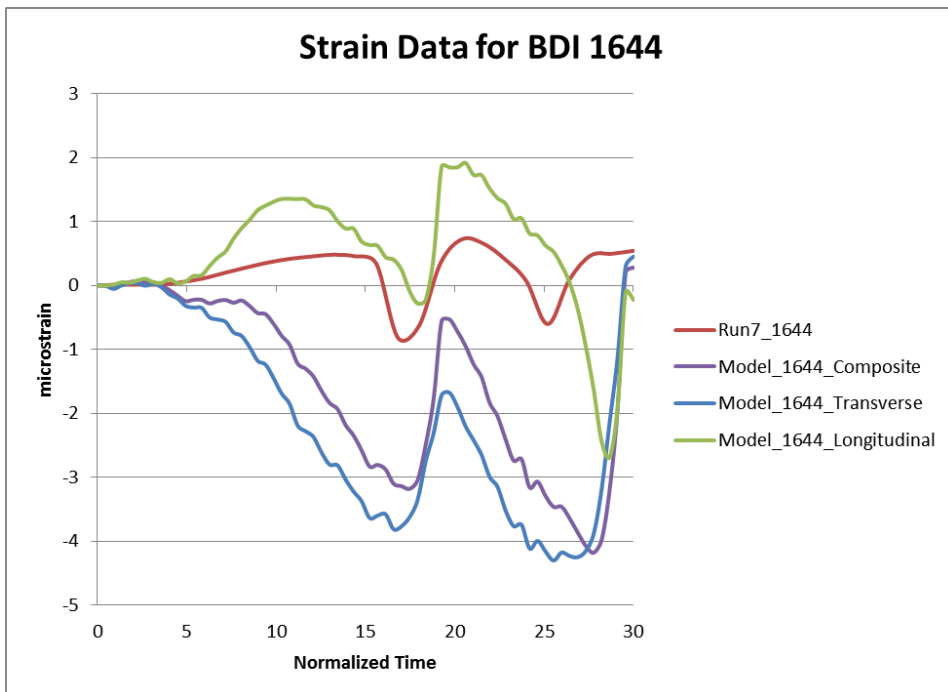

Figure 4-14: BDI Strain Transducer #1644 - Placed Normal to the Abutment on the Top Surface across a Crack between Beams 4 and 5; Model Data Based on an Approximately Equivalent Position on Beam 5.

65
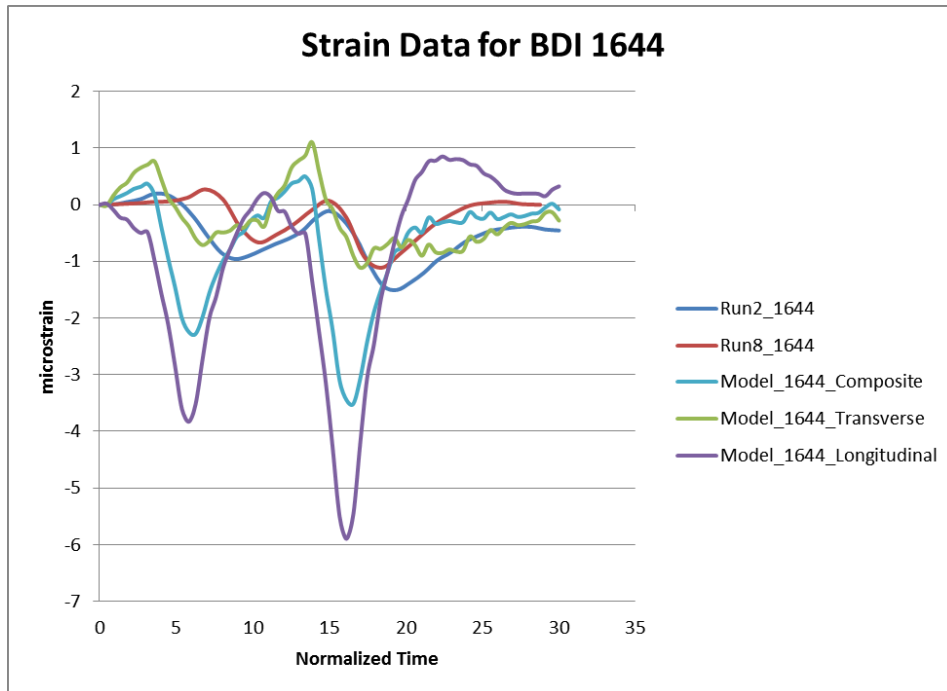
Figure 4-15: Field Test Data Based on BDI Strain Transducer #1644 - Placed Normal to the Abutment on the Top Surface across a Crack between Beams 4 and 5 Near the East Side of the Bridge; Model Data Based on an Equivalent Position on Beam 4 Near the West Side of the Bridge.

4.4 Finite Element Model Stress Distributions

The model that was created was then run with a static H-20 truck loading (a truck applying 8,000 pounds beneath the front axle and 32,000 pounds beneath the rear axle) on beams 6 and 7. The stress distribution at the beam-overlay interface and the top surface was then analyzed to examine if any conclusions could be reached as to why the top surface of the concrete overlay was cracking. The stress displayed in the following figures has units of pounds per square inch (psi). Generally, the greatest tensile stresses exist near the abutments and on the opposite side of the bridge from the loading (see Figures 4-16 to 4-22). The tensile stresses between the beams (along the shear key) are evident from the transverse, first principal, and second principal stresses.

66
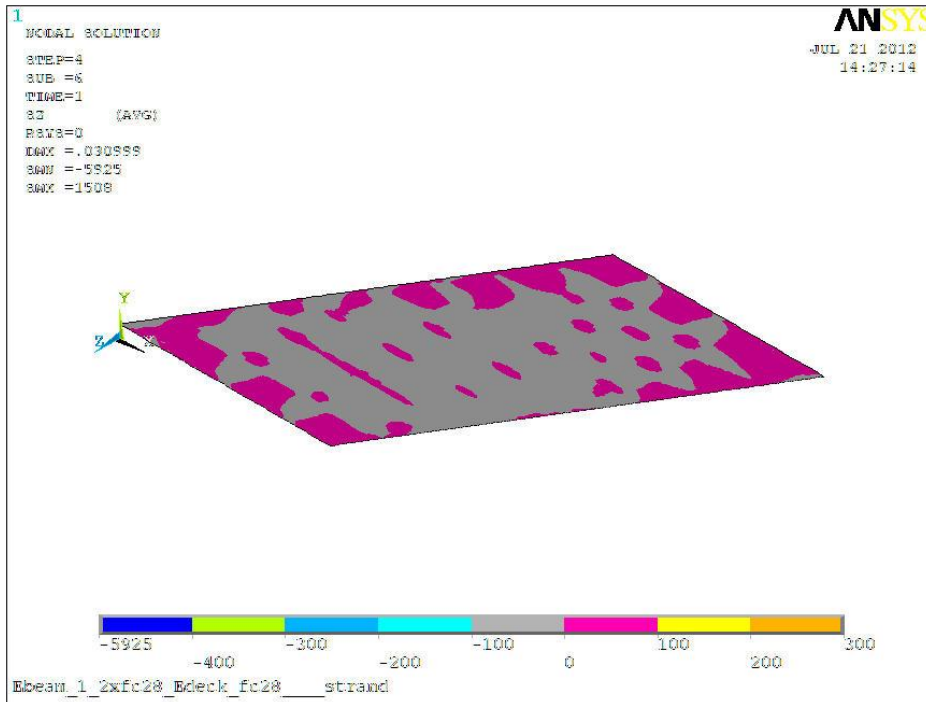
Figure 4-16: Transverse Stress at the Beam-Overlay Interface.
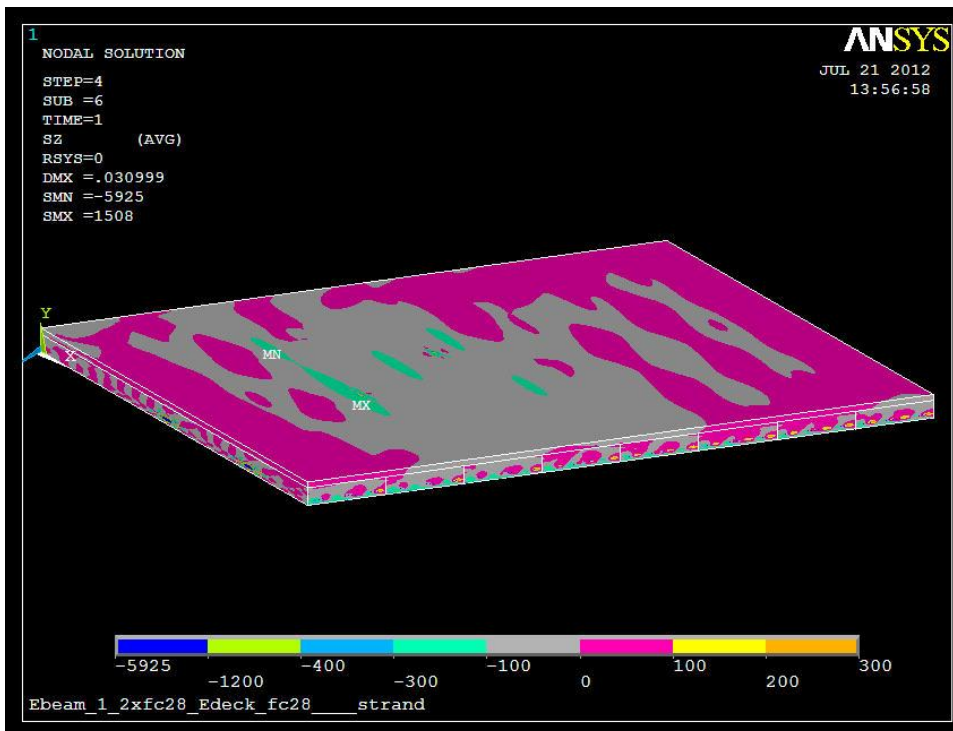
Figure 4-17: Transverse Stress at the Top Surface.
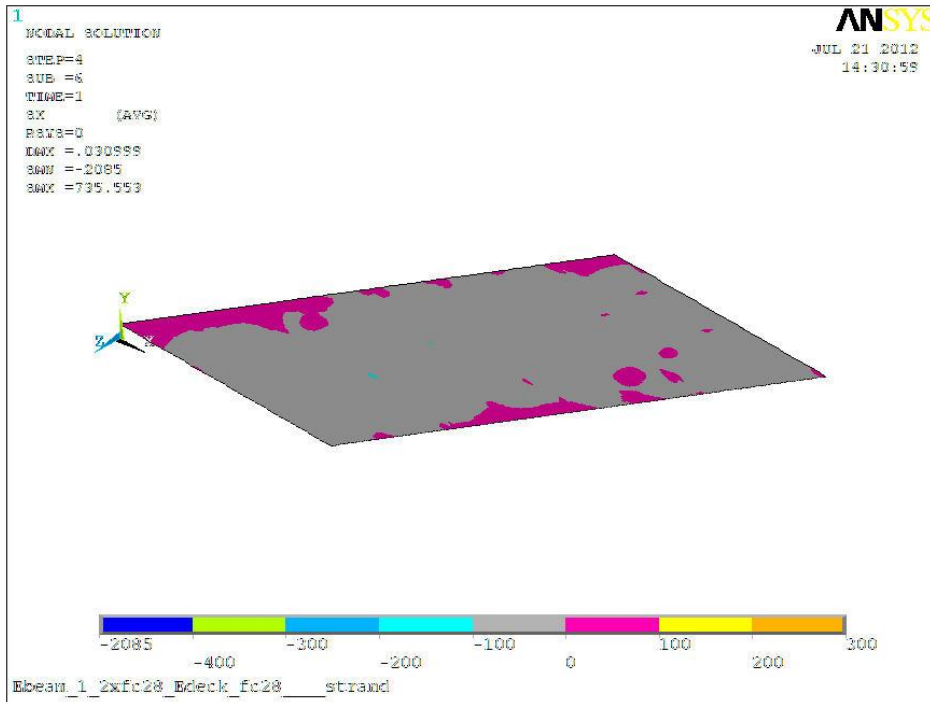
Figure 4-18: Longitudinal Stress at the Beam-Overlay Interface.
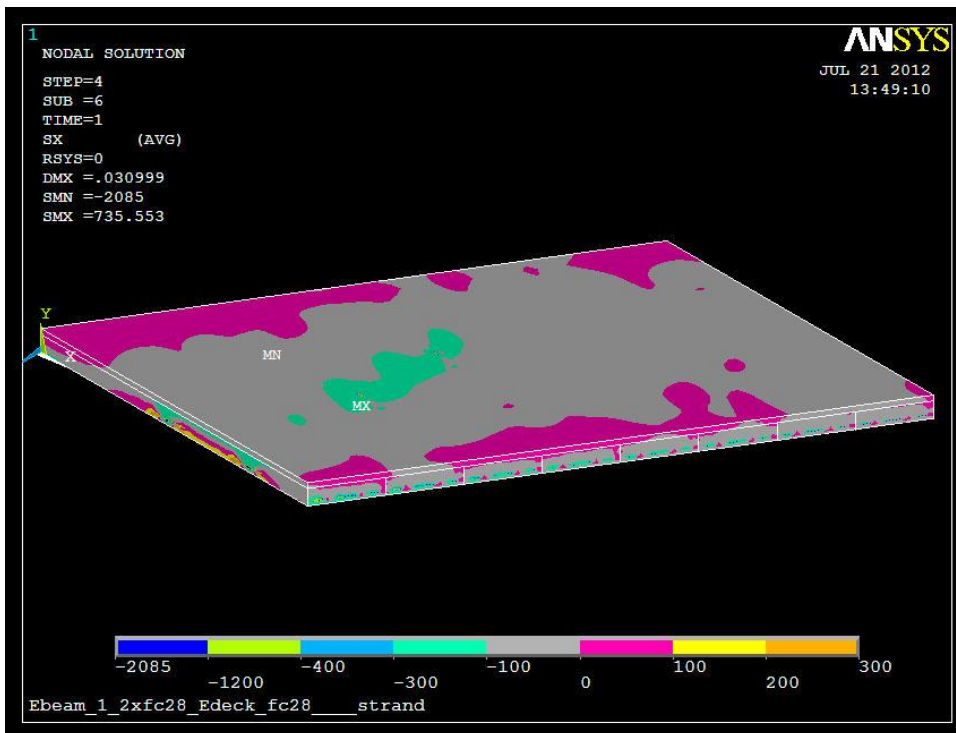
Figure 4-19: Longitudinal Stress at the Top Surface.
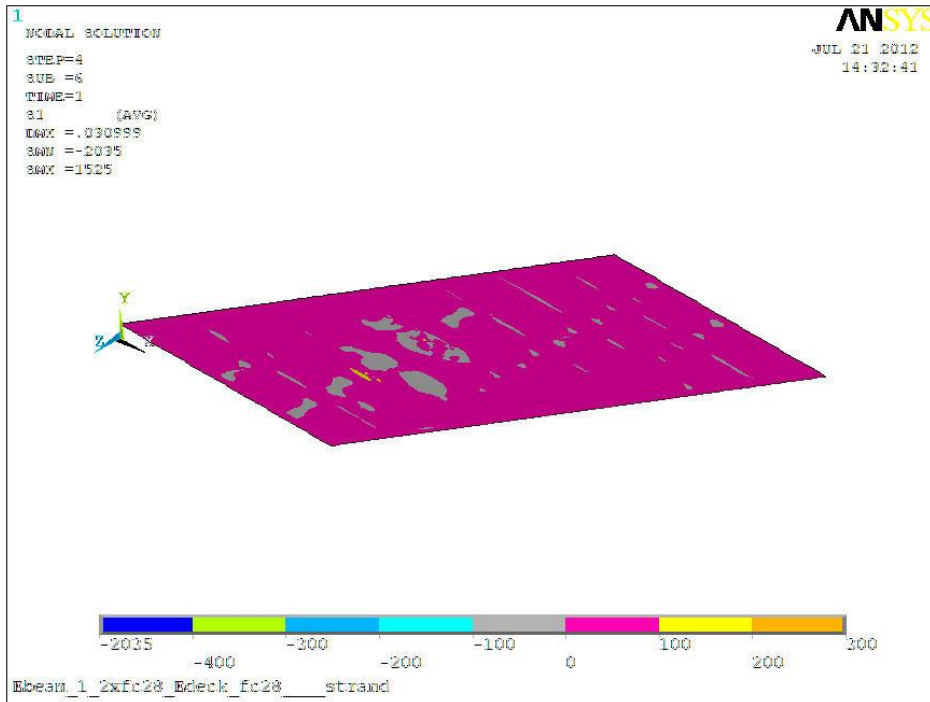
Figure 4-20: First Principal Stress at the Beam-Overlay Interface.
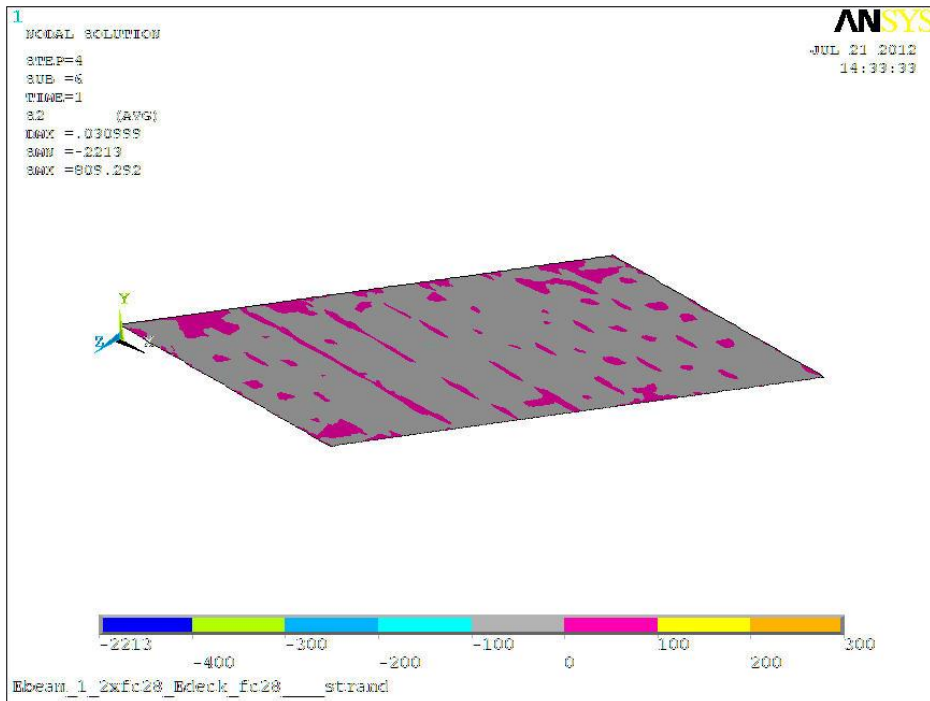
Figure 4-21: Second Principal Stress at the Beam-Overlay Interface.
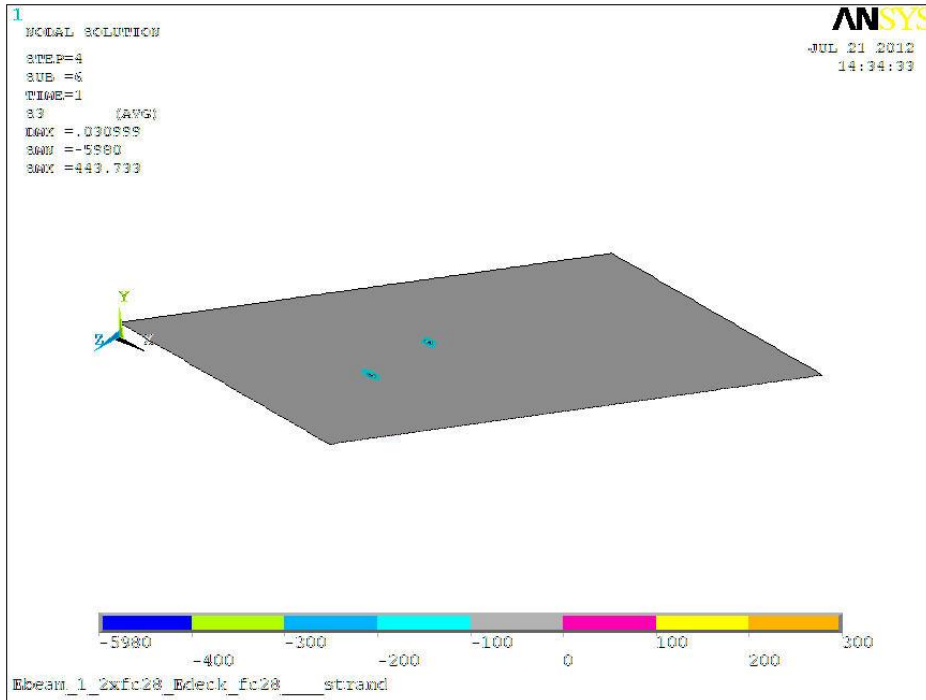
Figure 4-22: Third Principal Stress at the Beam-Overlay Interface.

70

Chapter 5: Skewed Bridge Parametric Study Using Finite Element Model Analyses

5.1 Parametric Analysis Details

### 5.1.1 Parametric Analysis Assumptions

To obtain a more complete idea of how the skew angle affects transversely post-tensioned adjacent concrete slab bridges, a parametric study was performed using twenty-one different finite element models. Each bridge was designed as a simply-supported two lane bridge with a width of 32'-0" made up of eight 4'-0" wide adjacent precast prestressed concrete slabs with a 5" concrete overlay. The transverse tie rod diameters and forces were based on the span length of each bridge model and designed according to the MDSHA standards. The transverse post-tensioning was designed as an ungrouted system. An H-20 truck loading (a truck with an 8,000-pound front axle and 32,000-pound rear axle) was applied to each model. The longitudinal, transverse, first principal, second principal, and third principal stresses were all examined for each model. The transverse stress at the slab-deck interface was chosen to be the critical analysis component as this stress predominately contributes to the longitudinal reflective cracking in the concrete overlay observed in the field. The longitudinal stress and the main component of the first principal stress are primarily carried by the concrete slabs which have not shown any structural or serviceability failures. The second and third principal stresses did not show a significant impact. The stress displayed in the stress distribution figures has units of pounds per square inch (psi). The full results for the stresses present at the slab-deck

71

interface for the first model as well as the longitudinal and first principal stresses for the remaining models can be referenced in Appendix C.

5.1.2 Parametric Analysis Process

Three main components of transversely post-tensioned adjacent concrete slab bridges were investigated to produce a set of recommendations: span length, skew angle, and post-tensioning orientation. Three standard span lengths were considered: 25'-0", 40'-0", and 55'-0". Two skew angles were considered: 15^0 and 30^0. Two orientations for the transverse post-tensioning were considered: parallel to the bridge abutments (skewed tie rods) and normal to the slabs (normal/staggered tie rods). For brevity, these orientations will be described only as "skewed" or "normal" in the descriptions in the following sections. For consistency, our recommended transverse post-tensioning orientation is always placed on the left side of the page when comparing with other possible transverse post-tensioning orientations. It is important to note that the behavior of the models changes as a function of not only the skew angle but also the length to width ratio. As the skew angle decreases and the bridge span length increases, the bridges act more similarly to a beam than a plate.

5.2 Twenty-Five Foot, Fifteen Degree Skewed Bridge

Six finite element models were created to determine the best transverse post-tensioning practice for a 25'-0", 15^0 skewed bridge. First two loading conditions were compared to determine a standard loading condition for the rest of the finite element models in the parametric study. Then, four possible transverse post-tensioning orientations were considered: four normal and staggered tie rods (connecting three or five beams together) located equivalent distances apart on the

bridge, two skewed tie rods located at the third points, two skewed tie rods located 3'-0" from each abutment, and three skewed tie rods located 2'-6" from each abutment and at the midspan.

5.2.1 Loading: One Truck vs. Two Truck

To determine the load that should be applied to each finite element model, a 25'-0", 15° skewed bridge model was created. A skewed post-tensioning tie rod was placed at each of the third points of the bridge as according to current practice. Then one H-20 truck loading was applied followed, in a separate run, by two H-20 trucks loading to provide a comparison. As seen in Figure 5-1, there is little difference in the transverse stress at the slab-deck interface, so for the rest of the models only one H-20 truck loading was applied.
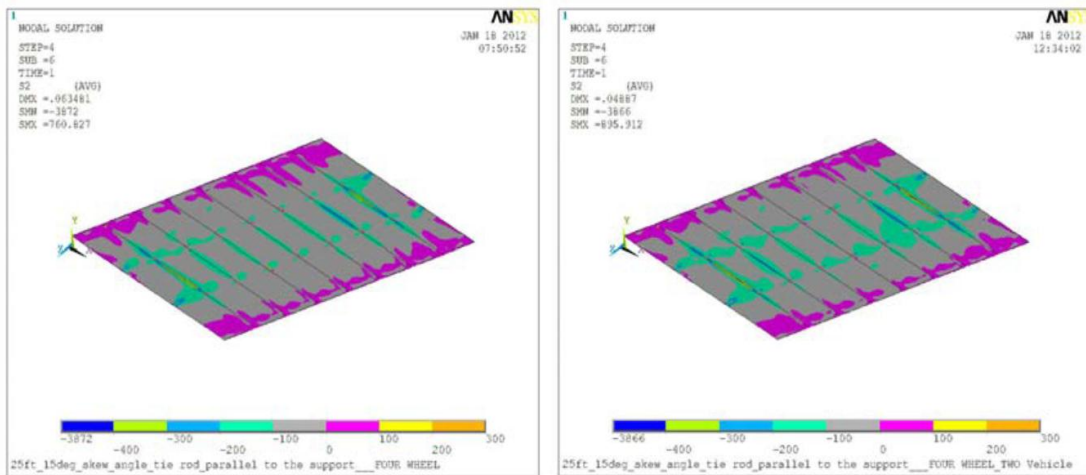
Figure 5-1: Transverse Stress Present at Slab-Deck Interface of a Twenty-Five Foot, Fifteen Degree Skewed Bridge. (On the left, one truck loading and third points skewed; on the right, two truck loading and third points skewed.)

The magnitude of the transverse stress in pounds per square inch (psi) is indicated by the color bar below each image with magnitude increasing to the right. Any negative transverse stress indicates compression while positive transverse stress

73

indicates tension. Since this project is concerned with the longitudinal cracking possibly initiated between the slabs at the abutments, post-tensioning orientations that result in significant positive transverse stresses (pink/purple, yellow, and orange colors) in those areas are discouraged.

5.2.2 Post-Tensioning Orientation: Third Points Skewed vs. Four Normal and Staggered

As can be seen in Figure 5-2, using two skewed tie rods located at the third points shows significant improvement over using four normal and staggered tie rods (connecting three or five beams together) located equivalent distances apart on the 25'-0", 15^0 skewed bridge.
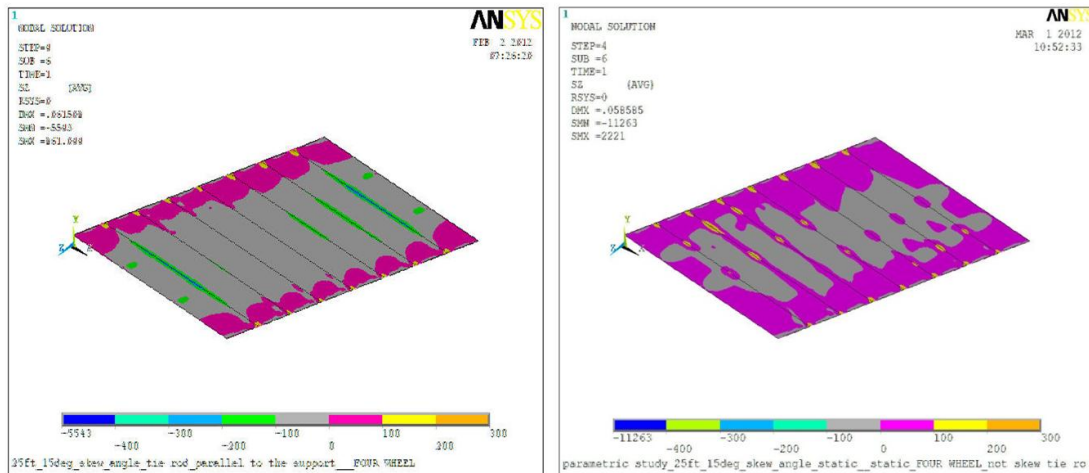

Figure 5-2: Transverse Stress Present at Slab-Deck Interface of a Twenty-Five Foot, Fifteen Degree Skewed Bridge. (On the left, third points skewed; on the right, four normal and staggered.)

5.2.3 Post-Tensioning Orientation: Third Points Skewed vs. Ends Skewed

As can be seen in Figure 5-3, using two skewed tie rods located 3'-0" from each abutment shows some but not significant improvement over using two skewed tie rods located at the third points of the 25'-0", 15^0 skewed bridge.

74
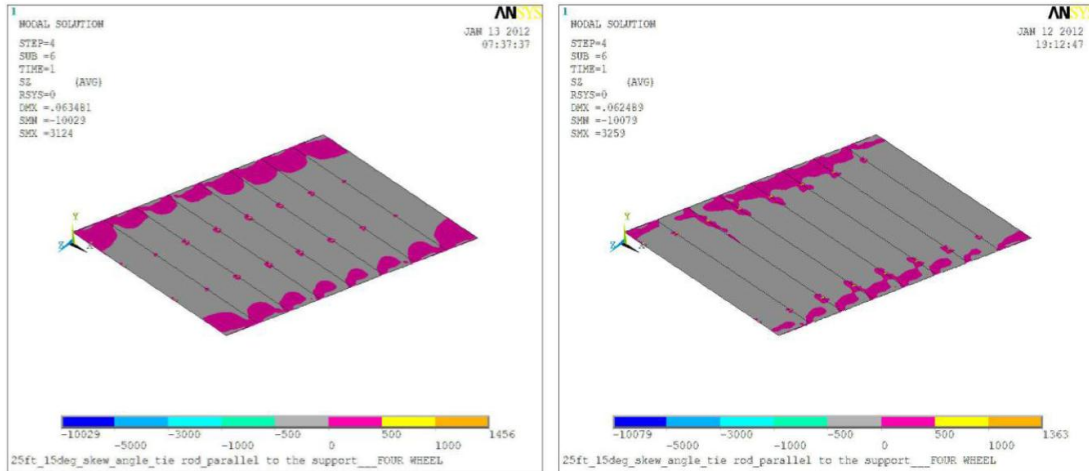
Figure 5-3: Transverse Stress Present at Slab-Deck Interface of a Twenty-Five Foot, Fifteen Degree Skewed Bridge. (On the left, third points skewed; on the right, ends skewed.)

5.2.4 Post-Tensioning Orientation: Third Points Skewed vs. Ends and Midspan

Skewed

As can be seen in Figure 5-4, using three skewed tie rods located 2'-6" from each abutment and at the midspan shows some but not significant improvement over using two skewed tie rods located at the third points of the 25'-0", 15^0 skewed bridge.
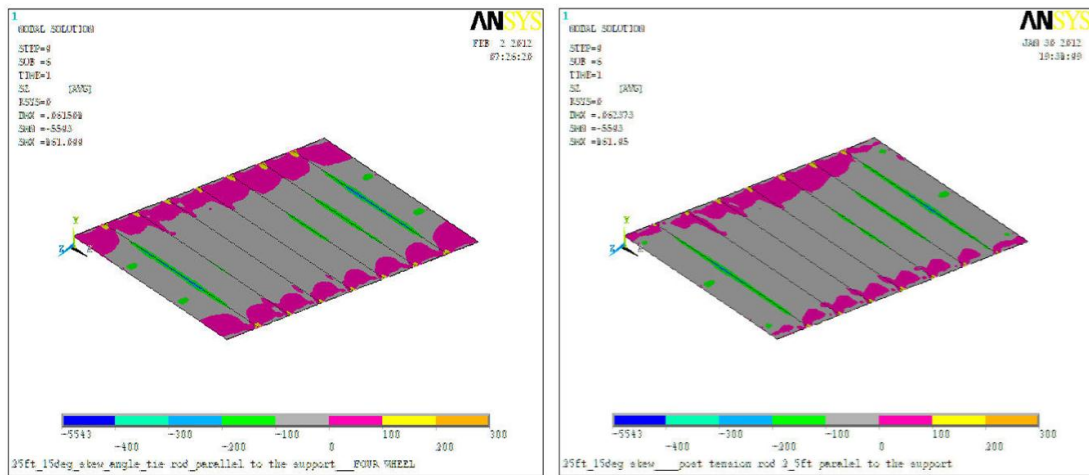

Figure 5-4: Transverse Stress Present at Slab-Deck Interface of a Twenty-Five Foot, Fifteen Degree Skewed Bridge. (On the left, third points skewed; on the right, ends and midspan skewed.)

75

5.3 Twenty-Five Foot, Thirty Degree Skewed Bridge

Two finite element models were created to determine the best transverse post-tensioning practice for a 25'-0", 30^0 skewed bridge. Two possible transverse post-tensioning orientations were considered: four normal and staggered tie rods (connecting three or five beams together) located equivalent distances apart on the bridge and two skewed tie rods located at the third points.

5.3.1 Post-Tensioning Orientation: Third Points Skewed vs. Four Normal and Staggered

As can be seen in Figure 5-5, using two skewed tie rods located at the third points shows significant improvement over using four normal and staggered tie rods (connecting three or five beams together) located equivalent distances apart on the 25'-0", 30^0 skewed bridge; but it is also important to note that there are significant stresses in both designs.
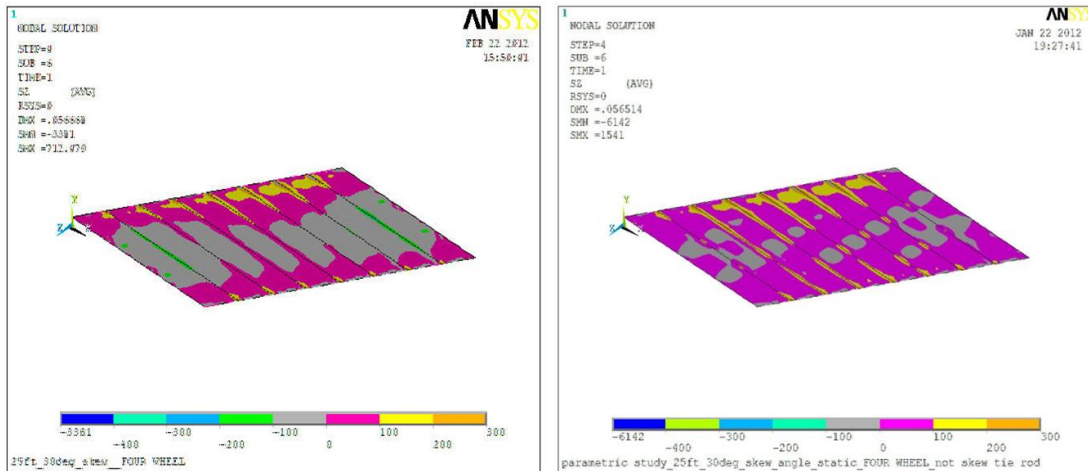

Figure 5-5 Transverse Stress Present at Slab-Deck Interface of a Twenty-Five Foot, Thirty Degree Skewed Bridge. (On the left, third points skewed; on the right, four normal and staggered.)

5.4 Forty Foot, Fifteen Degree Skewed Bridge

Five finite element models were created to determine the best transverse post-tensioning practice for a 40'-0", 15^0 skewed bridge. Five possible transverse post-tensioning orientations were considered: two normal tie rods (connecting all eight beams together) located at approximately the third points of the bridge, four normal and staggered tie rods (connecting three or five beams together) located equivalent distances apart, two skewed tie rods located at the third points, three skewed tie rods located 5'-0" from each abutment and at the midspan, and four skewed tie rods located 2'-0" and 14'-0" from each abutment.

5.4.1 Post-Tensioning Orientation: Ends and Midspan Skewed vs. Two Normal

As can be seen in Figure 5-6, using three skewed tie rods located 5'-0" from each abutment and at the midspan shows significant improvement over using two normal tie rods (connecting all eight beams together) located at approximately the third points of the 40'-0", 15^0 skewed bridge.
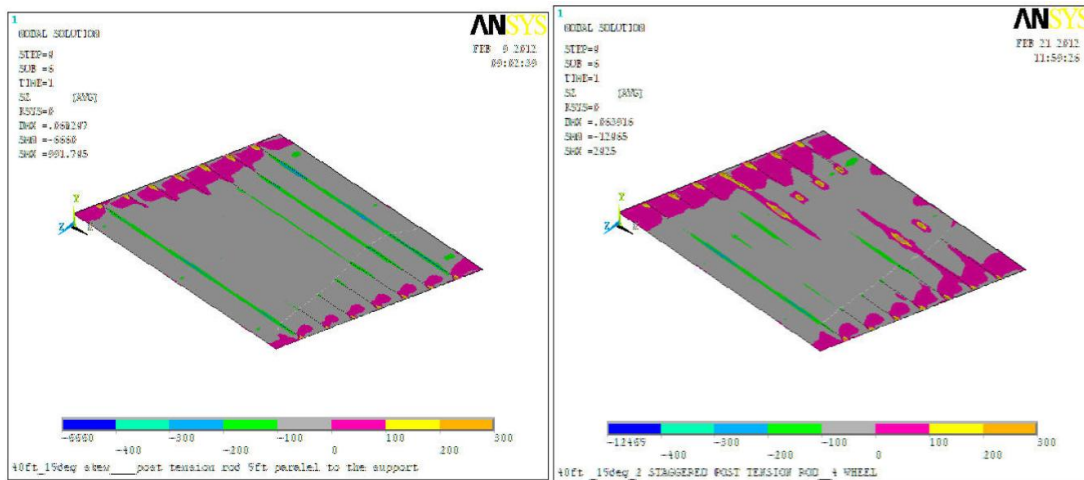
Figure 5-6: Transverse Stress Present at Slab-Deck Interface of a Forty Foot, Fifteen Degree Skewed Bridge. (On the left, ends and midspan skewed; on the right, two normal.)

5.4.2 Post-Tensioning Orientation: Ends and Midspan Skewed vs. Four Normal and

Staggered

As can be seen in Figure 5-7, using three skewed tie rods located 5'-0" from each abutment and at the midspan shows significant improvement over using four normal and staggered tie rods (connecting three or five beams together) located equivalent distances apart on the 40'-0", 15^0 skewed bridge.
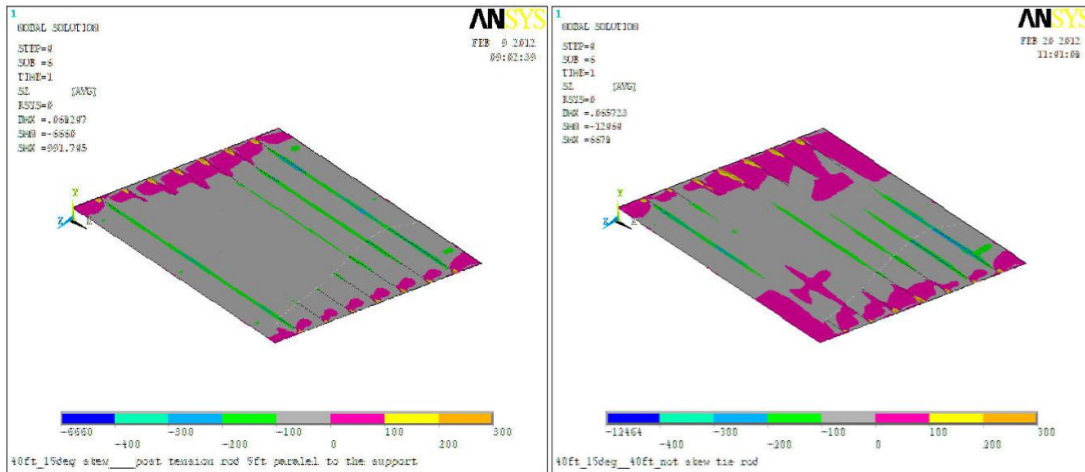

Figure 5-7: Transverse Stress Present at Slab-Deck Interface of a Forty Foot, Fifteen Degree Skewed Bridge. (On the left, ends and midspan skewed; on the right, four normal and staggered.)

5.4.3 Post-Tensioning Orientation: Ends and Midspan Skewed vs. Third Points

Skewed

As can be seen in Figure 5-8, using three skewed tie rods located 5'-0" from each abutment and at the midspan shows significant improvement over using two skewed tie rods located at the third points of the 40'-0", 15^0 skewed bridge.
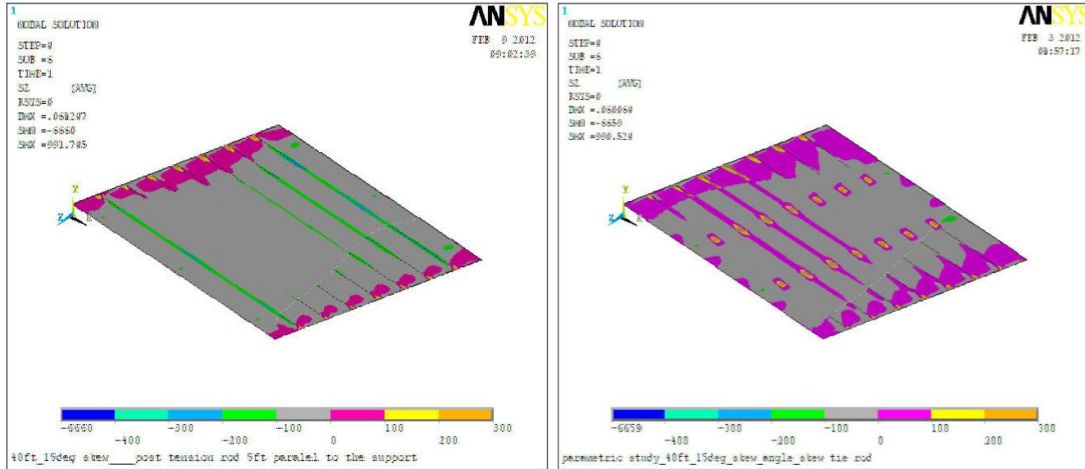
Figure 5-8: Transverse Stress Present at Slab-Deck Interface of a Forty Foot, Fifteen Degree Skewed Bridge. (On the left, ends and midspan skewed; on the right, third points skewed.)

5.4.4 Post-Tensioning Orientation: Ends and Midspan Skewed vs. Four Skewed

As can be seen in Figure 5-9, using four skewed tie rods located 2'-0" and 14'-0" from each abutment shows some but not significant improvement over using three skewed tie rods located 5'-0" from each abutment and at the midspan of the 40'-0", 15^0 skewed bridge.
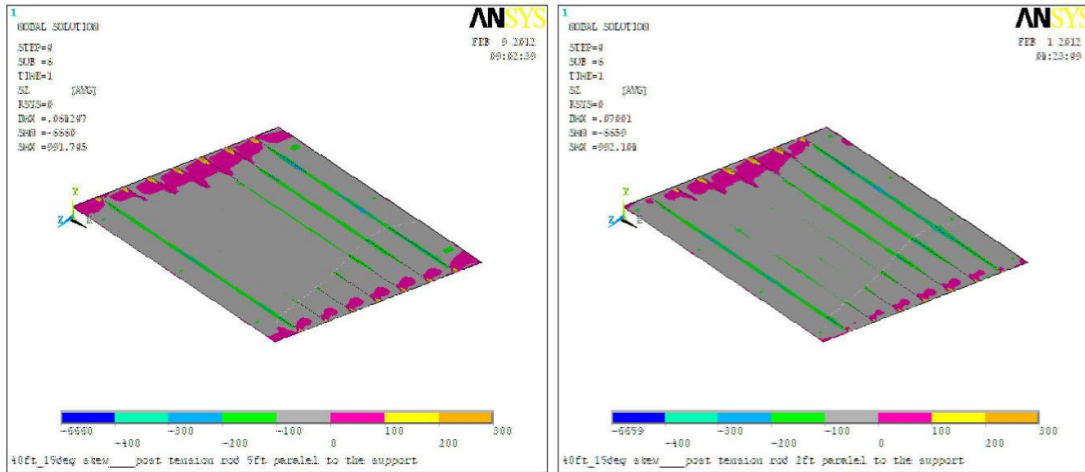

Figure 5-9: Transverse Stress Present at Slab-Deck Interface of a Forty Foot, Fifteen Degree Skewed Bridge. (On the left, ends and midspan skewed; on the right, four skewed.)

5.5 Forty Foot, Thirty Degree Skewed Bridge

Four finite element models were created to determine the best transverse post-tensioning practice for a 40'-0", 30^0 skewed bridge. Four possible transverse post-tensioning orientations were considered: two normal tie rods (connecting all eight beams together) located at approximately the third points of the bridge, four normal and staggered tie rods (connecting three or five beams together) located equivalent distances apart, two skewed tie rods located at the third points, and three skewed tie rods located 5'-0" from each abutment and at the midspan.

5.5.1 Post-Tensioning Orientation: Ends and Midspan Skewed vs. Two Normal

As can be seen in Figure 5-10, using three skewed tie rods located 5'-0" from each abutment and at the midspan shows some improvement over using two normal tie rods (connecting all eight beams together) located at approximately the third points of the 40'-0", 30^0 skewed bridge.
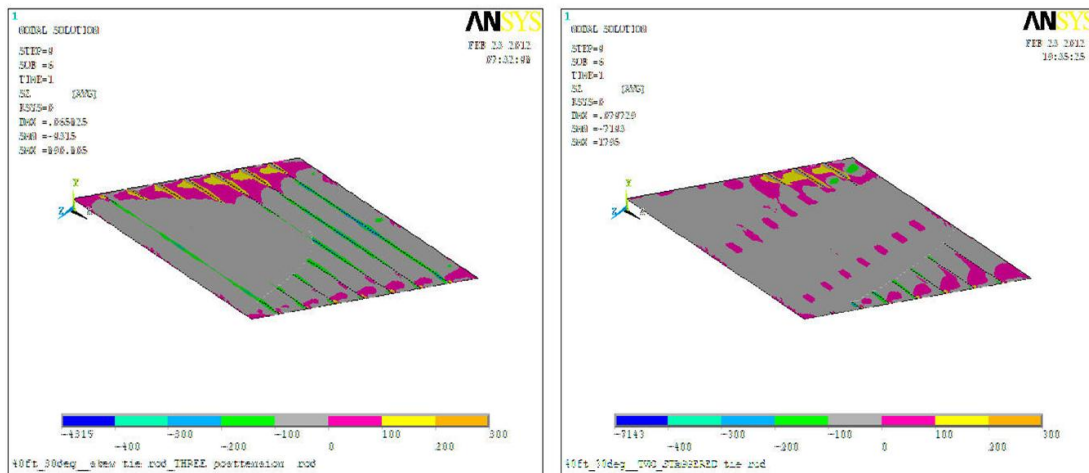

Figure 5-10: Transverse Stress Present at Slab-Deck Interface of a Forty Foot, Thirty Degree Skewed Bridge. (On the left, ends and midspan skewed; on the right, two staggered.)

5.5.2 Post-Tensioning Orientation: Ends and Midspan Skewed vs. Four Normal and

Staggered

As can be seen in Figure 5-11, using three skewed tie rods located 5'-0" from each abutment and at the midspan shows some improvement over using four normal and staggered tie rods (connecting three or five beams together) located equivalent distances apart on the 40'-0", 30^0 skewed bridge.
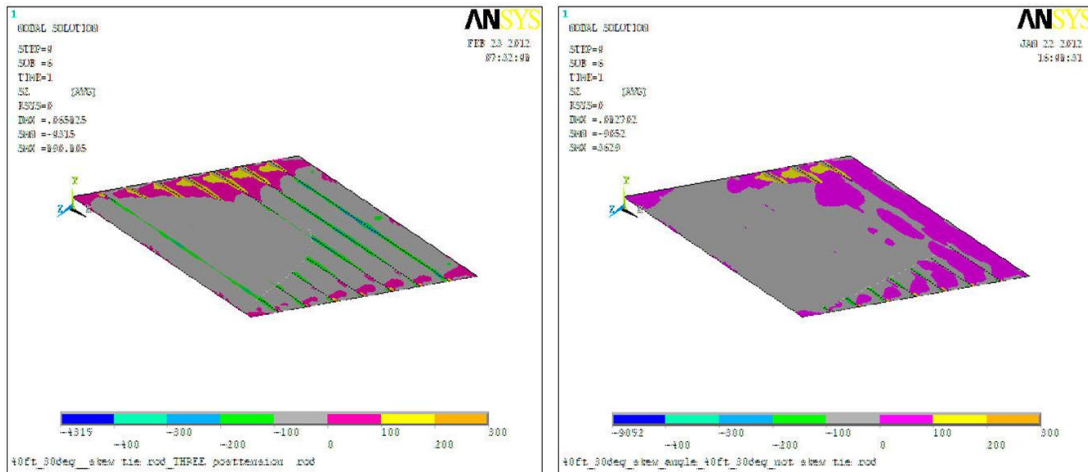

Figure 5-11: Transverse Stress Present at Slab-Deck Interface of a Forty Foot, Thirty Degree Skewed Bridge. (On the left, ends and midspan skewed; on the right, four normal and staggered.)

5.5.3 Post-Tensioning Orientation: Ends and Midspan Skewed vs. Third Points

Skewed

As can be seen in Figure 5-12, using three skewed tie rods located 5'-0" from each abutment and at the midspan shows some improvement over using two skewed tie rods located at the third points of the 40'-0", 30^0 skewed bridge.
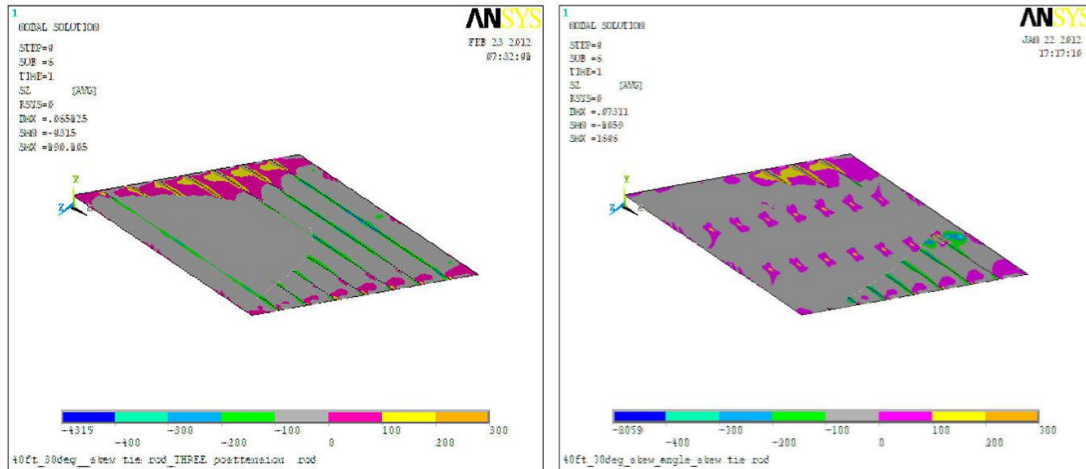
Figure 5-12: Transverse Stress Present at Slab-Deck Interface of a Forty Foot, Thirty Degree Skewed Bridge. (On the left, ends and midspan skewed; on the right, third points skewed.)

5.6 Fifty-Five Foot, Fifteen Degree Skewed Bridge

Two finite element models were created to determine the best transverse post-tensioning practice for a 55'-0", 15^0 skewed bridge. Two possible transverse post-tensioning orientations were considered: two normal tie rods (connecting all eight beams together) located at approximately the third points of the bridge and four skewed tie rods located 5'-0" and 20'-0" from each abutment.

5.6.1 Post-Tensioning Orientation: Four Skewed vs. Two Normal

As can be seen in Figure 5-13, using four skewed tie rods located 5'-0" and 20'-0" from each abutment shows little to no improvement over using two normal tie rods (connecting all eight beams together) located at approximately the third points of the 55'-0", 15^0 skewed bridge.
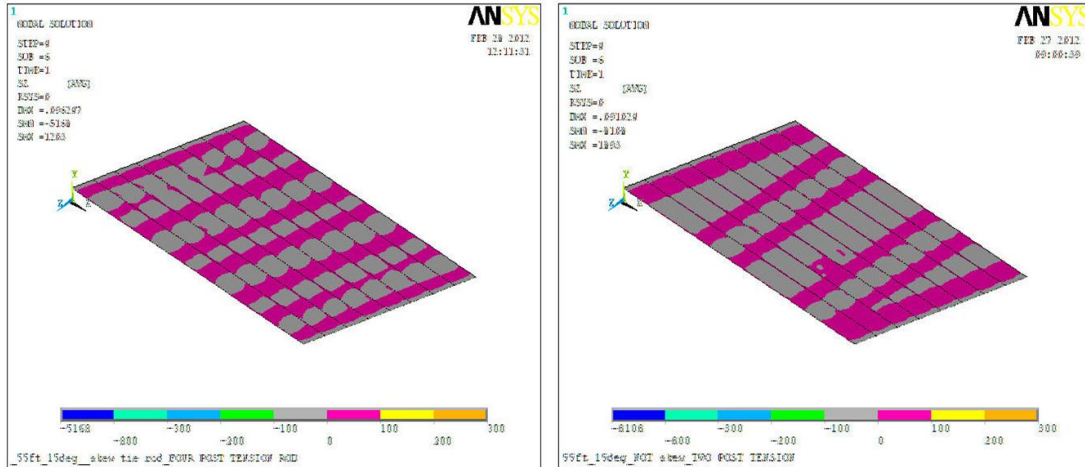
Figure 5-13: Transverse Stress Present at Slab-Deck Interface of a Fifty-Five Foot, Fifteen Degree Skewed Bridge. (On the left, four skewed; on the right, two normal.)

5.7 Fifty-Five Foot, Thirty Degree Skewed Bridge

Two finite element models were created to determine the best transverse post-tensioning practice for a 55'-0", 30^0 skewed bridge. Two possible transverse post-tensioning orientations were considered: two normal tie rods (connecting all eight beams together) located at approximately the third points of the bridge and four skewed tie rods located 5'-0" and 20'-0" from each abutment.

5.7.1 Post-Tensioning Orientation: Four Skewed vs. Two Normal

As can be seen in Figure 5-14, using four skewed tie rods located 5'-0" and 20'-0" from each abutment shows significant improvement over using two normal tie rods (connecting all eight beams together) located at approximately the third points of the 55'-0", 30^0 skewed bridge.
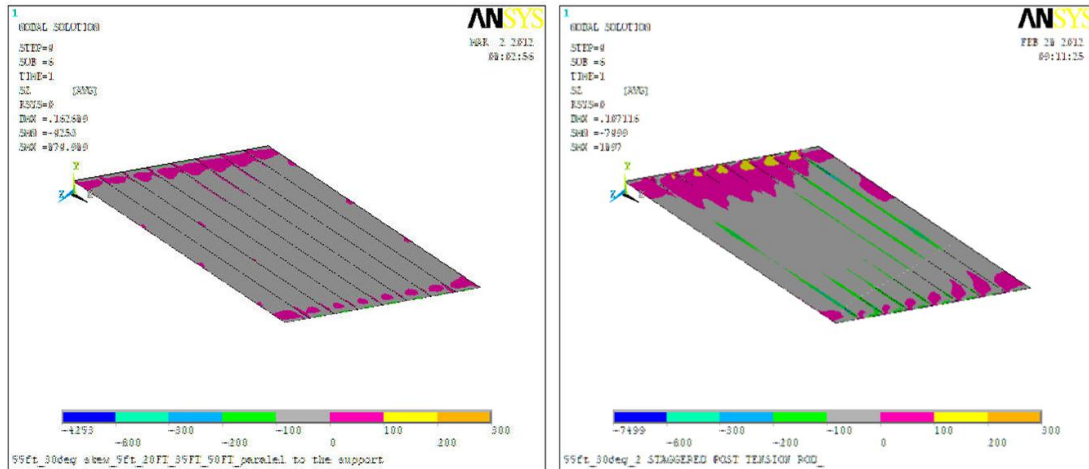
Figure 5-14: Transverse Stress Present at Slab-Deck Interface of a Fifty-Five Foot, Thirty Degree Skewed Bridge. (On the left, four skewed; on the right, two normal.)

5.8 MDSHA Requested Parametric Study Extension

5.8.1 Parametric Study Extension Description

Because constructing the transverse post-tensioning normal to the beams in the field is easier than constructing it parallel to the skew, the MDSHA requested that the parametric study be further extended to examine a combination of transverse post-tensioning orientations.   Previously, only two orientations for the transverse post-tensioning were considered: parallel to the bridge abutments (skewed tie rods) and normal to the slabs (normal/staggered tie rods). For this extension, a combination of these two orientations was considered: skewed tie rods near the abutments but normal tie rods near the midspan of the bridge. For brevity, this orientation combination will be referred to as "combined" in the descriptions in the following sections.   For consistency, our previously recommended transverse post-tensioning orientation is always placed on the left side of the page when comparing with these alternatives. When three tie rods are used in this combined configuration, only the middle tie rod is

84

normal to the beams; when four tie rods are used in this combined configuration, the two middle tie rods are normal to the beams. Miniature figures displaying the orientation of the transverse post-tensioning will be inset in the upper right of each of the following stress distribution figures. All other features of these six finite element models are the same as those created in the main parametric study.

5.8.2 Forty Foot, Fifteen Degree Skewed Bridge – Post-Tensioning Orientation: Three Skewed vs. Three Combined

As can be seen in Figure 5-15, using three skewed tie rods located 5'-0" from each abutment and at the midspan shows little to no improvement over using a combined configuration of two skewed tie rods located 5'-0" from each abutment and one normal tie rod (connecting all eight beams together) located at the midspan of the 40'-0", 15^0 skewed bridge.
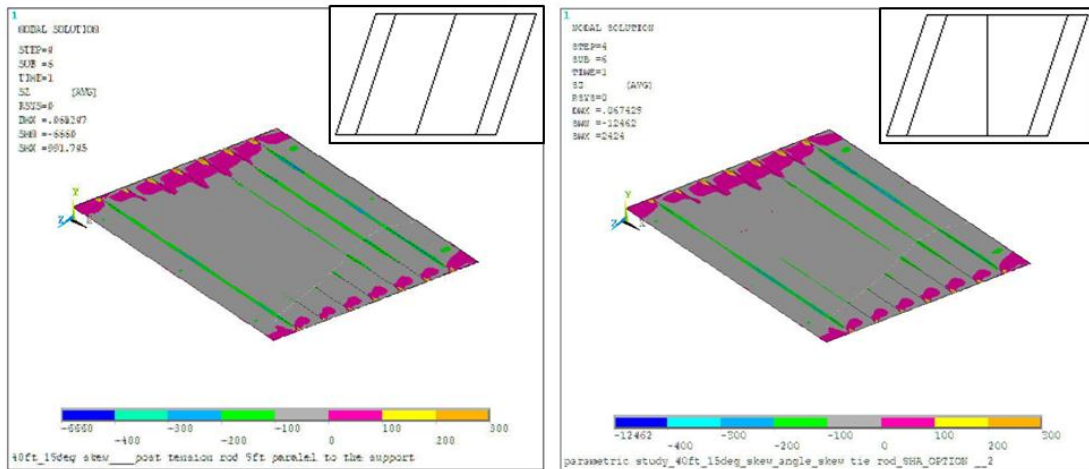

Figure 5-15: Transverse Stress Present at Slab-Deck Interface of a Forty Foot, Fifteen Degree Skewed Bridge. (On the left, ends and midspan skewed; on the right, three combined.)

85

5.8.3 Forty Foot, Thirty Degree Skewed Bridge – Post-Tensioning Orientation: Three

Skewed vs. Three Combined

As can be seen in Figure 5-16, using three skewed tie rods located 5'-0" from each abutment and at the midspan shows little to no improvement over using a combined configuration of two skewed tie rods located 5'-0" from each abutment and one normal tie rod (connecting all eight beams together) located at the midspan of the 40'-0", 30^0 skewed bridge, though there is a different stress distribution.
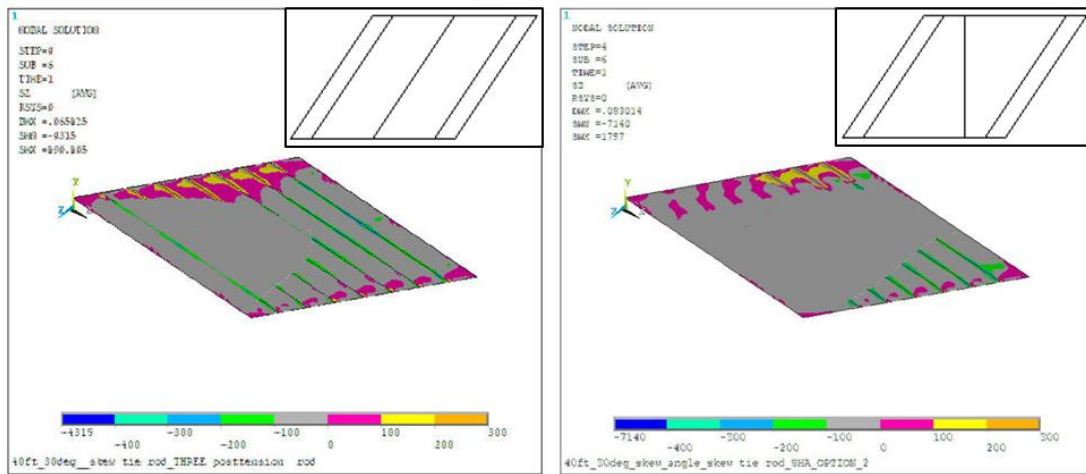
Figure 5-16: Transverse Stress Present at Slab-Deck Interface of a Forty Foot, Thirty Degree Skewed Bridge. (On the left, ends and midspan skewed; on the right, three combined.)

5.8.4 Fifty-Five Foot, Fifteen Degree Skewed Bridge – Post-Tensioning Orientation:

Four Skewed vs. Three Combined

As can be seen in Figure 5-17, using four skewed tie rods located 5'-0" and 20'-0" from each abutment shows little to no improvement over using a combined configuration of two skewed tie rods located 5'-0" from each abutment and one normal tie rod (connecting all eight beams together) located at the midspan of the 55'-0", 15^0 skewed bridge.
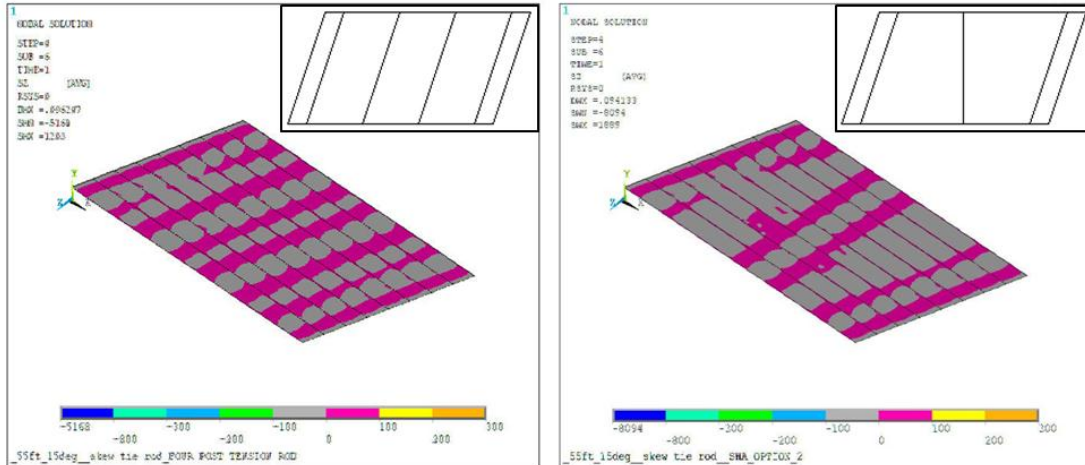
Figure 5-17: Transverse Stress Present at Slab-Deck Interface of a Fifty-Five Foot, Fifteen Degree Skewed Bridge. (On the left, four skewed; on the right, three combined.)

5.8.5 Fifty-Five Foot, Fifteen Degree Skewed Bridge – Post-Tensioning Orientation:

Four Skewed vs. Four Combined

As can be seen in Figure 5-18, using four skewed tie rods located 5'-0" and 20'-0" from each abutment shows little to no improvement over using a combined configuration of two skewed tie rods located 5'-0" from each abutment and two normal tie rods (connecting all eight beams together) located 20'-0" from each abutment of the 55'-0", 15^0 skewed bridge.
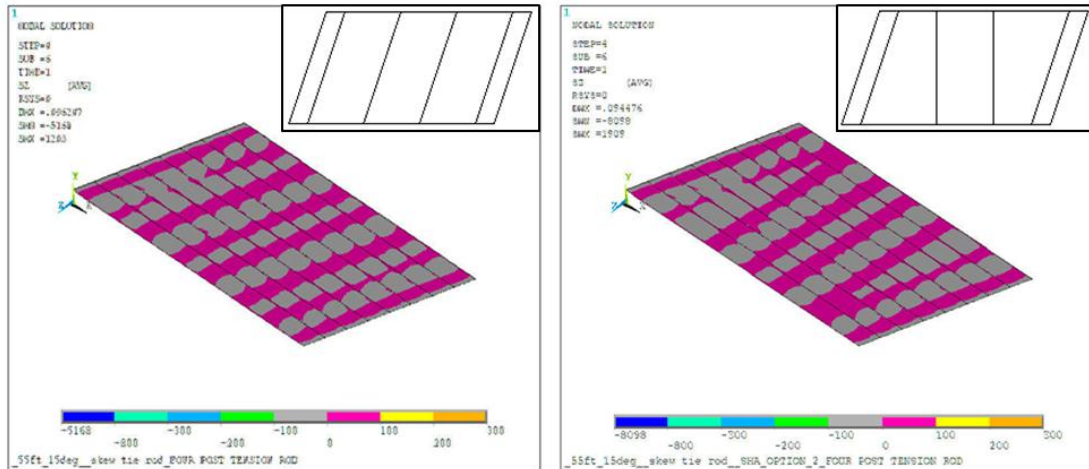
Figure 5-18: Transverse Stress Present at Slab-Deck Interface of a Fifty-Five Foot, Fifteen Degree Skewed Bridge. (On the left, four skewed; on the right, four combined.)

5.8.6 Fifty-Five Foot, Thirty Degree Skewed Bridge – Post-Tensioning Orientation:

Four Skewed vs. Three Combined

As can be seen in Figure 5-19, using four skewed tie rods located 5'-0" and 20'-0" from each abutment shows little to no improvement over using a combined configuration of two skewed tie rods located 5'-0" from each abutment and one normal tie rod (connecting all eight beams together) located 20'-0" located at the midspan of the 55'-0", 30^0 skewed bridge.
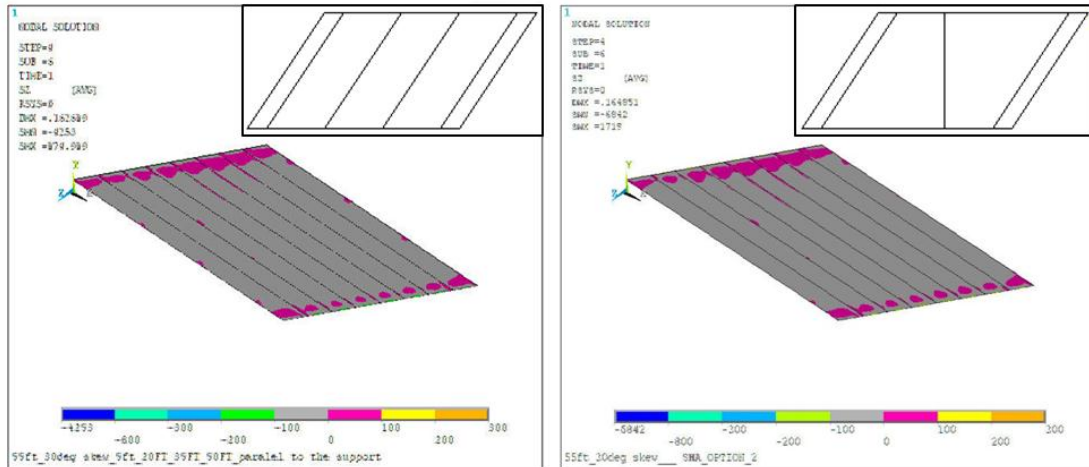
Figure 5-19: Transverse Stress Present at Slab-Deck Interface of a Fifty-Five Foot, Thirty Degree Skewed Bridge. (On the left, four skewed; on the right, three combined.)

5.8.7 Fifty-Five Foot, Thirty Degree Skewed Bridge – Post-Tensioning Orientation:

Four Skewed vs. Four Combined

As can be seen in Figure 5-20, using four skewed tie rods located 5'-0" and 20'-0" from each abutment shows little to no improvement over using a combined configuration of two skewed tie rods located 5'-0" from each abutment and two normal tie rods (connecting all eight beams together) located 20'-0" from each abutment of the 55'-0", 30^0 skewed bridge.
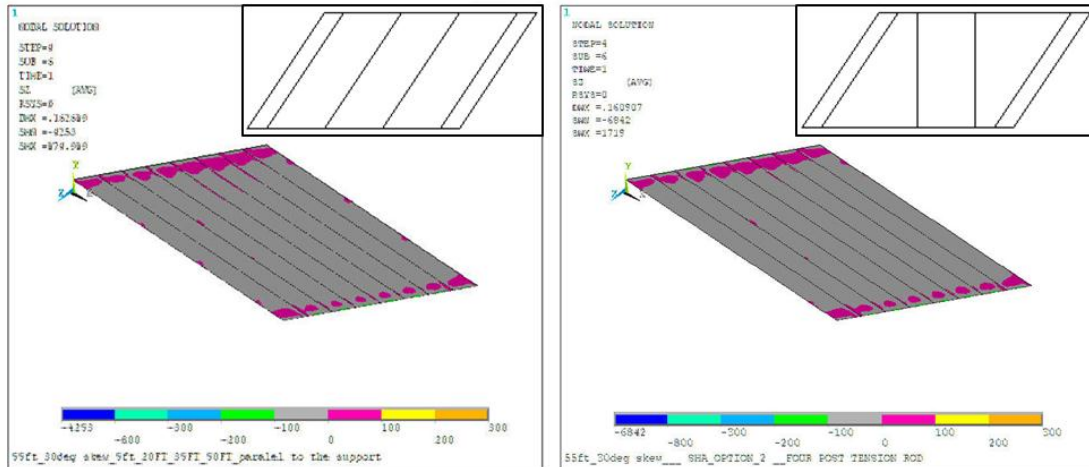
Figure 5-20: Transverse Stress Present at Slab-Deck Interface of a Fifty-Five Foot, Thirty Degree Skewed Bridge. (On the left, four skewed; on the right, four combined.)

5.8.8 Loading: Two Axle vs. Three Axle

In addition, one finite element model was created to examine loading effects on the longer bridges. An H-20 truck loading had been used for the parametric study for consistency within the study because only two axles (fourteen feet apart) could fit on the twenty-five foot span bridge. A standard HS-20 truck loading (a truck with an 8,000-pound front axle and two 32,000-pound rear axles with at least fourteen feet between each axle) was applied to the 55'-0", 15° skewed bridge model (with a combined transverse post-tensioning configuration using three tie rods) to confirm that there was no difference between the parametric study loading and the normal bridge design loading. As seen in Figure 5-21, there is negligible difference in the transverse stress at the slab-deck interface produced from the H-20 truck loading and the HS-20 truck loading.
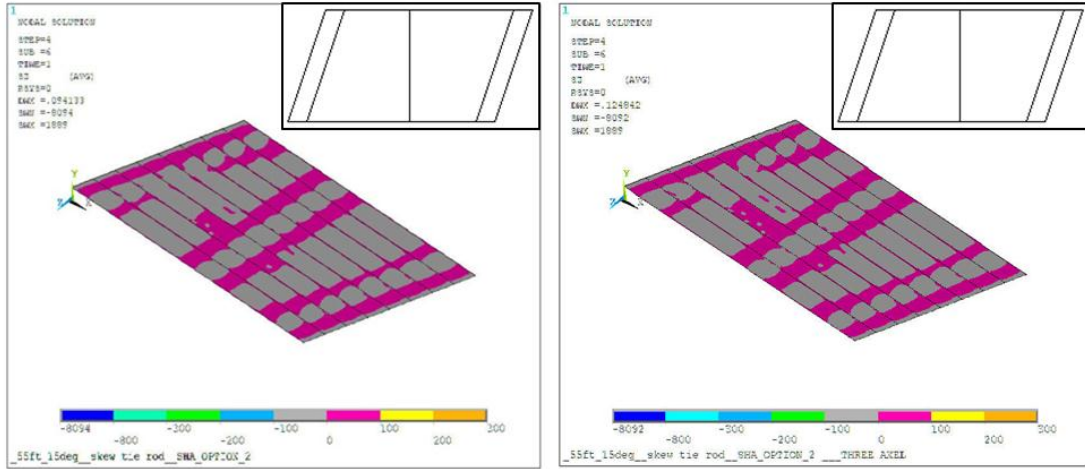
Figure 5-21: Transverse Stress Present at Slab-Deck Interface of a Fifty-Five Foot, Thirty Degree Skewed Bridge. (On the left, H-20 (two axle) load; on the right, HS-20 (three axle) load.)

Chapter 6: Conclusions and Recommendations

6.1 Causes of Knoxville Bridge Cracks

Four possible contributors to the reflective cracking on the top surface of the concrete overlay of the Knoxville, MD, bridge are temperature effects, shrinkage of the grout, the large skew angle, and the vehicle loads. It is often the bond between the shear key and the concrete beams that is the weakest point and the cause of failure; this is critical because the bond has a lower strength than either the grout or the concrete (Sharpe, 2007). It has been reported that often thermal loads are the cause of crack initiation, sometimes even before a bridge is opened to traffic, which may have contributed to this specific case (Sharpe, 2007, and Badwan and Liang, 2007). In addition, conventional grout has relatively low shear and tensile strength, approximately 360 psi and 220 psi, respectively, but tests have recorded failure at as little as 61 psi (longitudinal shear) and 75 psi (direct tension) (Sharpe, 2007). From this parametric study (discussed in Chapter 5), it is clear that large skew angles (as in this case where skew is 31.4°) significantly increase the amount of transverse stress (tension) applied to the shear keys, especially at the abutments. From the field test and the finite element model of the bridge conducted in this study, it is evident that the bridge is undergoing large strains and significant enough stresses to at least continue to propagate the existing cracks.

6.2 Parametric Study Recommendations for Skewed Transversely Post-Tensioned Slab Bridges

Based on the results from the twenty-eight finite element models in the parametric study and extension, a few conclusions were reached to reduce the likelihood of reflective cracking on the top surfaces of precast concrete multi-beam bridges. The transverse post-tensioning orientation and locations can greatly decrease the stresses caused by vehicular loads. Transversely post-tensioning should be done parallel to the supports (i.e. parallel to the skew), especially when near the abutments, of a skewed adjacent precast concrete slab bridge instead of normal to the beams due to the decrease of transverse stresses present at the slab-deck interface. It is preferred to build bridges with as small a skew as is practical, but certainly not greater than 30^0 due to the significant increase in transverse stress as the skew angle increases. Table 6-1 summarizes the preliminary recommendations for the MDSHA bridge design standards.

Table 6-1: Recommended Skew Particulars for Transversely Post-Tensioned Adjacent Precast Concrete Slab Bridge Standard in Maryland.

Span (feet)	Maximum Skew Angle (degrees)	Number of Transverse Tie Rods	Orientation of Transverse Tie Rods	Location of Transverse Tie Rods
< 30	30	2	Parallel to Skew	Third Points (L/3)
30 – 45	30	3	Parallel to Skew	5'-0" from Supports and Midspan (L/2)
> 45	30	4	Parallel to Skew	5'-0" and 20'-0" from Supports

From the extension of the parametric study requested by the MDSHA, placing the transverse post-tensioning tie rods normal to the beams instead of parallel to the skew near the midspan of the bridge has a negligible effect on the resulting transverse

stress at the slab-deck interface. As a result, it is also recommended that the MDSHA bridge design standards provide the following notes: (1) the tie rods closest to the abutment are required to be constructed parallel to the skew of the bridge, (2) the tie rods near the midspan of the bridge may be constructed normal to the beams as long as the maximum spacing between the ends of adjacent tie rods on both sides of the bridge is less than twenty-five feet, and (3) transverse post-tensioning may be staggered (i.e. one tie rod not connecting all of the beams) as long as it is overlapping should the bridge width require it.

6.3 Construction Details Recommendations

It is recommended that full-depth shear key designs be looked into further as full-depth shear keys have been shown to be much more effective than partial-depth shear keys at transferring shear force between beams and can reduce shear key-related longitudinal cracking up to 50% (Russell, 2009). It is also recommended that the construction sequence be changed to grouting the shear keys before transversely post-tensioning the slabs. When the slabs are post-tensioned before grouting, the transverse stress at the points where the slabs are in contact increase and the grout merely acts as a filler, transferring a minimal amount of shear force and only transferring the compressive stress of any transverse bending moments (Russell, 2009). Conversely, grouting before post-tensioning places compressive stress in the grout and across the interface, both allowing the shear key to transfer more shear force and providing a higher moment capacity while minimizing any tensile stresses that may occur in the shear key leading to longitudinal cracking (Russell, 2009). A few states have included a construction sequence detail in their bridge design

specifications and reported it successfully reducing the amount cracking in adjacent precast concrete multi-beam bridges where first the transverse tendons are tensioned to approximately a tenth of the total force, then the shear keys are filled with grout, and finally the transverse tendons are tensioned to the full post-tensioning force (Massachusetts Department of Transportation, 2009, Rhode Island Department of Transportation, 2010, Russell, 2011, and Vermont Agency of Transportation, 2011).

Appendix A: Source Websites for the Survey of State

Practices for Transversely Post-Tensioned Bridges

Arizona Department of Transportation (ADOT) (2007). *Bridge Design Guidelines*. August 17, 2011. <http://www.azdot.gov/Highways/bridge/Guidelines/DesignGuidelines/>.

District of Columbia Department of Transportation (DDOT) (2009). *Design and Engineering Manual*. August 17, 2011. <http://ddot.dc.gov/DC/DDOT/Projects+and+Planning/Standards+and+Guidelines/Design+and+Engineering+Manual/DDOT+Design+and+Engineering+Manual+-+April+2009>.

Indiana Department of Transportation (INDOT) (2011). *The Indiana Design Manual*. August 25, 2011. <http://www.in.gov/dot/div/contracts/standards/dm/2011/index.html>.

Kentucky Department of Highways (2008). *Kentucky Standard Drawings*. August 25, 2011. <http://transportation.ky.gov/Highway-Design/Standard%20Drawing%20%20Sepia%20PDFs/Structure-SERIES2008.pdf#bdp004-03>.

Massachusetts Department of Transportation (MassDOT) (2009). *2009 LRFD Bridge Manual*. August 25, 2011. <http://www.mhd.state.ma.us/default.asp?pgid=bridge/bridgemanual_01&sid=about>.

Michigan Department of Transportation (MDOT) (2011). *Bridge Design Guides*. August 25, 2011. <http://mdotwas1.mdot.state.mi.us/public/design/englishbridgeguides/>.

New York State Department of Transportation (NYSDOT) (2011). *Bridge Manual*. August 25, 2011. <https://www.dot.ny.gov/divisions/engineering/structures/manuals/bridge-manual-usc>.

North Carolina Department of Transportation (NCDOT) (2012). *Standard Specifications for Roads and Structures*. February 20, 2012. <http://www.ncdot.gov/doh/preconstruct/ps/specifications/2012draft.pdf>.

Ohio Department of Transportation (ODOT) (2007). *Bridge Design Manual (BDM 2007)*. August 29, 2011.

<http://www.dot.state.oh.us/Divisions/Engineering/Structures/standard/Bridge
s/Pages/BDM2007.aspx>.

Ohio Department of Transportation (ODOT) (2011). *Standard Bridge Drawings*.
August 25, 2011.
<http://www.dot.state.oh.us/Divisions/Engineering/Structures/standard/Bridge
s/Pages/StandardBridgeDrawings.aspx>.

Oregon Department of Transportation (ODOT) (2004, rev. April 2011). *Bridge
Design and Drafting Manual*. February 20, 2012.
<http://www.oregon.gov/ODOT/HWY/BRIDGE/docs/BDDM/apr-
2011_finals/section_1-2004_apr2011.pdf>.

Pennsylvania Department of Transportation (2011). *Bridge Standard Drawings*.
February 20, 2012.
<http://www.dot.state.pa.us/Internet/BQADStandards.nsf/home?OpenFramese
t>.

Rhode Island Department of Transportation (RIDOT) (2010). *Bridge Design
Standard Details*. August 29, 2011.
<http://www.dot.ri.gov/documents/engineering/BlueBook/RIDOT_Bridge_St
andards%202010.pdf>.

South Carolina Department of Transportation (SCDOT) (2007). *2007 Standard
Specifications for Highway Construction*. February 22, 2012.
<http://www.scdot.org/doing/construction_StandardSpec.aspx>.

South Carolina Department of Transportation (SCDOT) (2010). *Bridge Drawings and
Details*. February 22, 2012.
<http://www.scdot.org/doing/structural_Drawings.aspx>.

State of Connecticut Department of Transportation (ConnDOT) (2003). *Bridge
Design Manual*. August 17, 2011.
<http://www.ct.gov/dot/lib/dot/documents/dpublications/bridge/bdm.pdf>.

Texas Department of Transportation (TXDOT) (2011). *Bridge Design Manual -
LRFD*. February 20, 2012.
<http://onlinemanuals.txdot.gov/txdotmanuals/lrf/index.htm>.

Texas Department of Transportation (TXDOT) (2012). *Superstructure Design
Information*. February 20, 2012.
<http://www.txdot.gov/business/contractors_consultants/bridge/super_design.
htm>.

Vermont Agency of Transportation (VTrans) (2010). *Structures Design Manual*.
February 20, 2012.
<http://www.aot.state.vt.us/progdev/Publications/DocumentsPUBLICATION
S/Structures_Design_Manual.pdf>.

Vermont Agency of Transportation (VTrans) (2011). *2011 Standard Specifications
for Construction Book*. February 20, 2012.
<http://www.aot.state.vt.us/conadmin/2011StandardSpecs.htm>.

Washington Department of Transportation (WSDOT) (2012). *Bridge Design Manual
LRFD*. February 22, 2012.
<http://www.wsdot.wa.gov/Publications/Manuals/M23-50.htm>.

West Virginia Division of Highways (WVDOH) (2004). *Bridge Design Manual*.
February 22, 2012.
<http://www.transportation.wv.gov/highways/engineering/files/WVBDML.pd
f>.

Wisconson Department of Transportation (WisDOT) (2012). *LRFD Bridge Manual*.
February 22, 2012.
<http://on.dot.wi.gov/dtid_bos/extranet/structures/LRFD/LRFDManualIndex.
htm>.

Wyoming Department of Transportation (WYDOT) (2008). *Bridge Applications
Manual*. February 22, 2012.
<http://www.dot.state.wy.us/wydot/engineering_technical_programs/bridge/br
idge_applications_manual>.

Appendix B: Knoxville, MD, Test Bridge Plans
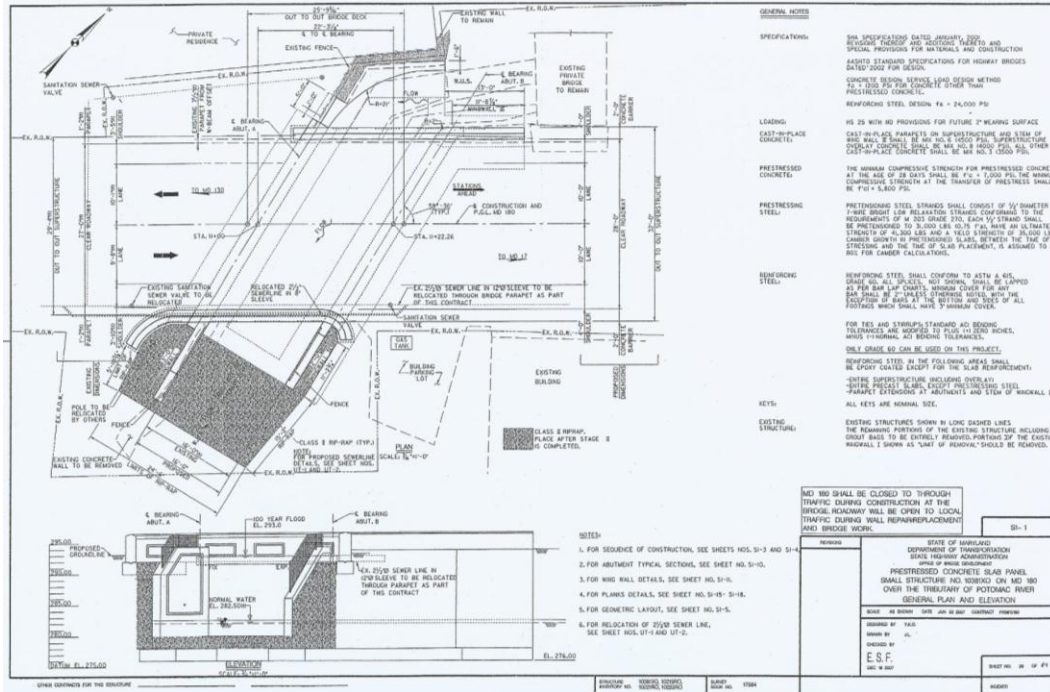
Figure B-1: General Plan and Elevation View of the Knoxville Bridge.

Figure B-2: Information Summary of the Knoxville Bridge.

Figure B-3: Abutment and Corner Details of the Knoxville Bridge
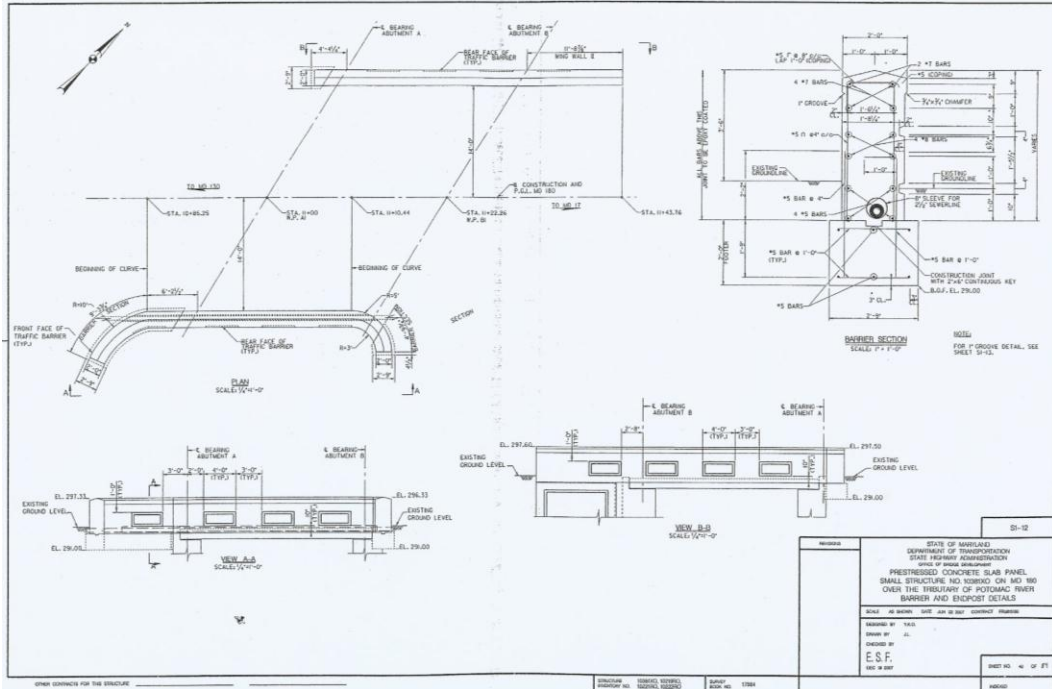
Figure B-4: Parapet Details of the Knoxville Bridge
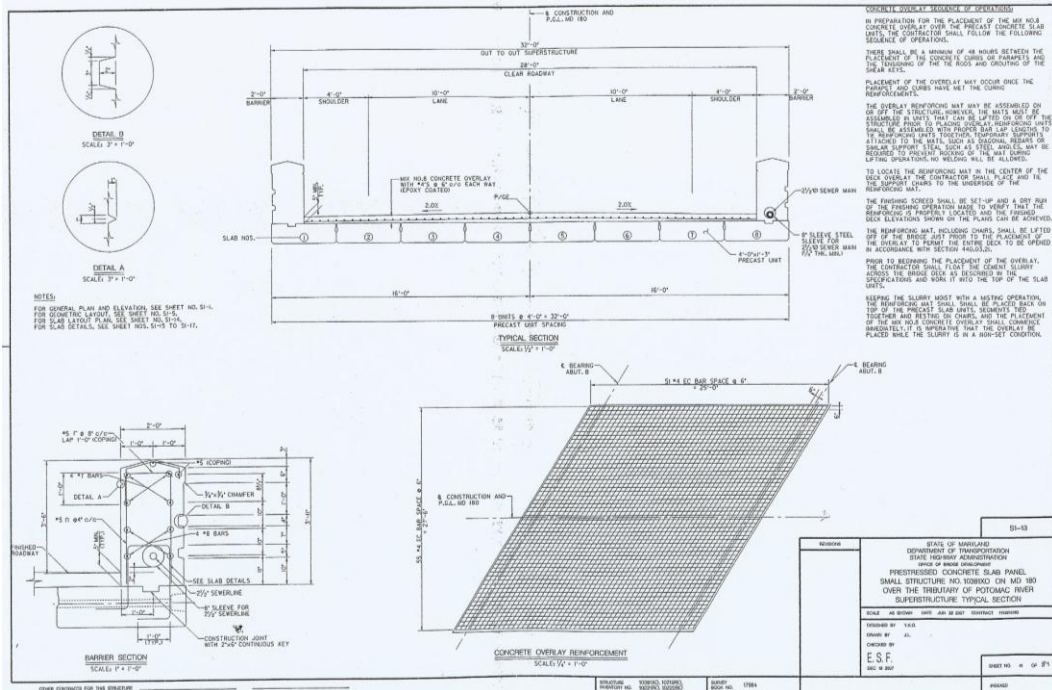
Figure B-5: Knoxville Bridge Superstructure Typical Section.

101
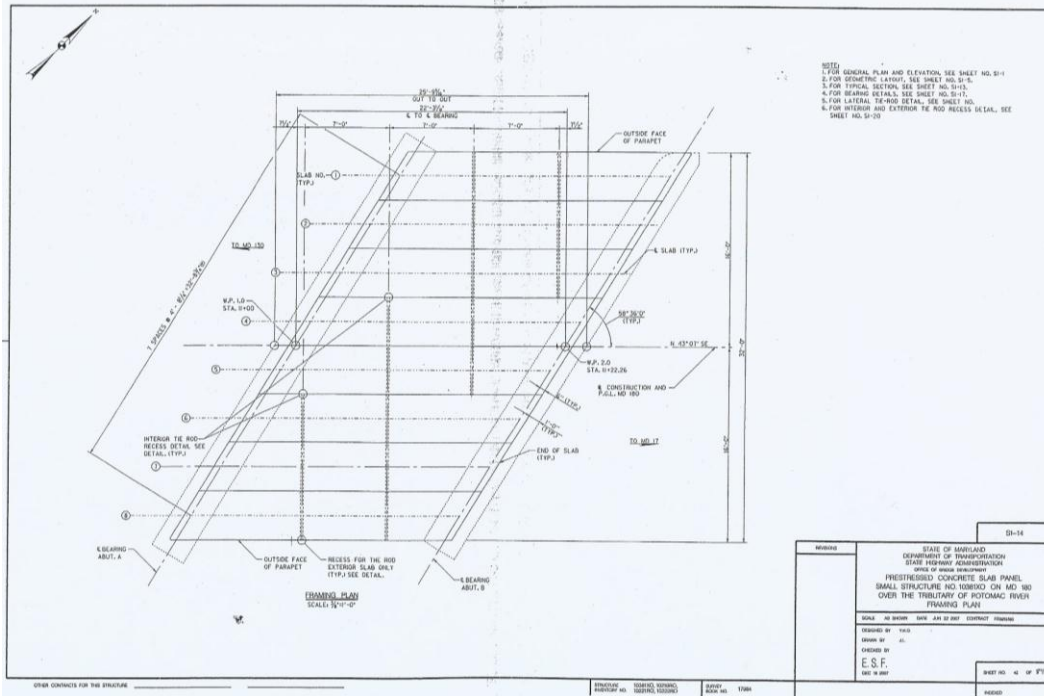
Figure B-6: Knoxville Bridge Framing Plan.
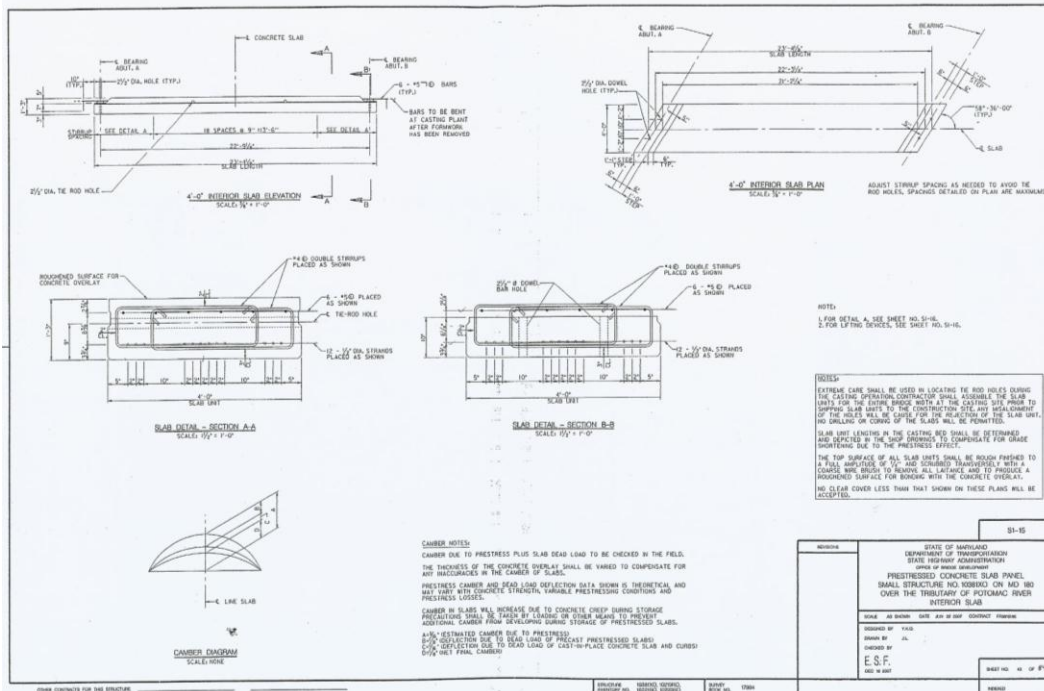
Figure B-7: Slab Details of the Knoxville Bridge.
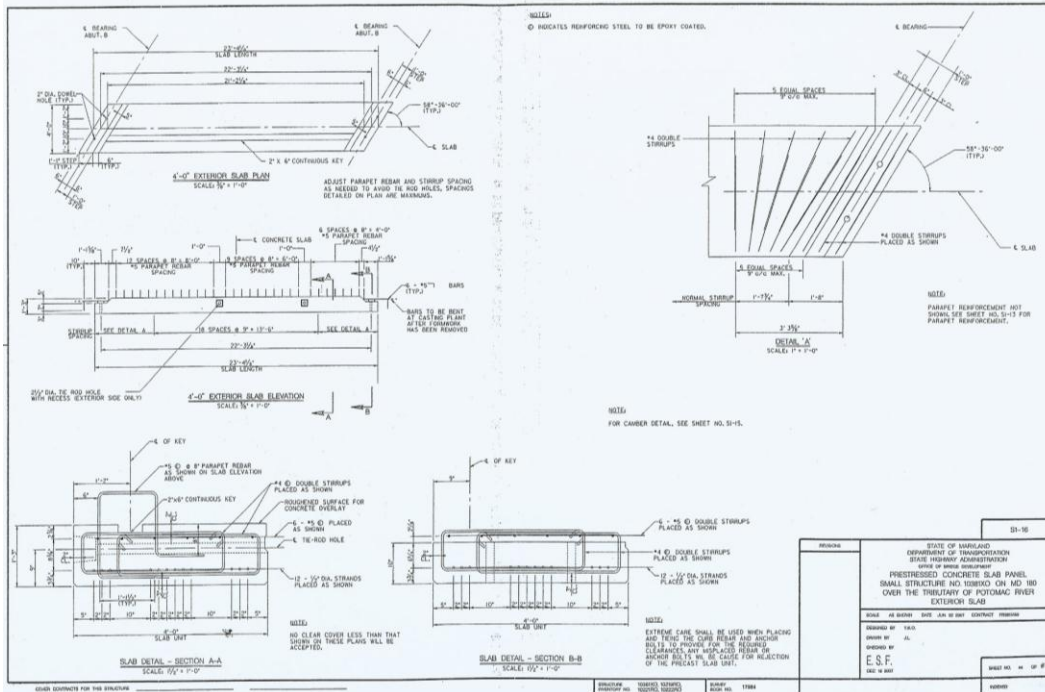
Figure B-8: Reinforcement Details of the Knoxville Bridge.
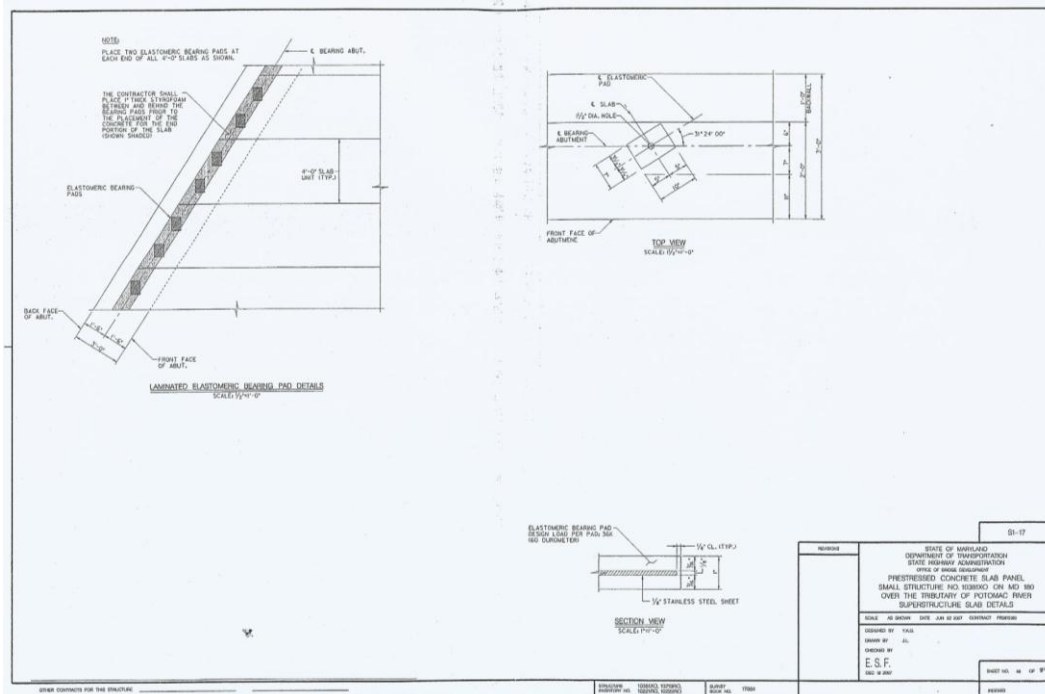
Figure B-9: Bearing Details of the Knoxville Bridge.

103

Figure B-10: Transverse Post-Tensioning Details of the Knoxville Bridge.

Appendix C: Full Results from Parametric Study

C.1 Twenty-Five Foot, Fifteen Degree Skewed Bridge – One Truck Loading
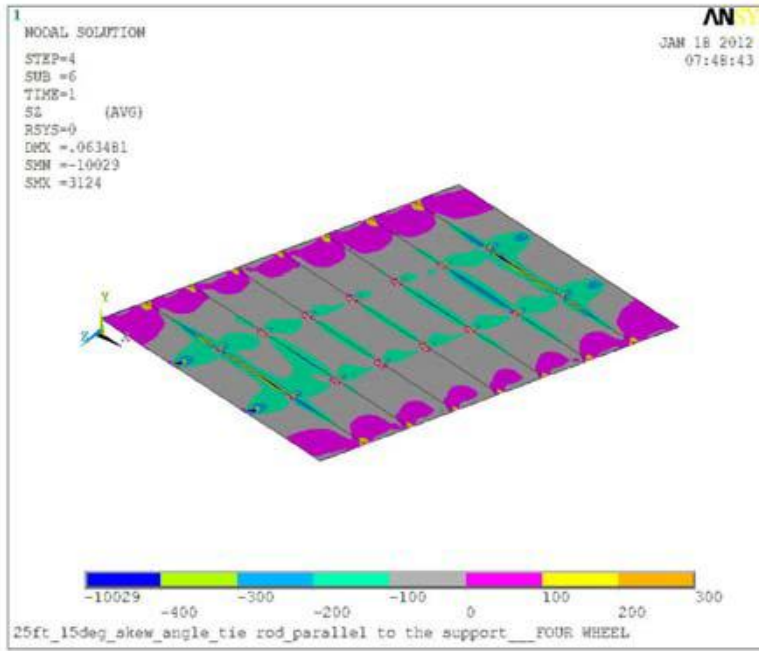

**Figure C-1: Transverse Stress at the Beam-Overlay Interface.**
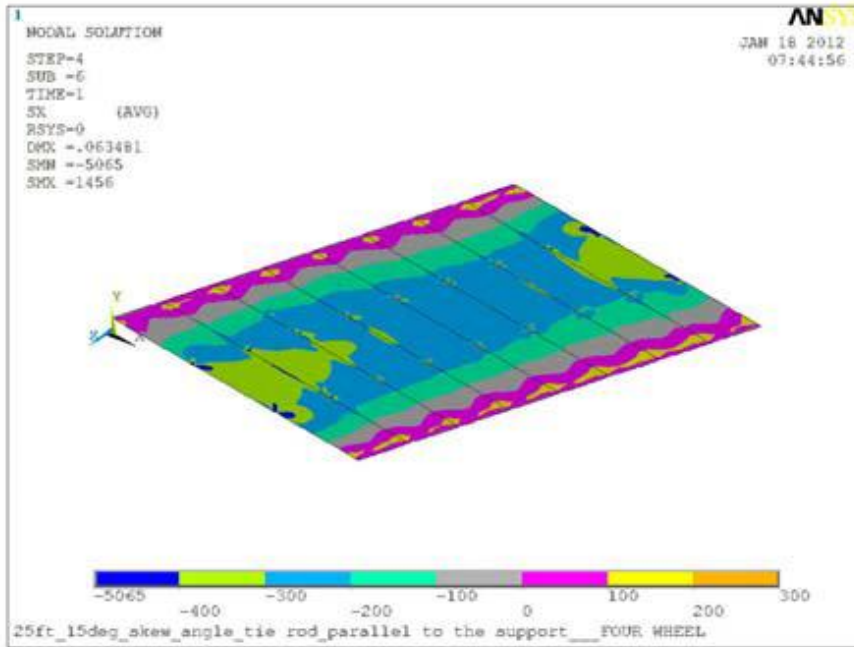
Figure C-2: Longitudinal Stress at the Beam-Overlay Interface.
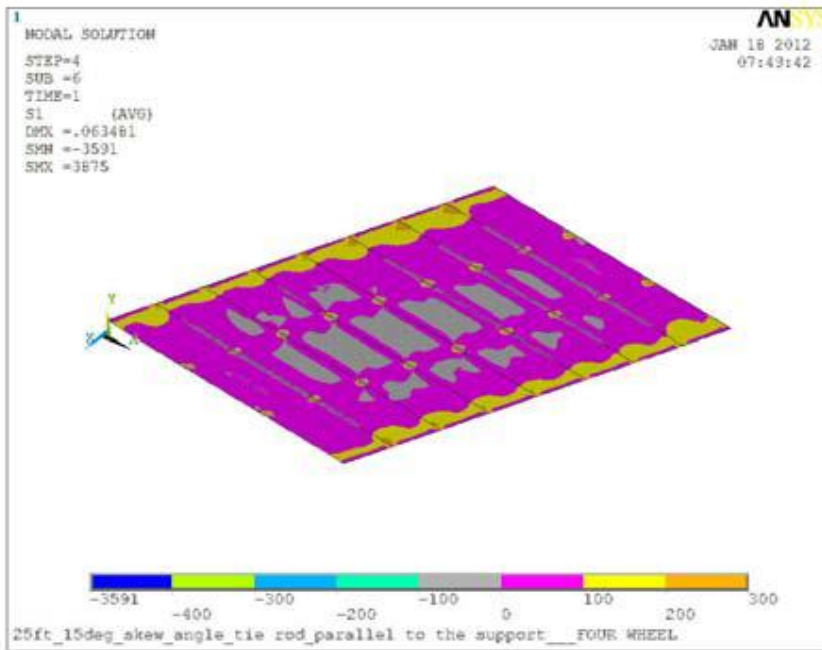
Figure C-3: First Principal Stress at the Beam-Overlay Interface.

106
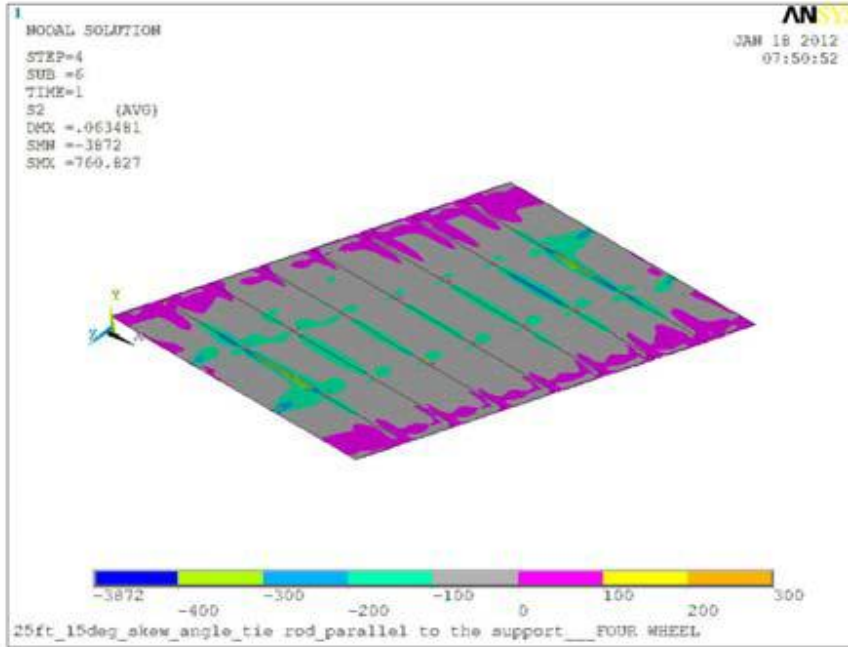
Figure C-4: Second Principal Stress at the Beam-Overlay Interface.
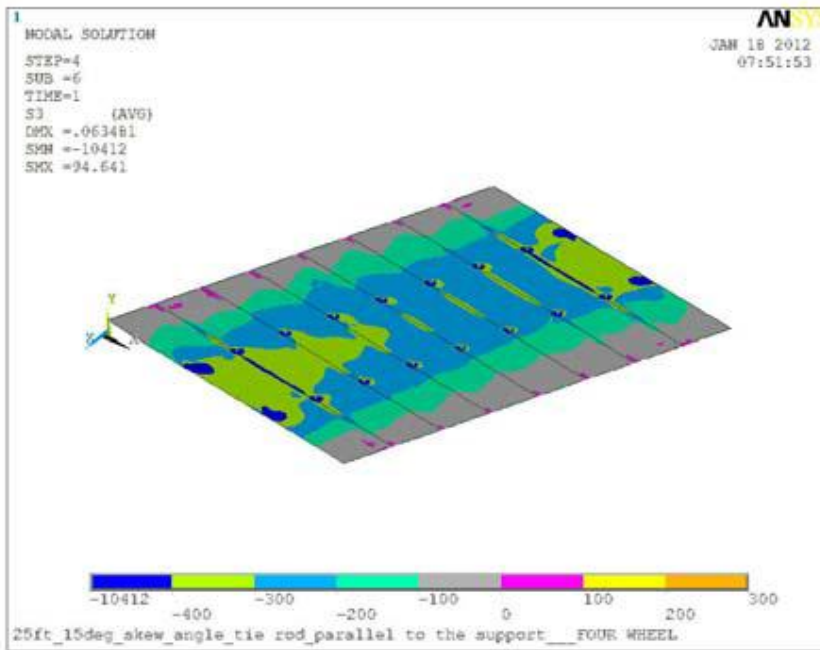
Figure C-5: Third Principal Stress at the Beam-Overlay Interface.

C.2 Twenty-Five Foot, Fifteen Degree Skewed Bridge – Two Truck Loading
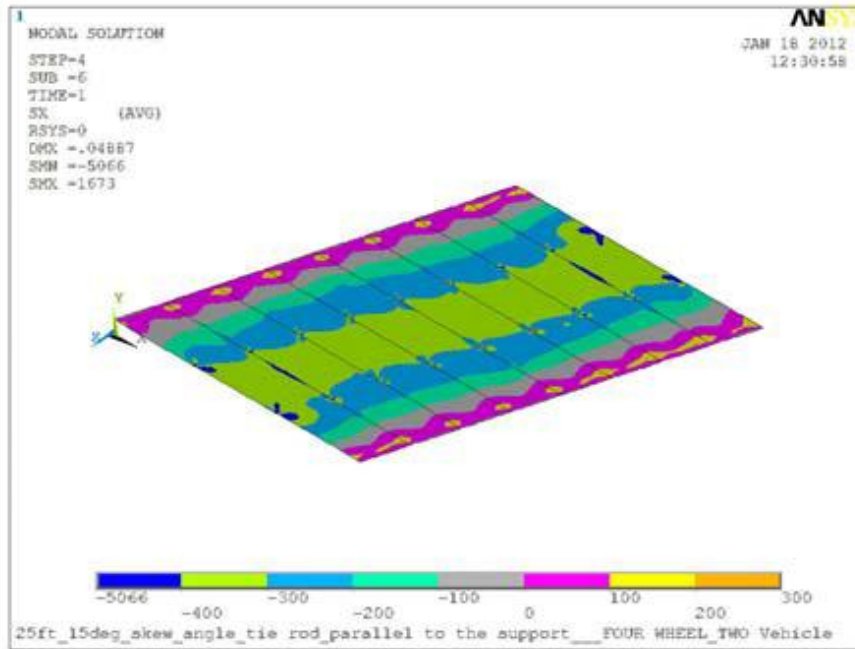
Figure C-6: Longitudinal Stress at the Beam-Overlay Interface.
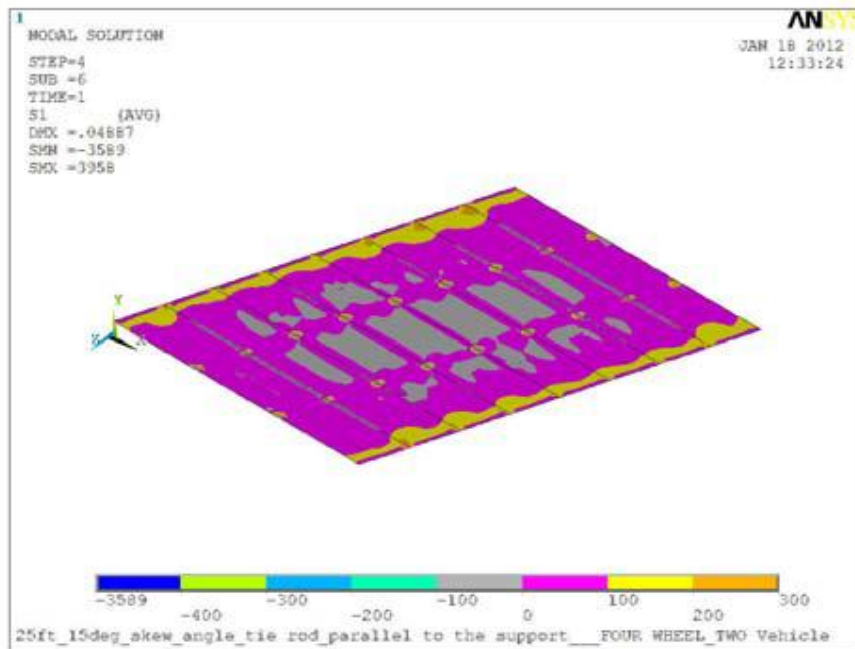
Figure C-7: First Principal Stress at the Beam-Overlay Interface.

C.3 Twenty-Five Foot, Fifteen Degree Skewed Bridge – Four Normal and Staggered
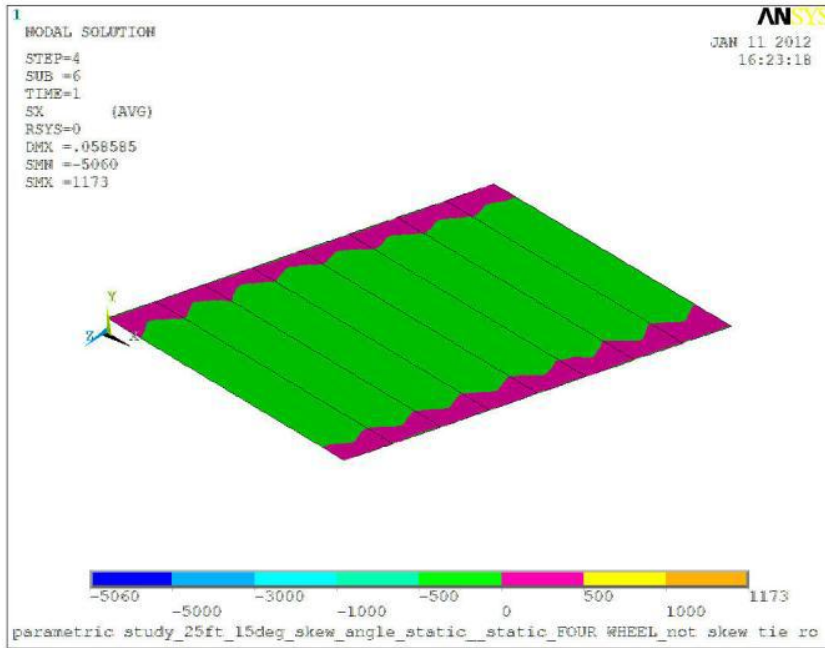
Figure C-8: Longitudinal Stress at the Beam-Overlay Interface.
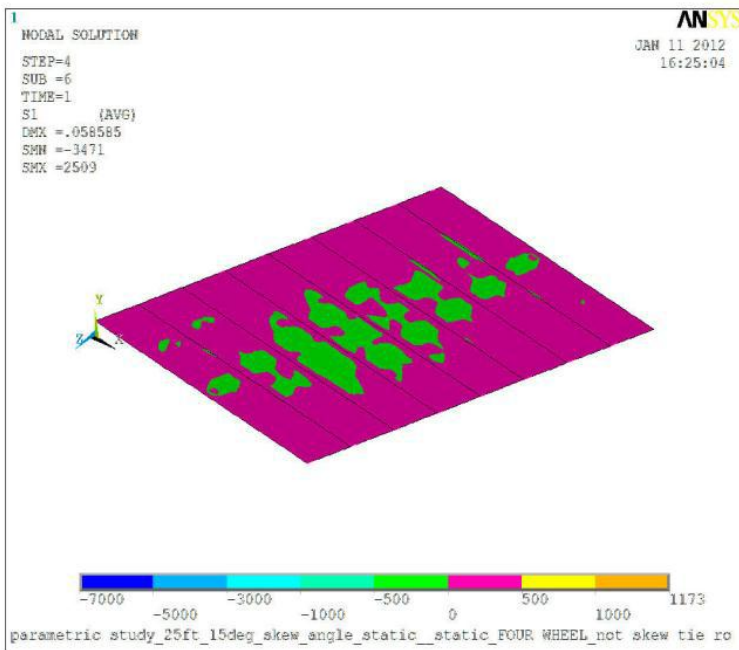
**Figure C-9: First Principal Stress at the Beam-Overlay Interface.**

109

C.4 Twenty-Five Foot, Fifteen Degree Skewed Bridge – Third Points Skewed
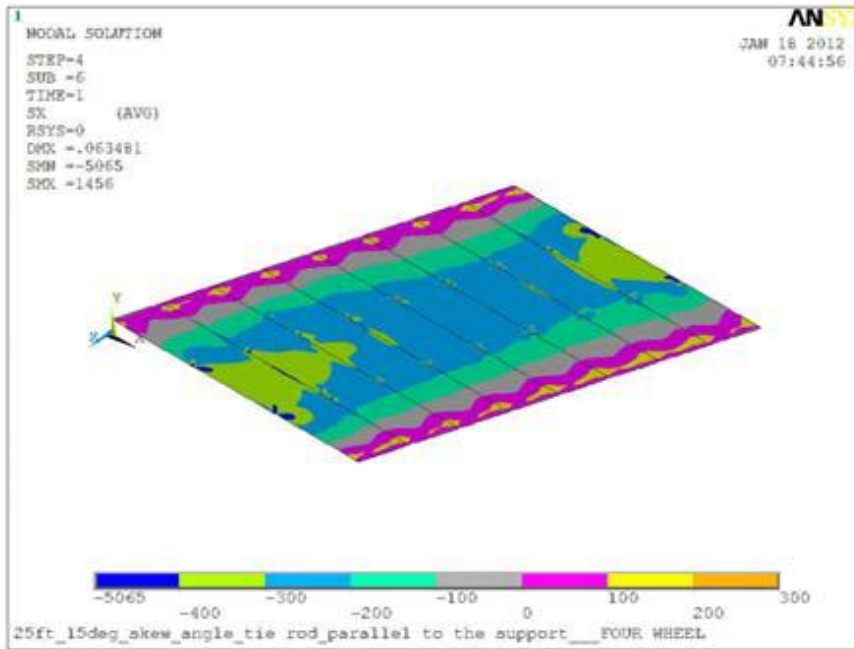
**Figure C-10: Longitudinal Stress at the Beam-Overlay Interface.**
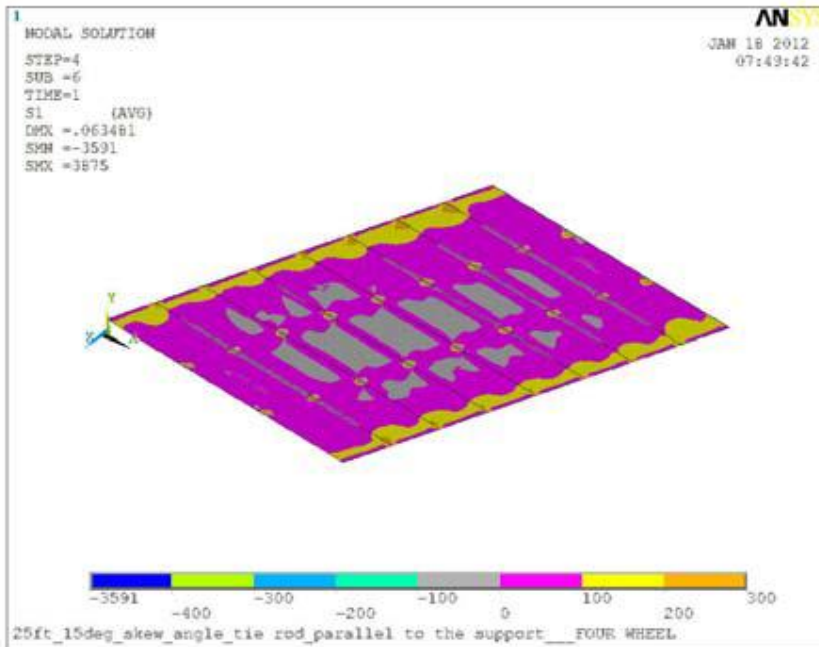
Figure C-11: First Principal Stress at the Beam-Overlay Interface.

C.5 Twenty-Five Foot, Fifteen Degree Skewed Bridge – Ends Skewed
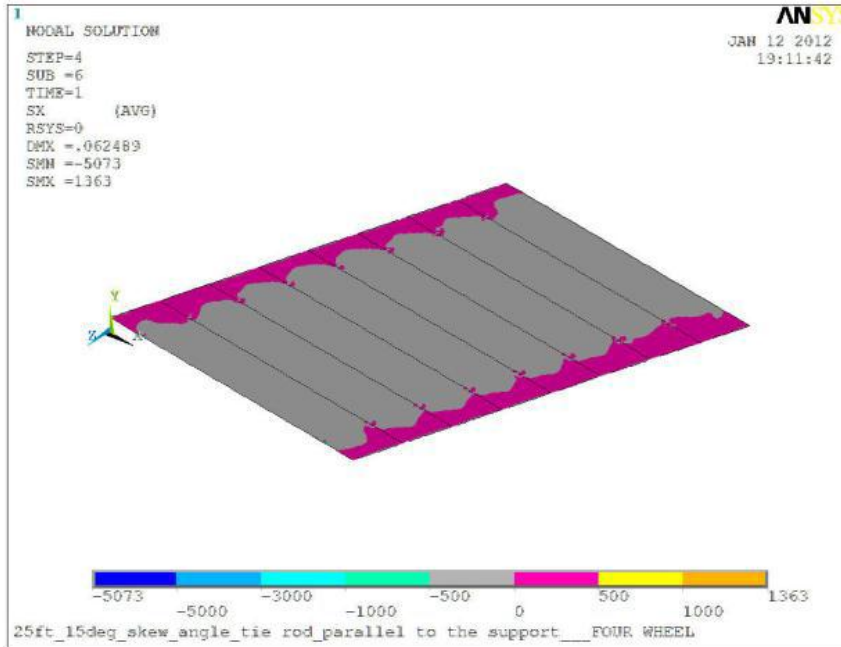
**Figure C-12: Longitudinal Stress at the Beam-Overlay Interface.**
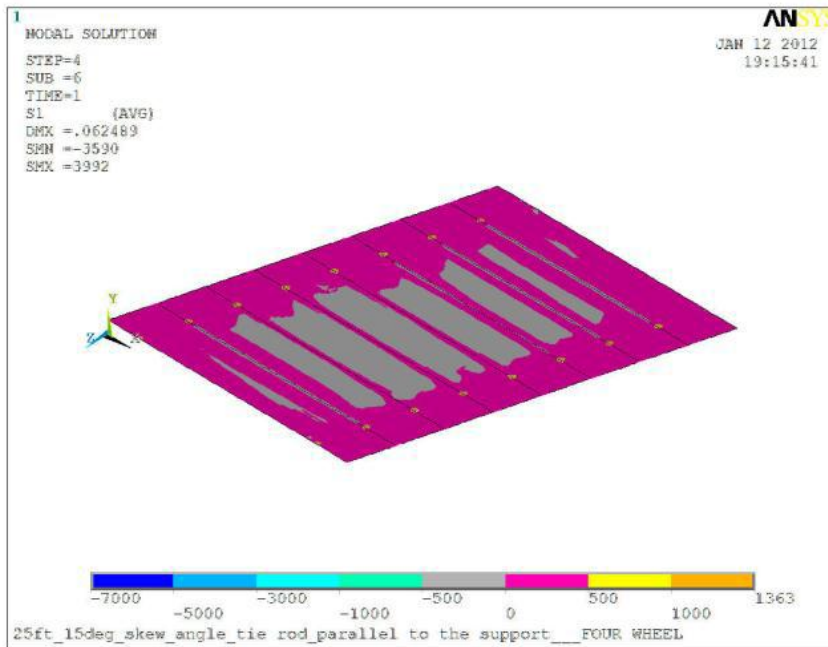
Figure C-13: First Principal Stress at the Beam-Overlay Interface.

## C.6 Twenty-Five Foot, Fifteen Degree Skewed Bridge – Ends and Midspan
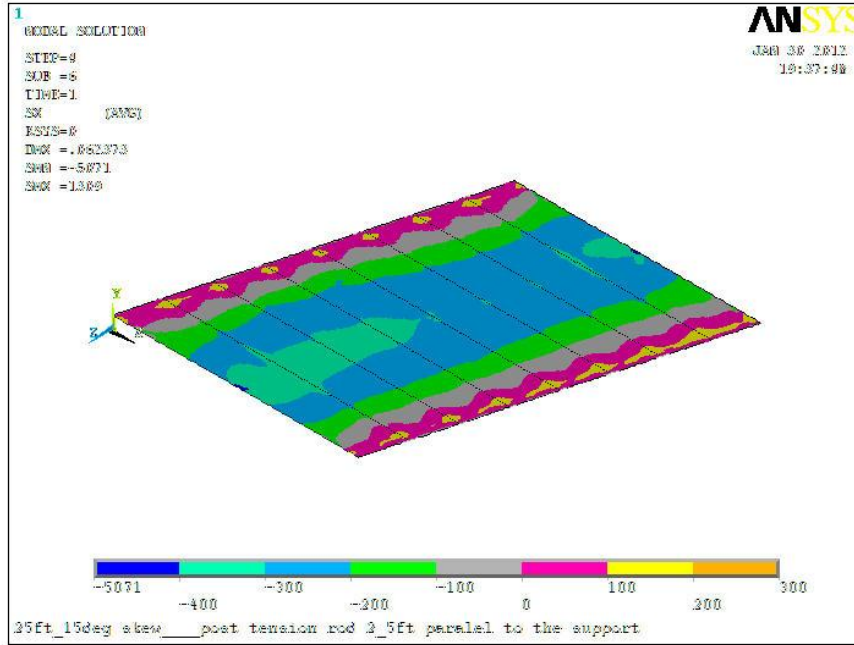
Skewed

Figure C-14: Longitudinal Stress at the Beam-Overlay Interface.
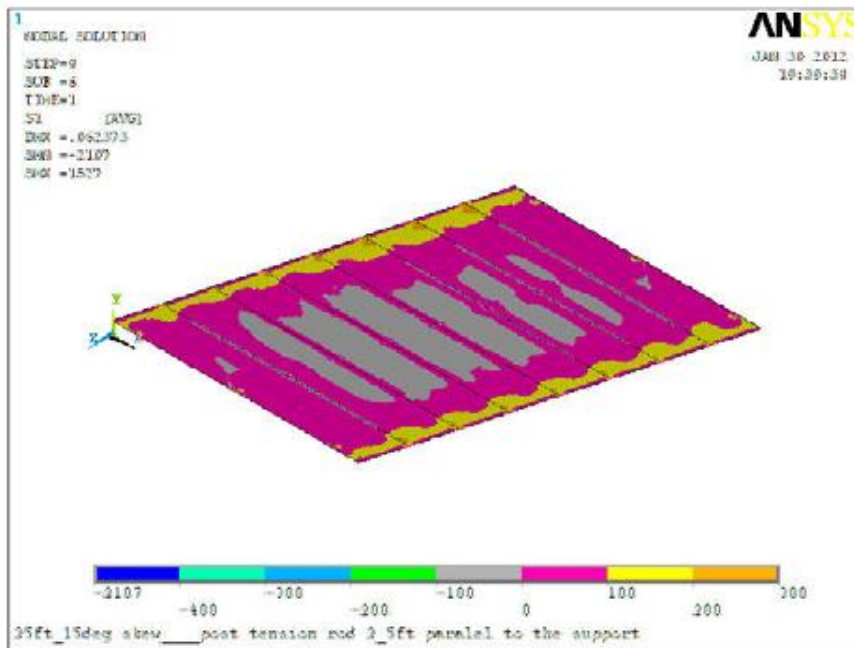
Figure C-15: First Principal Stress at the Beam-Overlay Interface.

112

C.7 Twenty-Five Foot, Thirty Degree Skewed Bridge – Four Normal and

Staggered
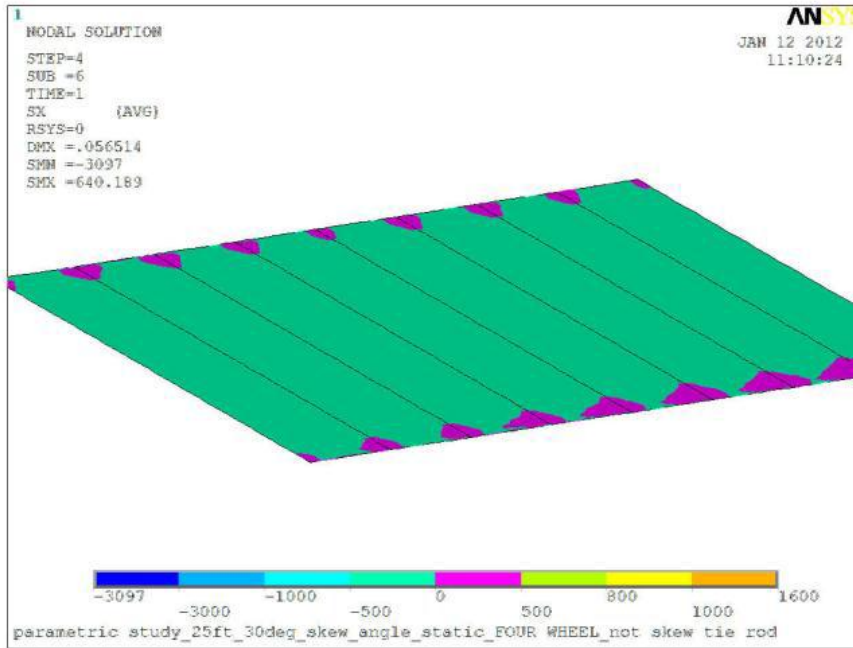
Figure C-16: Longitudinal Stress at the Beam-Overlay Interface.
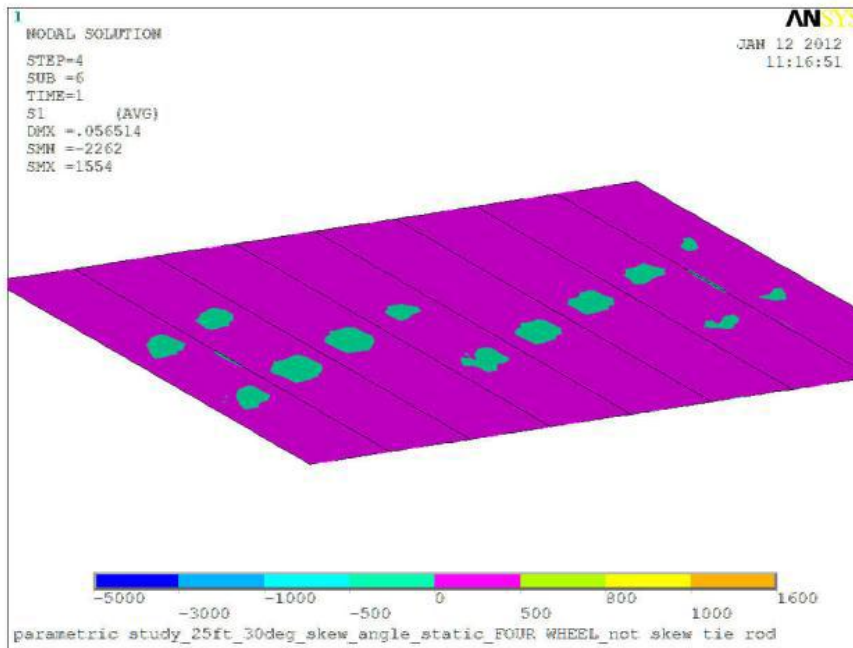
Figure C-17: First Principal Stress at the Beam-Overlay Interface.

113

C.8 Twenty-Five Foot, Thirty Degree Skewed Bridge – Third Points Skewed
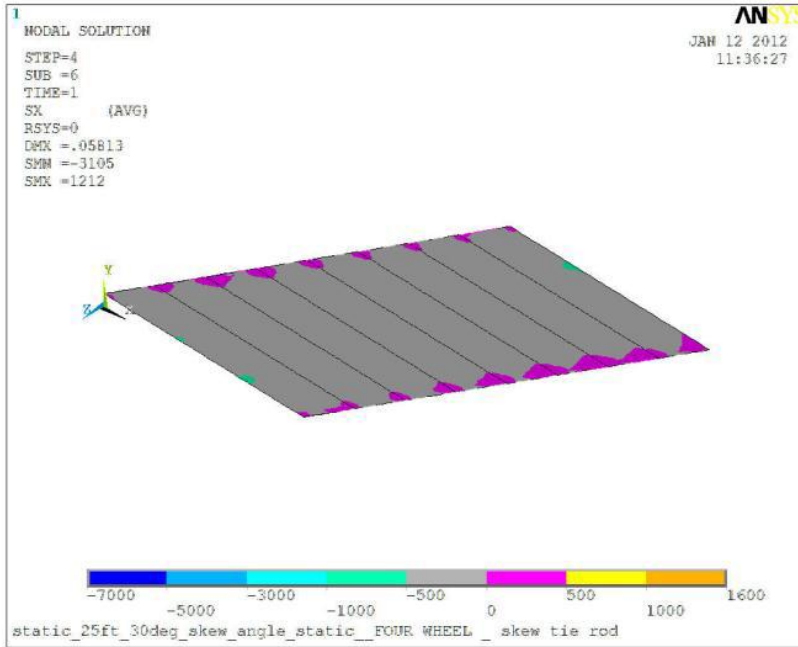

Figure C-18: Longitudinal Stress at the Beam-Overlay Interface.
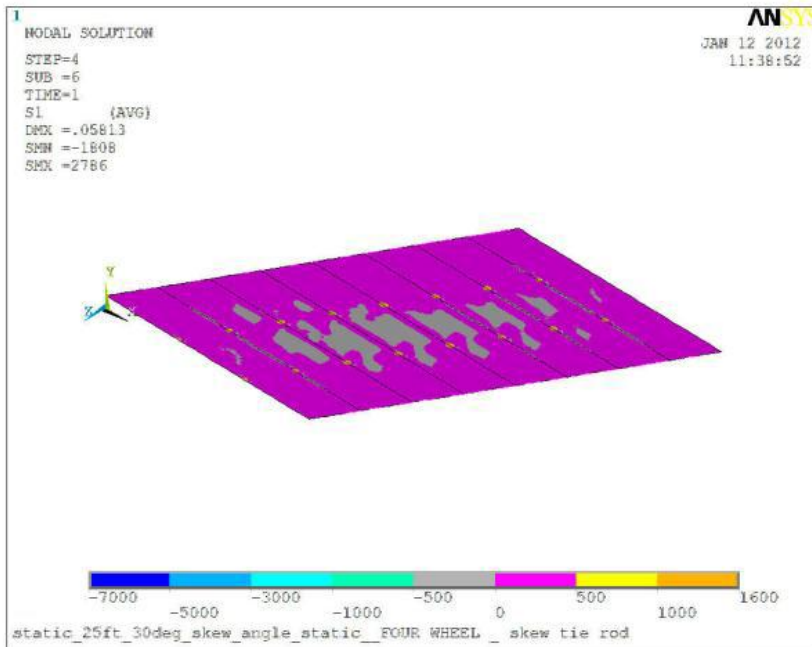
Figure C-19: First Principal Stress at the Beam-Overlay Interface.

C.9 Forty Foot, Fifteen Degree Skewed Bridge – Four Normal and Staggered
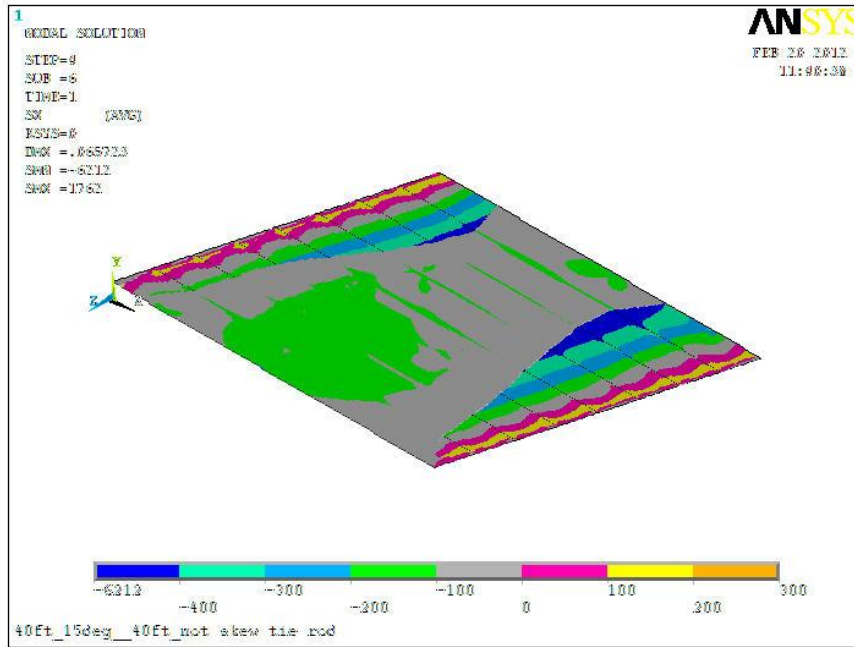
**Figure C-20: Longitudinal Stress at the Beam-Overlay Interface.**
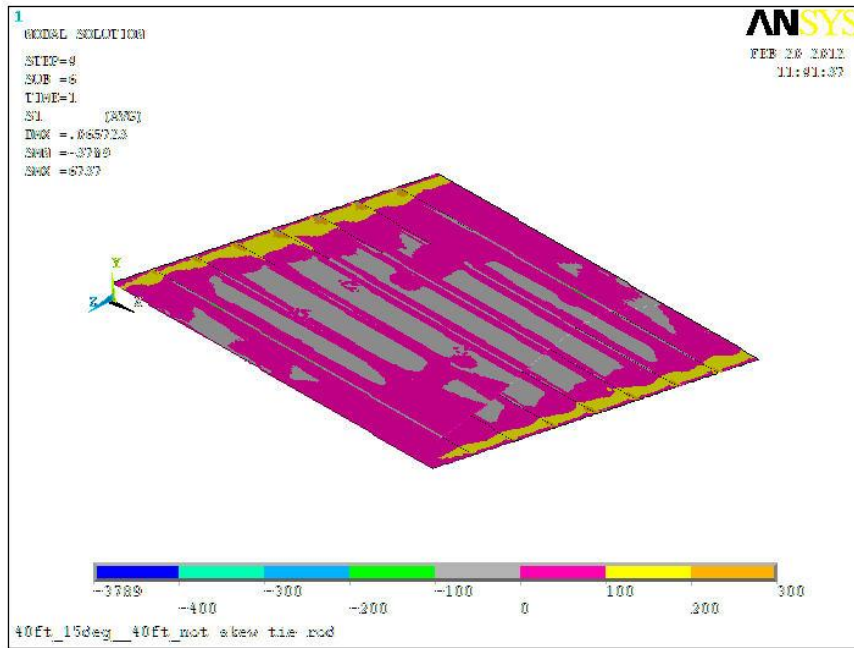
Figure C-21: First Principal Stress at the Beam-Overlay Interface.

C.10 Forty Foot, Fifteen Degree Skewed Bridge – Third Points Skewed
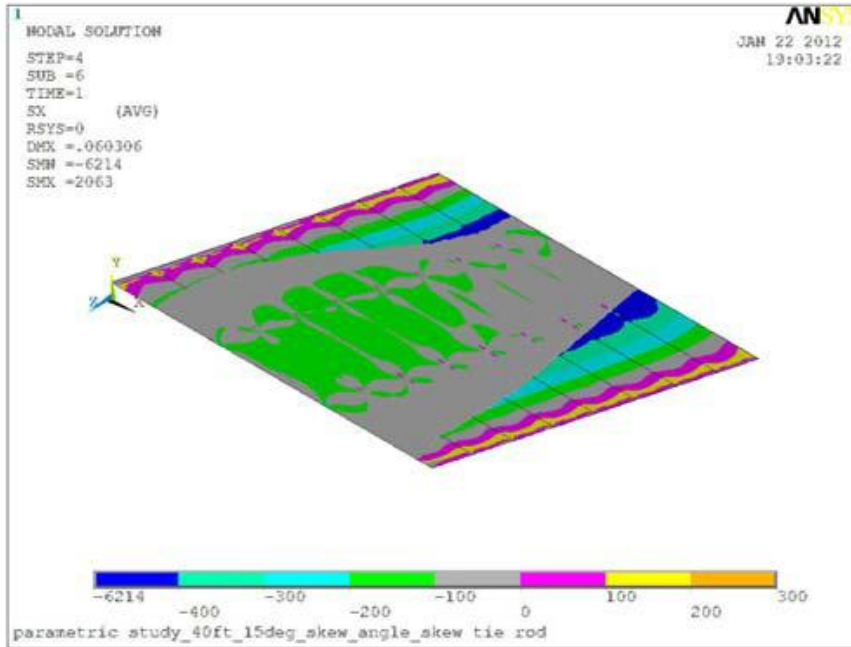
Figure C-22: Longitudinal Stress at the Beam-Overlay Interface.
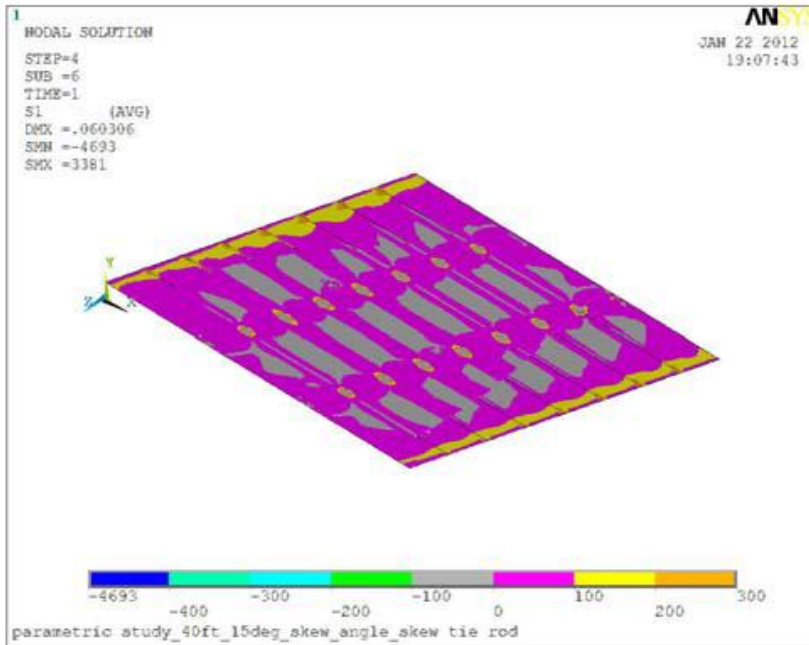

Figure C-23: First Principal Stress at the Beam-Overlay Interface.

C.11 Forty Foot, Fifteen Degree Skewed Bridge – Ends and Midspan Skewed
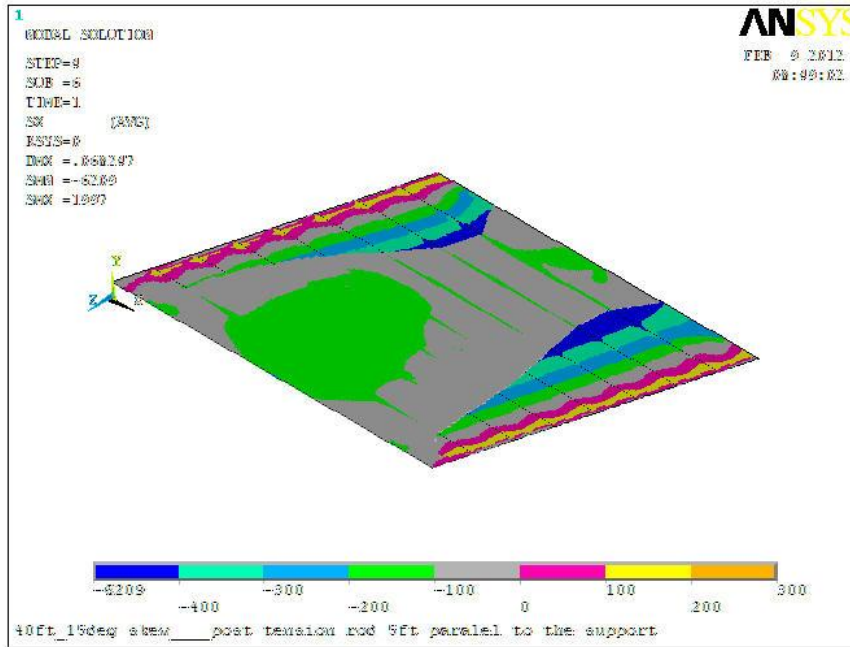
Figure C-24: Longitudinal Stress at the Beam-Overlay Interface.
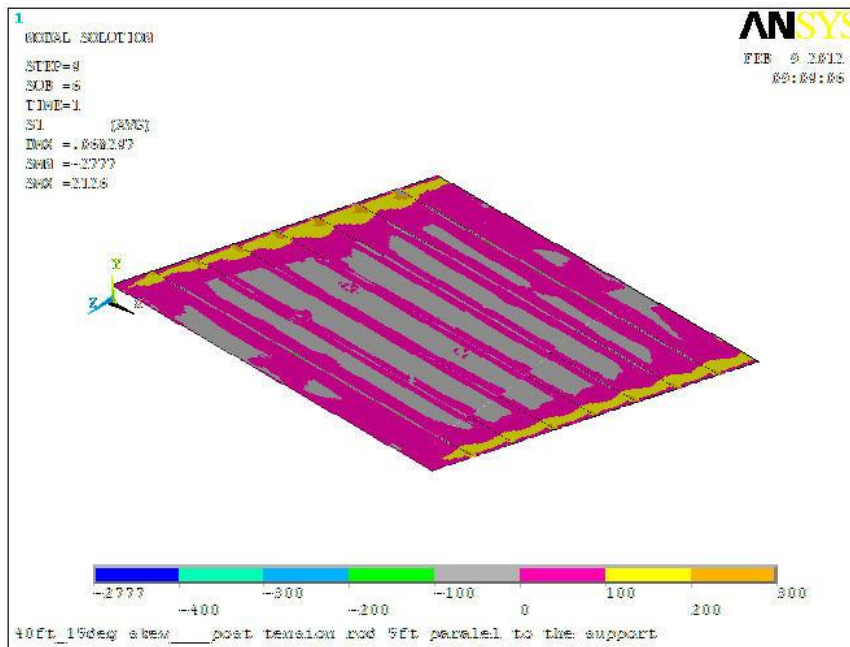
Figure C-25: First Principal Stress at the Beam-Overlay Interface.

117

## C.12 Forty Foot, Thirty Degree Skewed Bridge – Two Normal
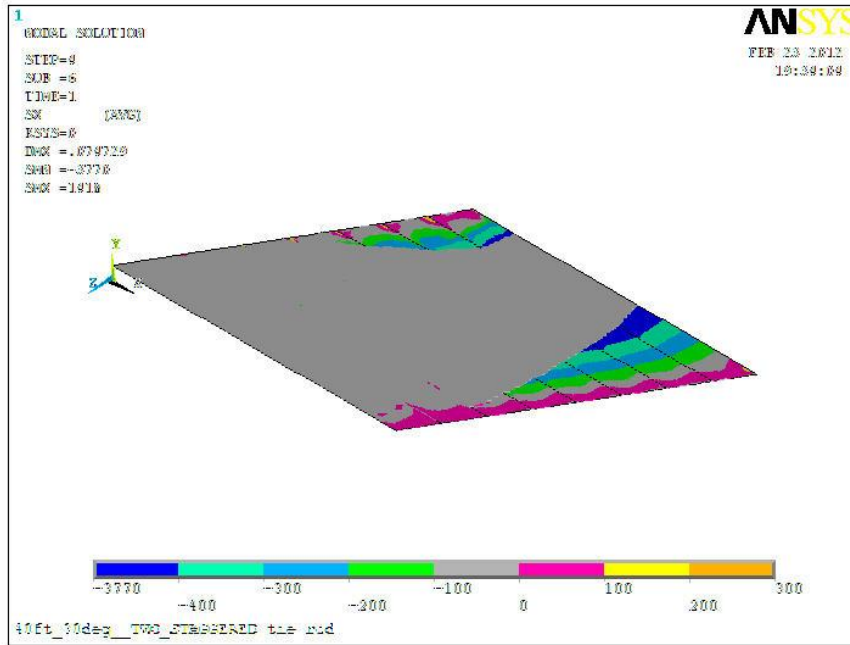
Figure C-26: Longitudinal Stress at the Beam-Overlay Interface.
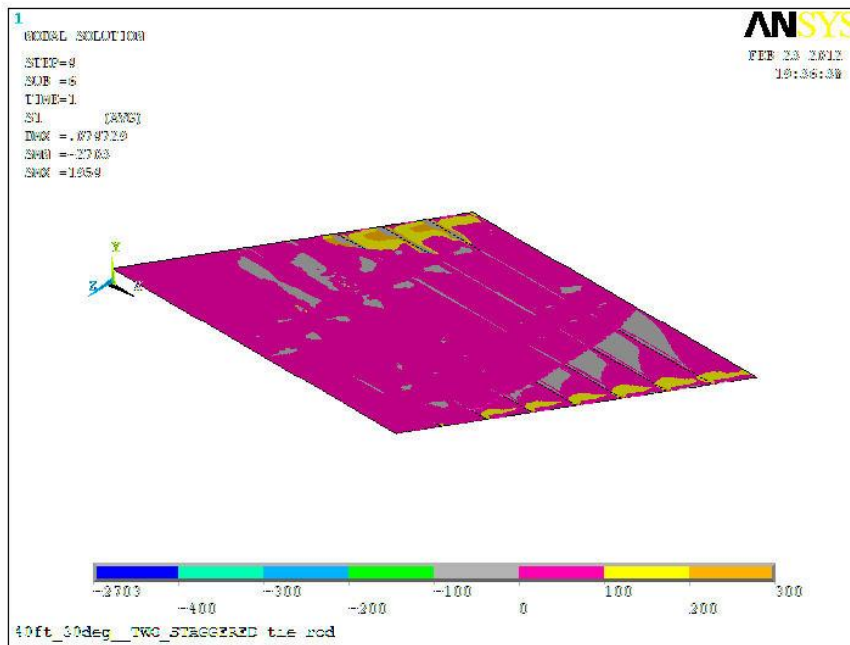
Figure C-27: First Principal Stress at the Beam-Overlay Interface.

## C.13 Forty Foot, Thirty Degree Skewed Bridge – Four Normal and Staggered
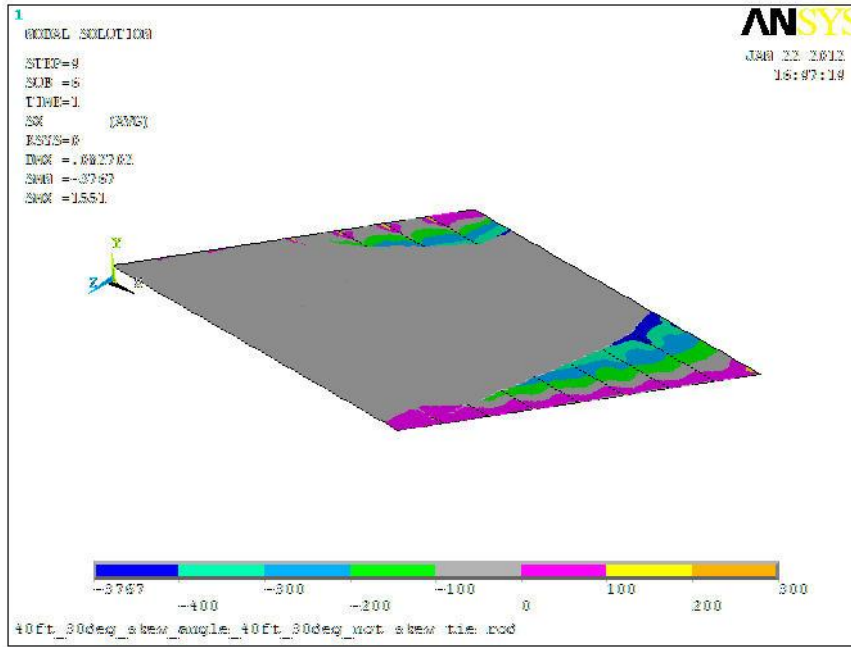
Figure C-28: Longitudinal Stress at the Beam-Overlay Interface.
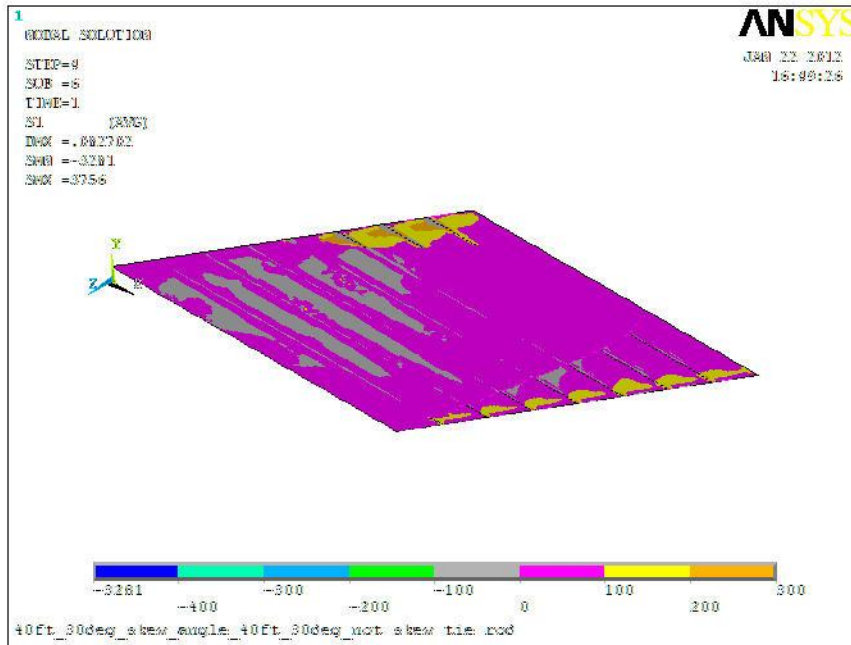
Figure C-29: First Principal Stress at the Beam-Overlay Interface.

C.14 Forty Foot, Thirty Degree Skewed Bridge – Third Points Skewed
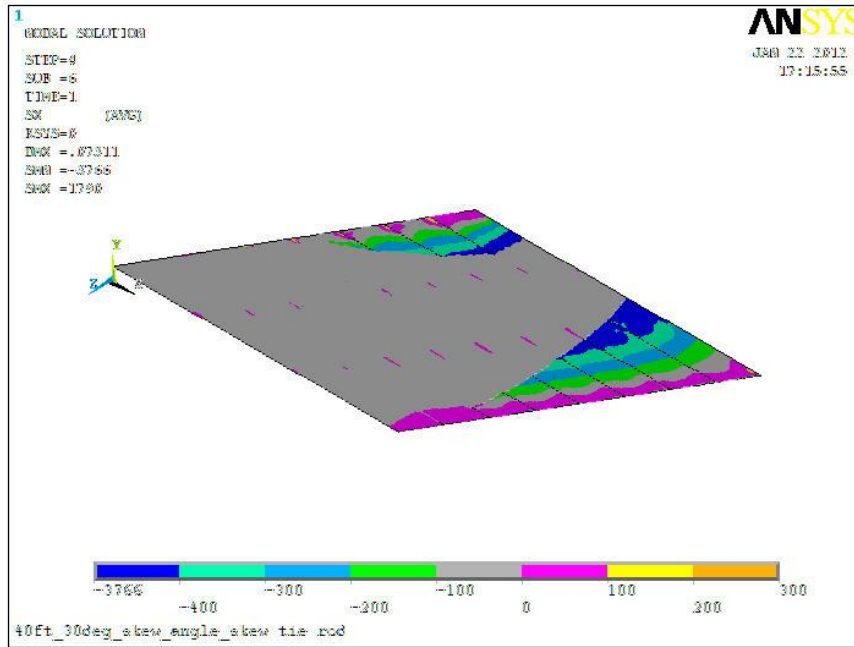
Figure C-30: Longitudinal Stress at the Beam-Overlay Interface.
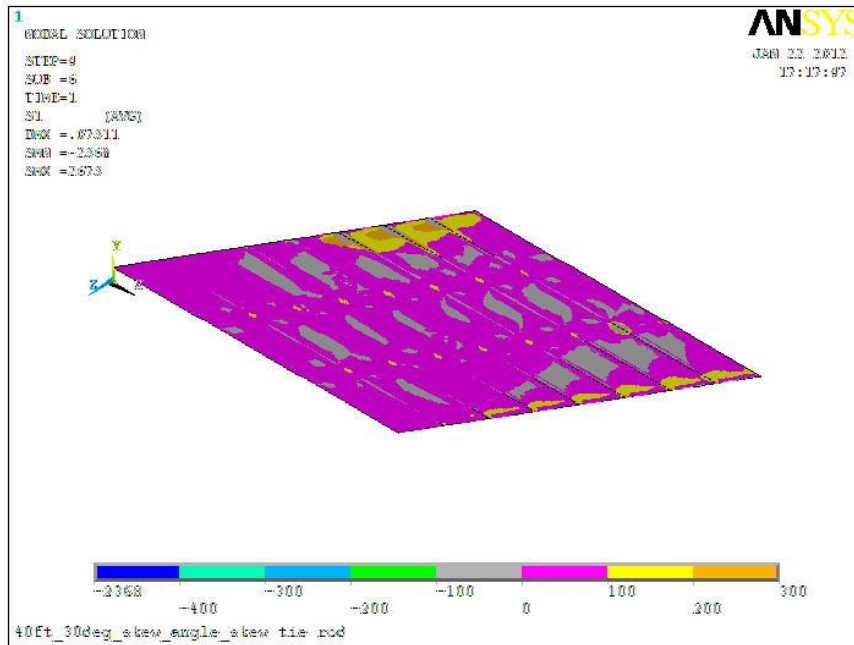
Figure C-31: First Principal Stress at the Beam-Overlay Interface.

C.15 Forty Foot, Thirty Degree Skewed Bridge – Ends and Midspan Skewed
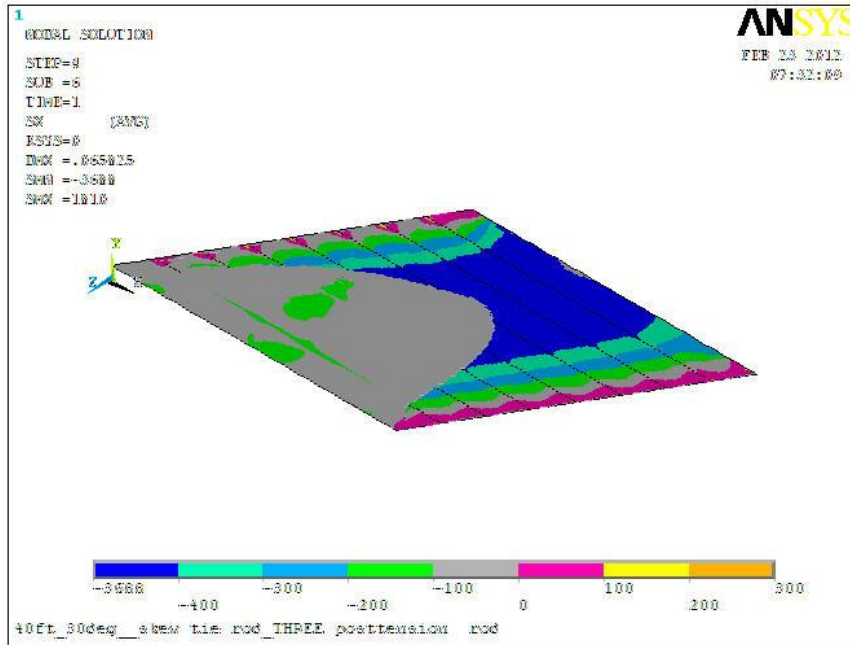
**Figure C-32: Longitudinal Stress at the Beam-Overlay Interface.**
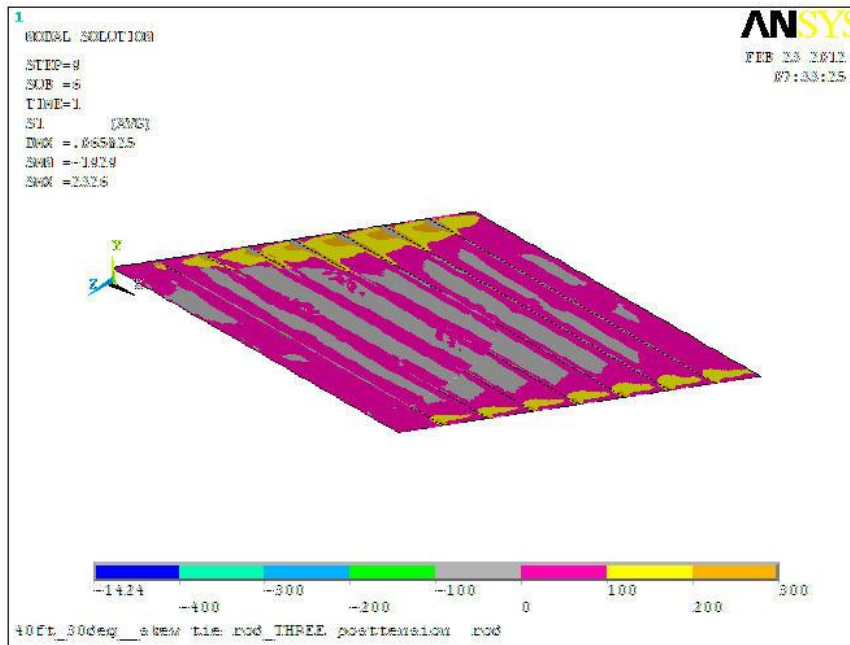
Figure C-33: First Principal Stress at the Beam-Overlay Interface.

121

C.16 Fifty-Five Foot, Fifteen Degree Skewed Bridge – Two Normal
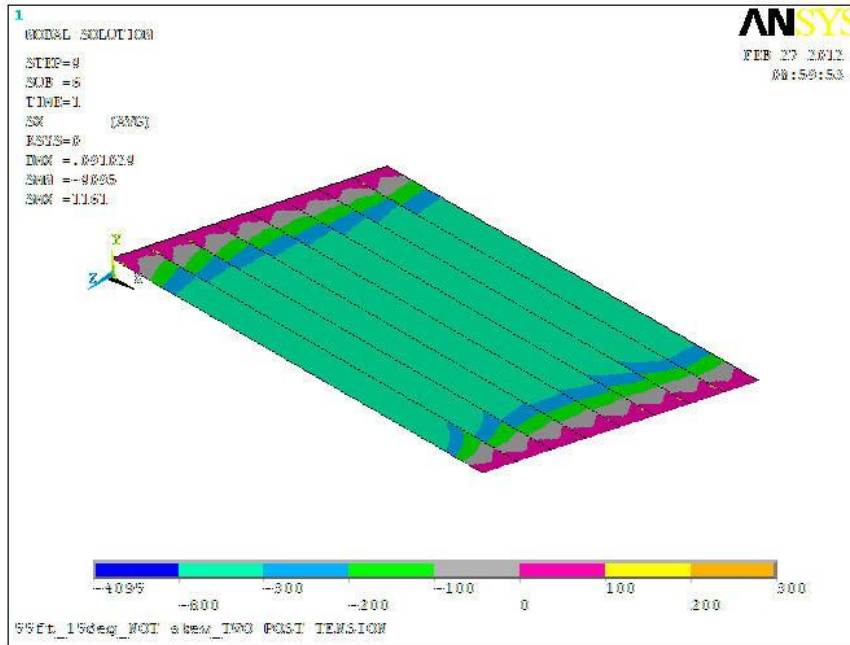
Figure C-34: Longitudinal Stress at the Beam-Overlay Interface.
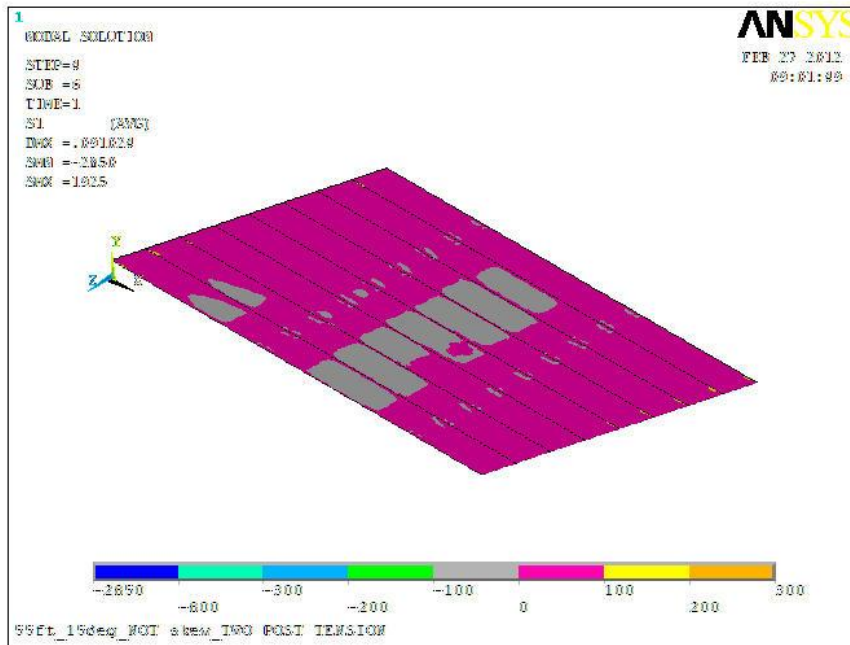
Figure C-35: First Principal Stress at the Beam-Overlay Interface.

C.17 Fifty-Five Foot, Fifteen Degree Skewed Bridge – Four Skewed
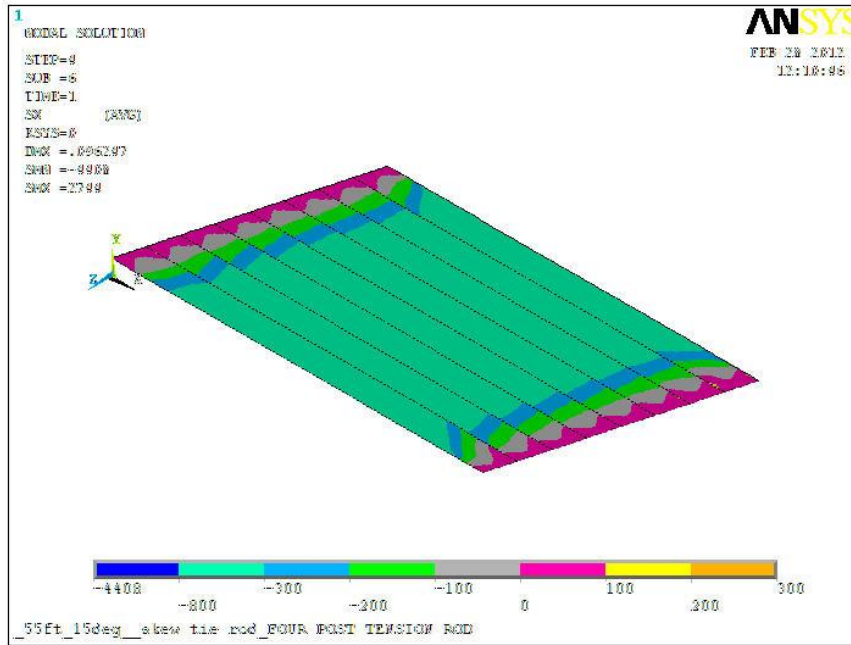
**Figure C-36: Longitudinal Stress at the Beam-Overlay Interface.**
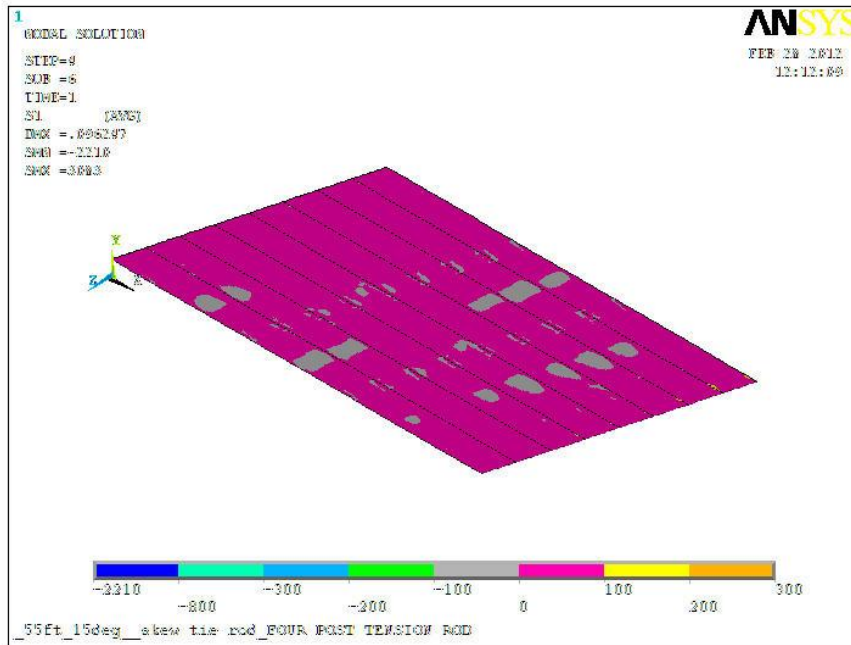
Figure C-37: First Principal Stress at the Beam-Overlay Interface.

## C.18 Fifty-Five Foot, Thirty Degree Skewed Bridge – Two Normal
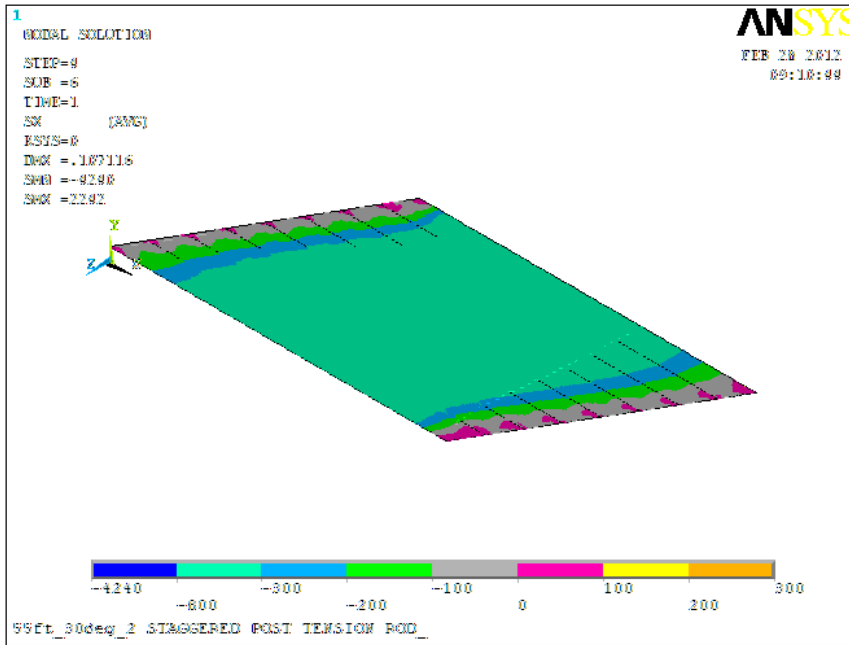
**Figure C-38: Longitudinal Stress at the Beam-Overlay Interface.**
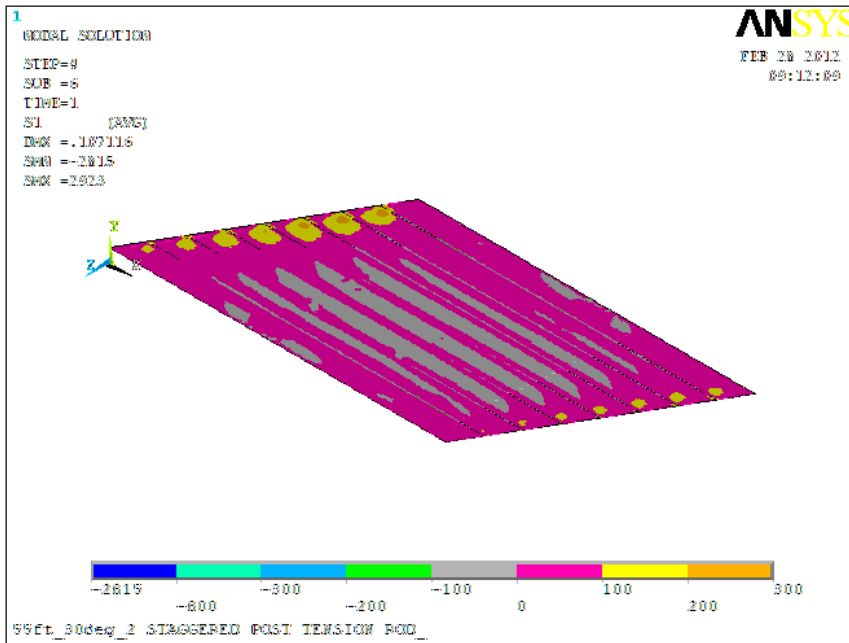
Figure C-39: First Principal Stress at the Beam-Overlay Interface.

124

C.19 Fifty-Five Foot, Thirty Degree Skewed Bridge – Three Skewed
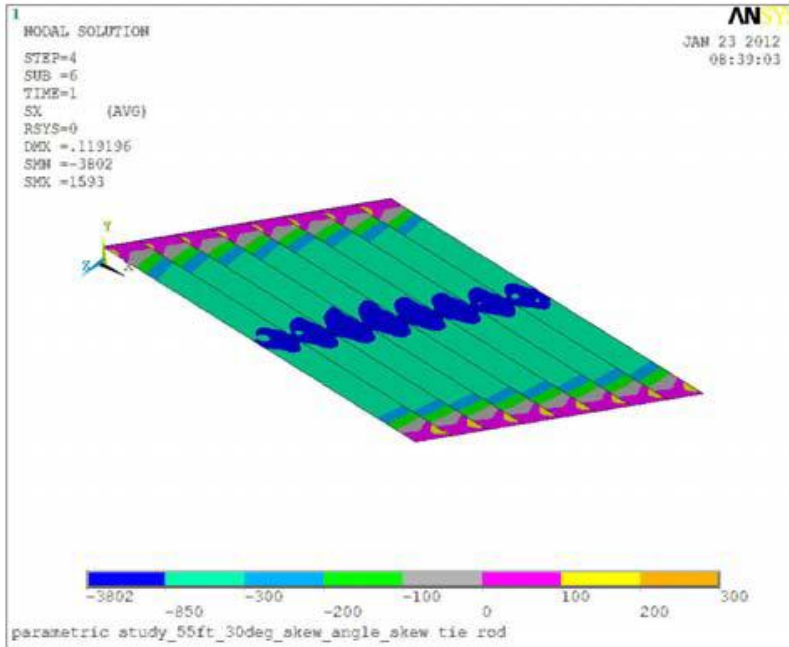

Figure C-40: Longitudinal Stress at the Beam-Overlay Interface.
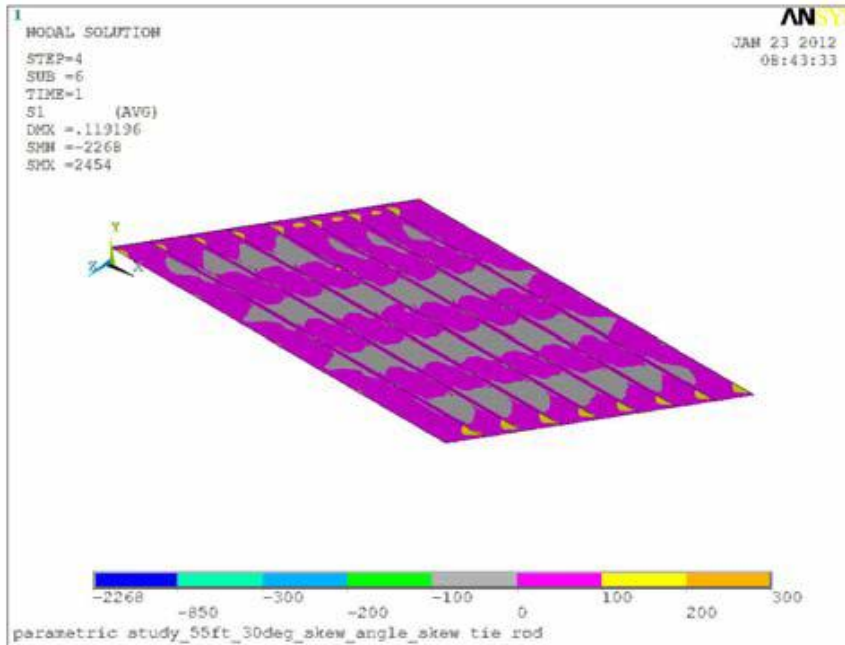

Figure C-41: First Principal Stress at the Beam-Overlay Interface.

## C.20 Fifty-Five Foot, Thirty Degree Skewed Bridge – Four Skewed
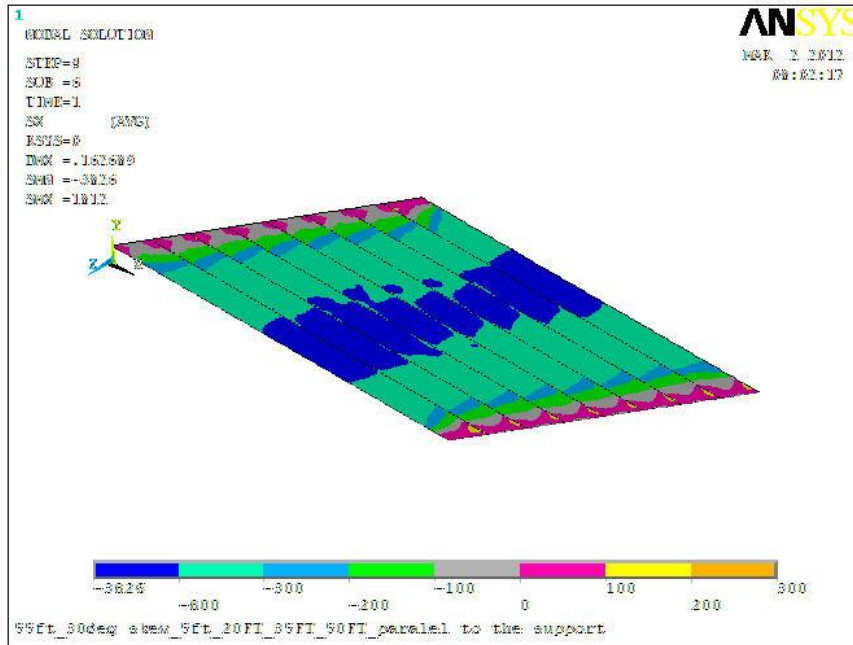
Figure C-42: Longitudinal Stress at the Beam-Overlay Interface.
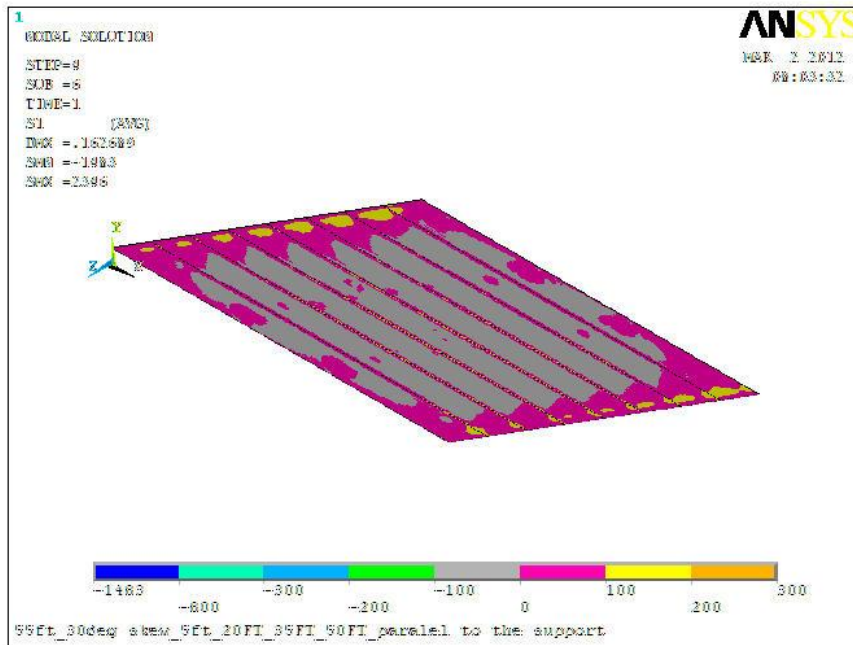

Figure C-43: First Principal Stress at the Beam-Overlay Interface.

C.21 Extension: Forty Foot, Fifteen Degree Skewed Bridge – Three Combined
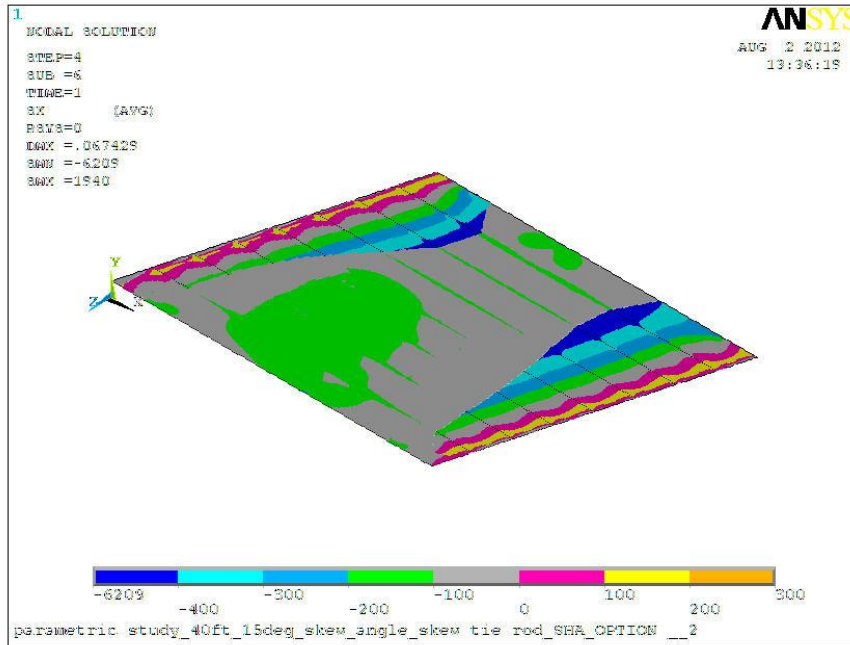
Figure C-44: Longitudinal Stress at the Beam-Overlay Interface.
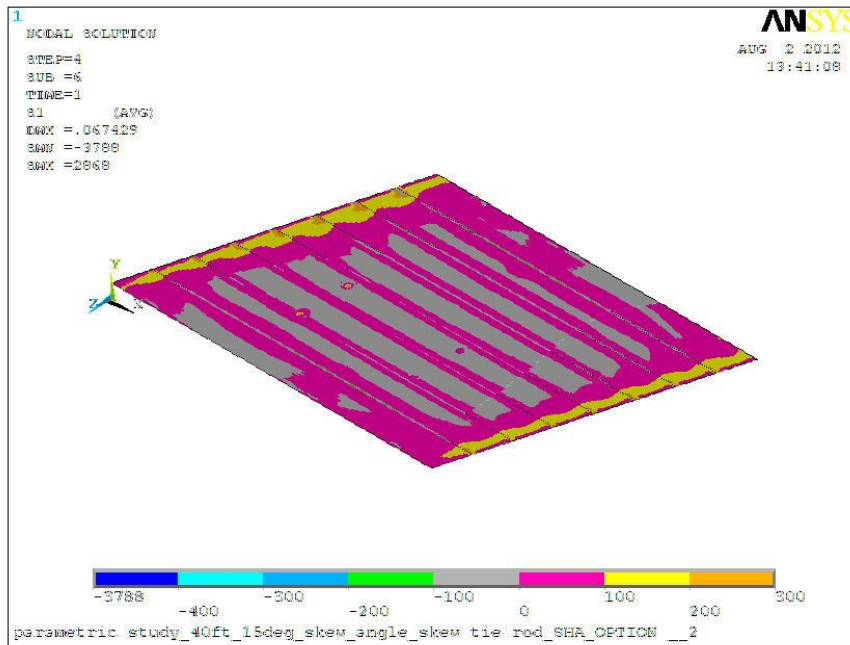
Figure C-45: First Principal Stress at the Beam-Overlay Interface.

C.22 Extension: Forty Foot, Thirty Degree Skewed Bridge – Three Combined
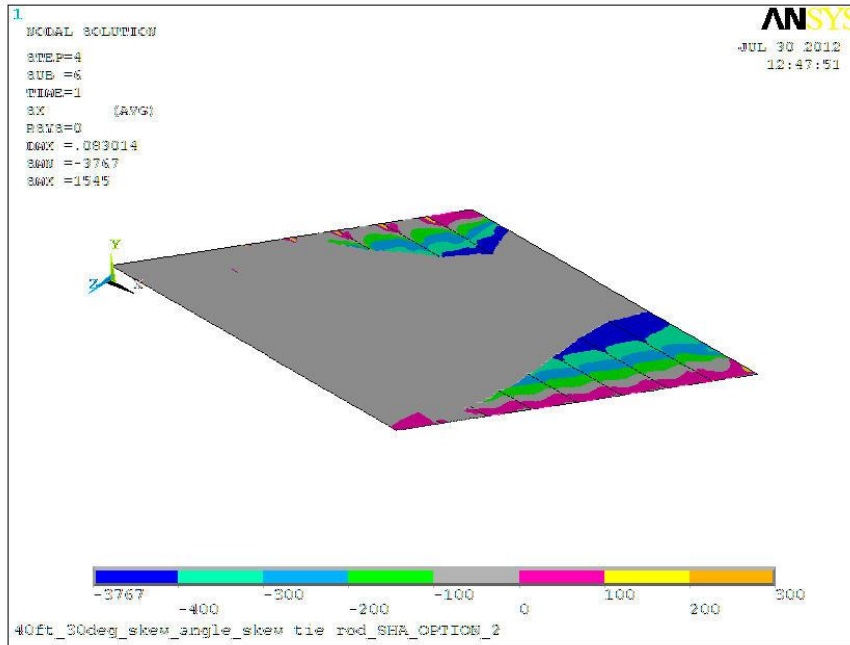

Figure C-46: Longitudinal Stress at the Beam-Overlay Interface.
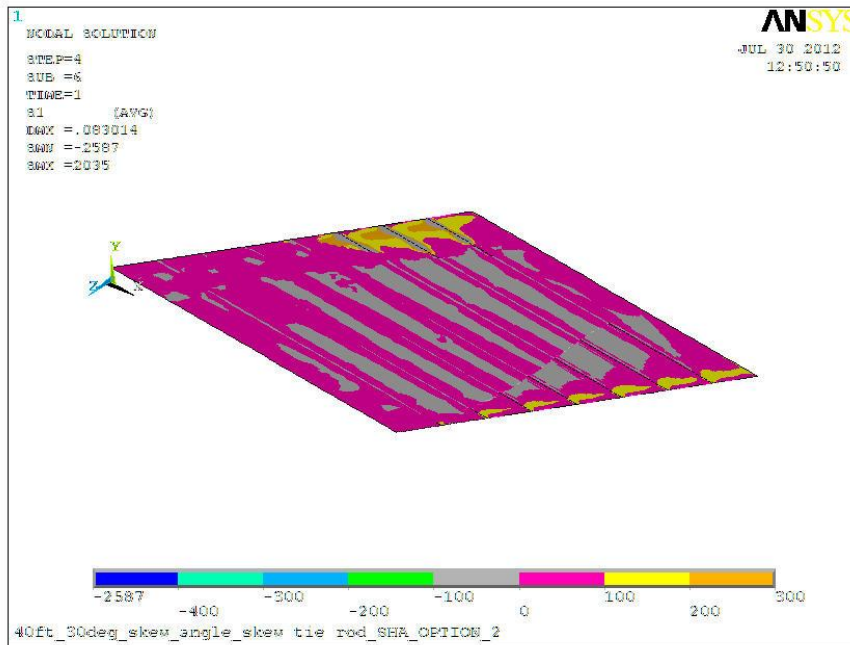
Figure C-47: First Principal Stress at the Beam-Overlay Interface.

C.23 Extension: Fifty-Five Foot, Fifteen Degree Skewed Bridge – Three
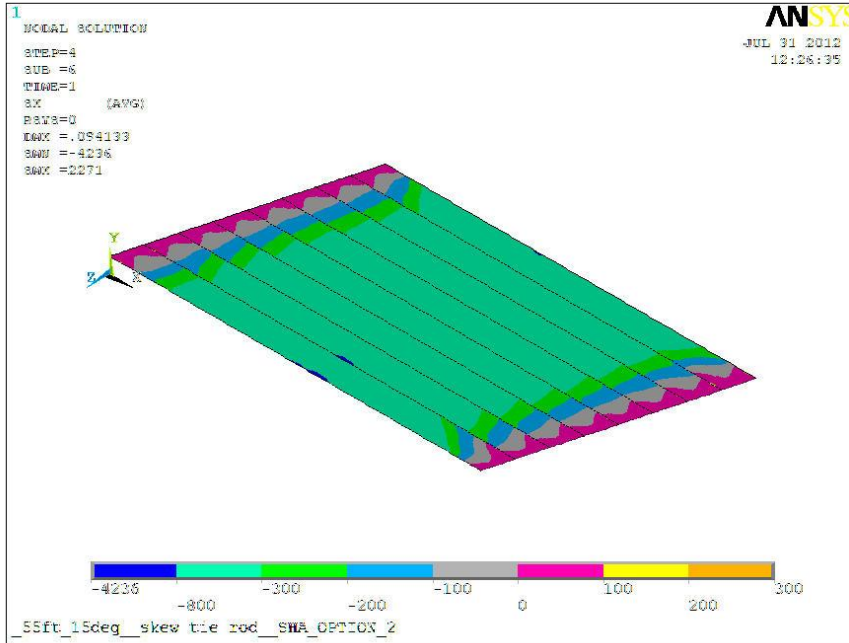
Combined

Figure C-48: Longitudinal Stress at the Beam-Overlay Interface.
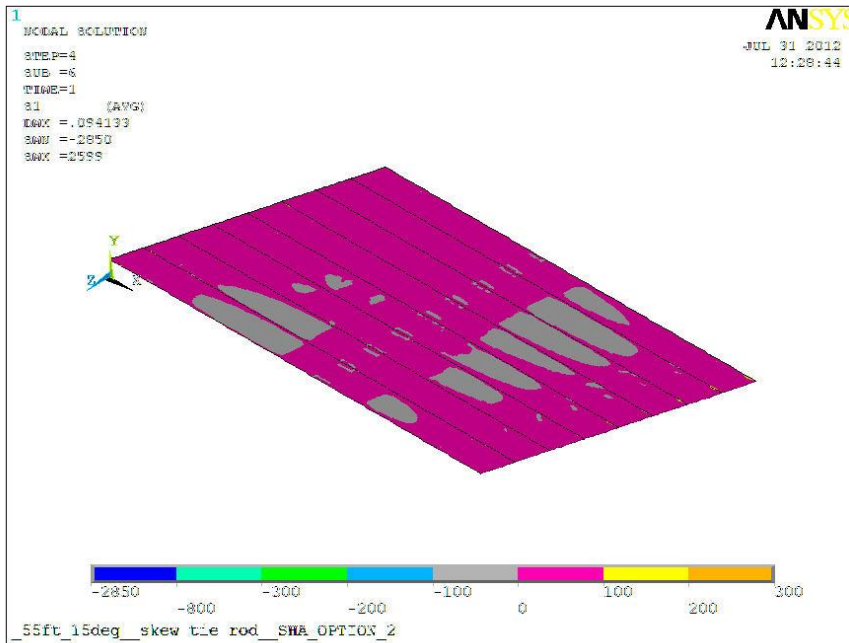
Figure C-49: First Principal Stress at the Beam-Overlay Interface.

C.24 Extension: Fifty-Five Foot, Fifteen Degree Skewed Bridge – Three

## Combined – HS-20 (Three Axle) Loading
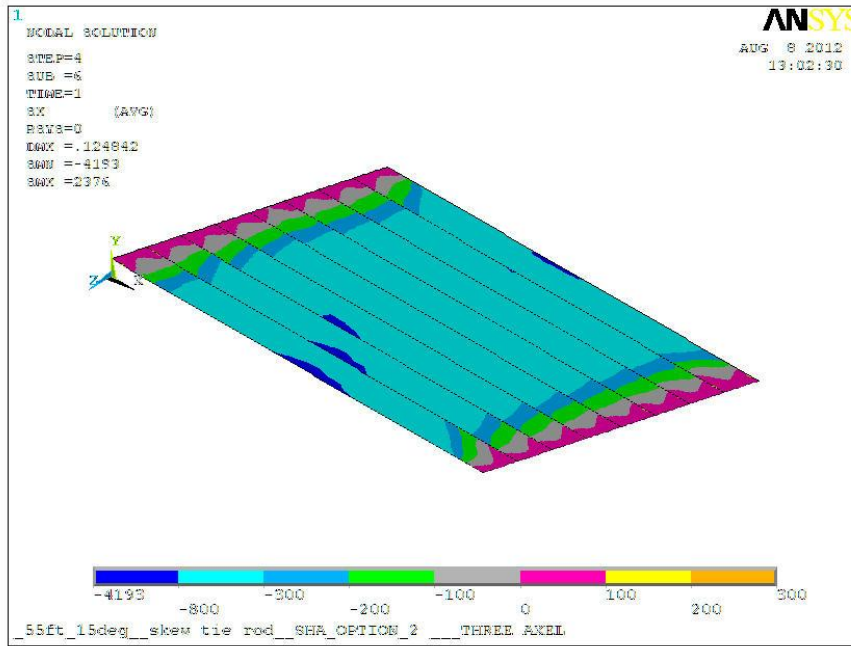
Figure C-50: Longitudinal Stress at the Beam-Overlay Interface.
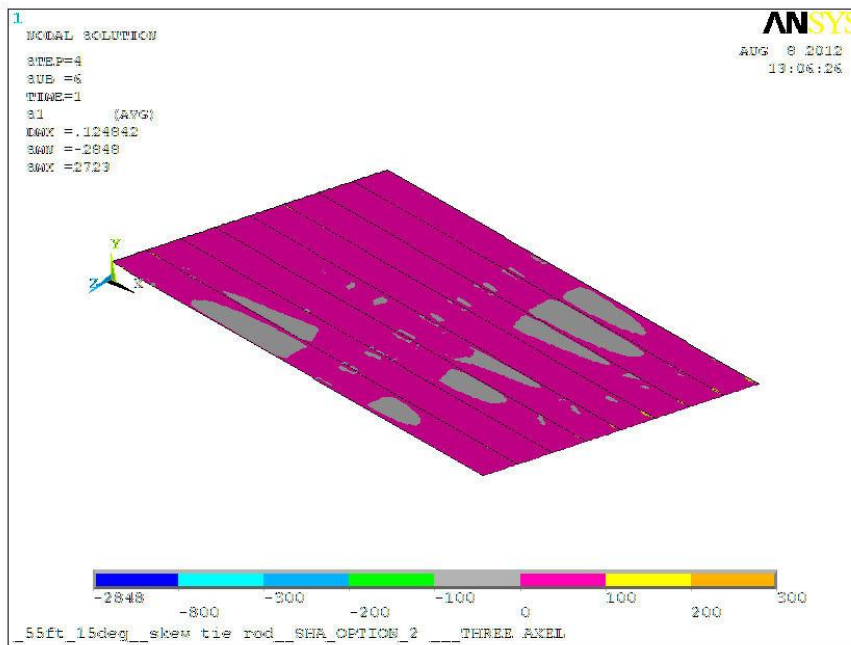
Figure C-51: First Principal Stress at the Beam-Overlay Interface.

C.25 Extension: Fifty-Five Foot, Fifteen Degree Skewed Bridge – Four
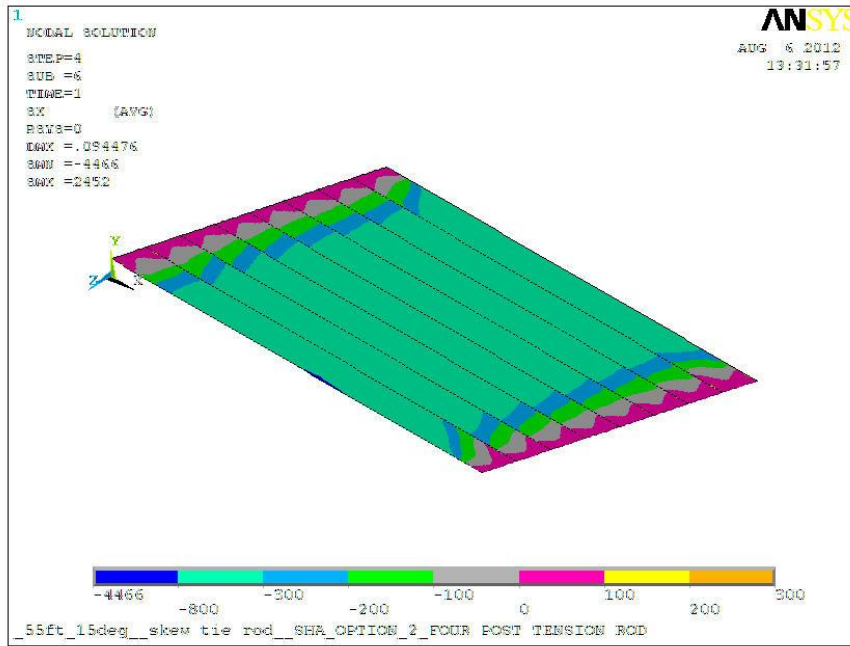
Combined

**Figure C-52: Longitudinal Stress at the Beam-Overlay Interface.**
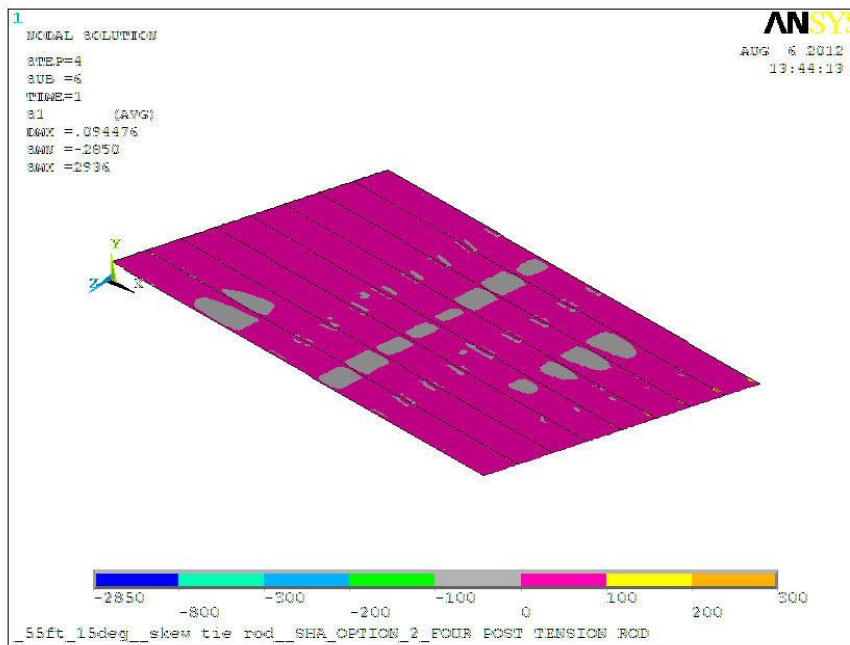
Figure C-53: First Principal Stress at the Beam-Overlay Interface.

C.26 Extension: Fifty-Five Foot, Thirty Degree Skewed Bridge – Three
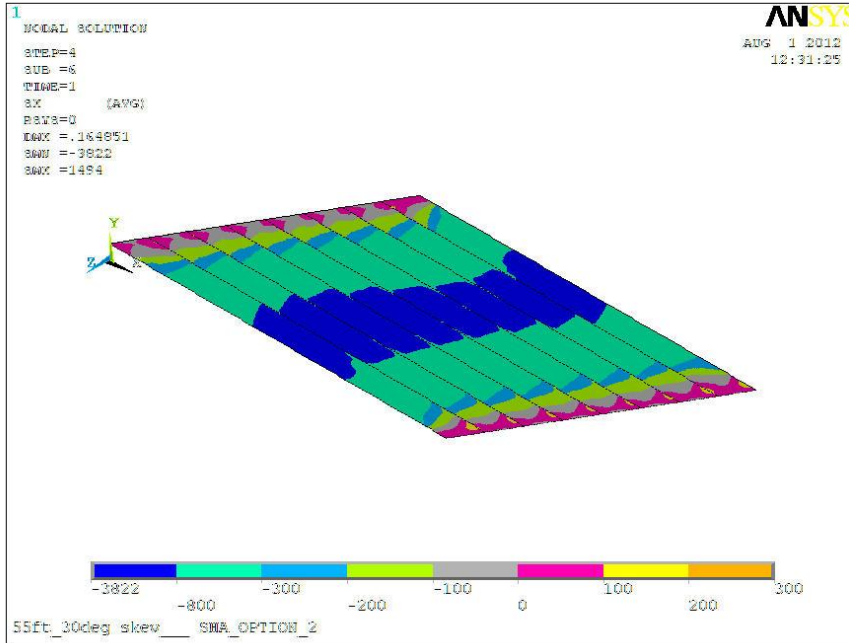
Combined

Figure C-54: Longitudinal Stress at the Beam-Overlay Interface.
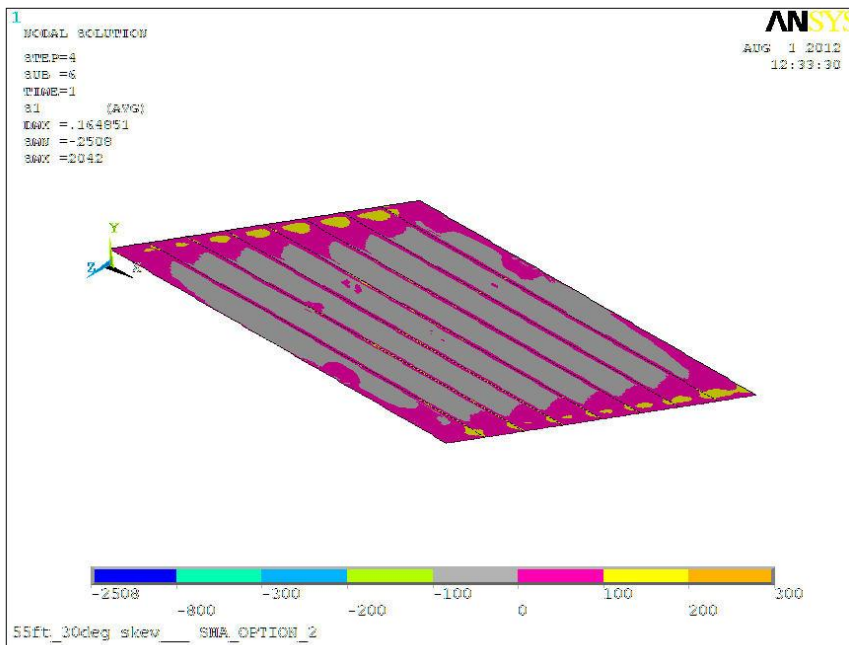
Figure C-55: First Principal Stress at the Beam-Overlay Interface.

C.27 Extension: Fifty-Five Foot, Thirty Degree Skewed Bridge – Four Combined
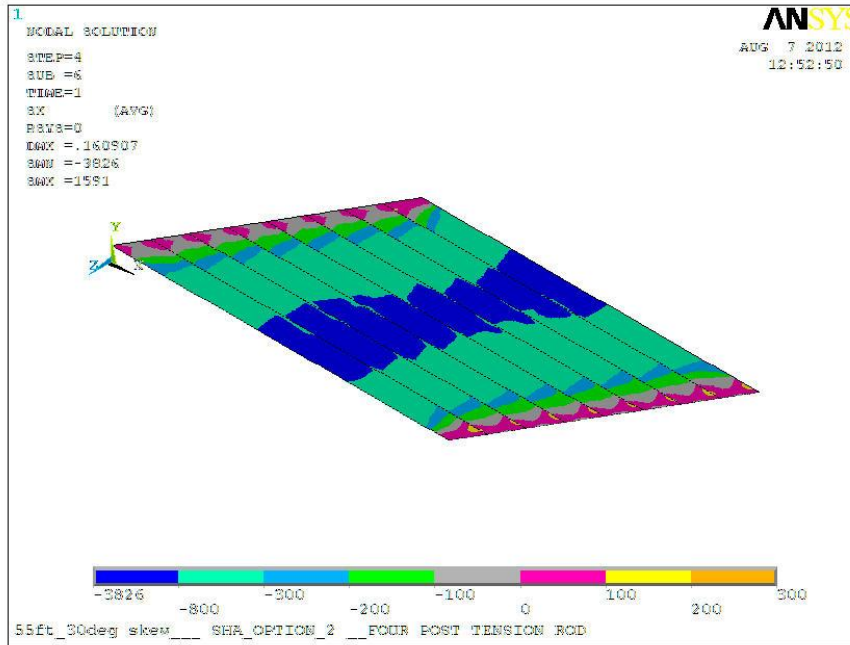
**Figure C-56: Longitudinal Stress at the Beam-Overlay Interface.**
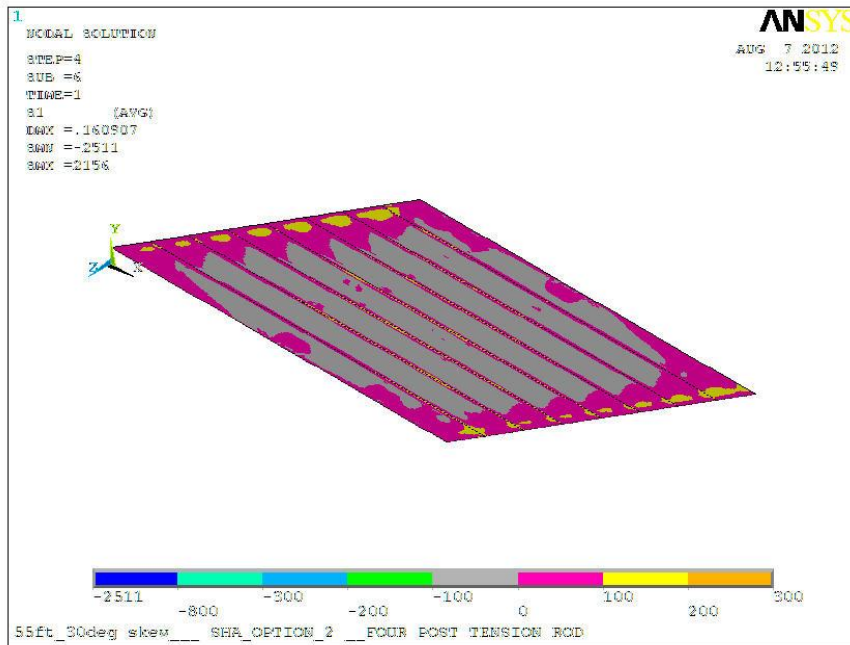
Figure C-57: First Principal Stress at the Beam-Overlay Interface.

133

References

AASHTO (2012). *AASHTO LRFD Bridge Design Specifications*, 6th Ed., American Association of State Highway and Transportation Officials, Washington, DC.

American Concrete Institute (ACI) (2011). "Building Code Requirements for Structural Concrete and Commentary." *ACI 318-11/ACI 318R-11*, Farmington Hills, MI.

ANSYS 10.0 [Computer software]. (2005). Cononsberg, PA, ANSYS.

Badwan, I. Z. and Liang, R. Y. (2007). "Performance Evaluation of Precast Posttensioned Concrete Multibeam Deck." *Journal of Performance of Constructed Facilities*, *21*(5), 368-374.

Bridge Diagnostics, Inc. (BDI). *BDI Strain Transducer Specifications*. June 13, 2012. <http://bridgetest.com/products/bdi-strain-transducers/>.

Bridge Engineering Software and Technology (BEST) Center, 2009. "Behavior and Analysis of an Instrumented MD355 over Wallace Creek Slab Bridge," Report to Maryland State Highway Administration and Federal Highway Administration (IBRC Program), Revision 0, University of Maryland, College Park.

Coletti, D., Chavel, B., and Gatti, W. (2011). "Challenges of Skew in Bridges with Steel Girders." *Transportation Research Record: Journal of the Transportation Research Board*, *2251*(5), 47-56.

Corven, J. and Moreton, A. (2004). "Post-Tensioning Tendon Installation and Grouting Manual," Report to Federal Highway Administration, Corven Engineering, Inc., Tallahassee, FL.

Federal Highway Administration (FHWA) (2011). *Deficient Bridges by State and Highway System*. February 21, 2012. <http://www.fhwa.dot.gov/bridge/deficient.cfm>.

Federal Highway Administration (FHWA) (2011). *Prefabricated Bridge Elements and Systems*. February 15, 2012. <http://www.fhwa.dot.gov/bridge/prefab/if09010/02b.cfm>.

Fu, C. C., Pan, Z., and Ahmed, M. S. (2011). "Transverse Posttensioning Design of Adjacent Precast Solid Multibeam Bridges." *Journal of Performance of Constructed Facilities*, *25*(3), 223-230.

Huang, H., Shenton, H. W., and Chajes, M. J. (2004). "Load Distribution for a Highly Skewed Bridge: Testing and Analysis." *Journal of Bridge Engineering*, *9*(6), 558-562.

Jeong, S. (2009). *Behavior and Analysis of an Instrumented Slab Bridge* (Master's thesis). University of Maryland, College Park, MD.

Marcuzzi, A. and Morassi, A. (2010). "Dynamic Identification of a Concrete Bridge with Orthotropic Plate-Type Deck." *Journal of Structural Engineering*, *136*(5), 586-602.

Mari, A. and Valdes, M. (2000). "Long-Term Behavior of Continuous Precast Concrete Bridge Model." *Journal of Bridge Engineering*, *5*(1), 22-30.

Massachusetts Department of Transportation (MassDOT) (2009). *2009 LRFD Bridge Manual*. August 25, 2011. <http://www.mhd.state.ma.us/default.asp?pgid=bridge/bridgemanual_01&sid =about>.

Menassa, C., Mabsout, M., Tarhini, K., and Frederick, G. (2007). "Influence of Skew Angle on Reinforce Concrete Slab Bridges." *Journal of Bridge Engineering*, *12*(2), 205-214.

Modjeski and Masters, Inc. (2002). "Shear in Skewed Multi-beam Bridges", Report to National Cooperative Highway Research Program (Project 20-7/Task 107).

Narer, J. W. (1997). "A New Generation of Precast Prestressed Concrete Slab Bridges for Maryland's Rural Highways." *PCI Journal*, May/June, 16-20.

Oregon Department of Transportation (ODOT) (2004, rev. April 2011). *Bridge Design and Drafting Manual*. February 20, 2012. <http://www.oregon.gov/ODOT/HWY/BRIDGE/docs/BDDM/apr-2011_finals/section_1-2004_apr2011.pdf>.

Precast/Prestressed Concrete Institute (PCI) (2003). *PCI Bridge Design Manual*, 2nd Ed., Chicago, IL.

Ramirez, J. A. and Smith, J. P. (2003). *An Investigation on Transversely Prestressed Concrete Bridge Decks*. Joint Transportation Research Program, Indiana Department of Transportation and Purdue University, West Lafayette, Indiana.

Rhode Island Department of Transportation (RIDOT) (2010). *Bridge Design Standard Details*. August 29, 2011.

<http://www.dot.ri.gov/documents/engineering/BlueBook/RIDOT_Bridge_St andards%202010.pdf>.

Roschke, P. N., Pruski, K. R., and Sripadanna, N. (1999). "Time-Dependent Behavior of Post-Tensioned Slab Bridge." *ACI Structural Journal*, *96*(3), 400-409.

Russell, H. G. (2009). *Adjacent Precast Concrete Box Beam Bridges: Connection Details*. National Cooperative Highway Research Program Synthesis 393, National Research Council Transportation Research Board, Washington, DC.

Russell, H. G. (2011). "Adjacent Precast Concrete Box-Beam Bridges: State of Practice." *PCI Journal*, Winter, 75-91.

Saber, A. and Alaywan, W. (2011). "Full-Scale Test of Continuity Diaphragms in Skewed Concrete Bridge Girders." *Journal of Bridge Engineering*, *16*(1), 21-28.

Schaffer, T. (1967). *Structural Response of a 45° Skew Prestressed Concrete Box-Girder Highway Bridge Subjected to Vehicular Loading Brookville Bridge* (Master's thesis). Lehigh University, Bethlehem, PA.

Sharpe, G. P. (2007). *Reflective Cracking of Shear Keys in Multi-Beam Bridges* (Master's thesis). Texas A&M University, College Station, TX.

"Strain Gauge." *Wikipedia*. June 13, 2012. <http://en.wikipedia.org/wiki/Strain_gauge>.

Vermont Agency of Transportation (VTrans) (2011). *2011 Standard Specifications for Construction Book*. February 20, 2012. <http://www.aot.state.vt.us/conadmin/2011StandardSpecs.htm>.

"Wheatstone Bridge." *Wikipedia*. June 13, 2012. <http://en.wikipedia.org/wiki/Wheatstone_bridge>.